Synthesis of Borocations and their Catalytic Application in Cyanosilylation

A Thesis

Submitted to

Indian Institute of Science Education and Research Pune in partial fulfillment of the requirements for the MSc. Degree Programme

by

Bhavsar Parth Kalpesh

IISER PUNE

Indian Institute of Science Education and Research, Pune

Dr. Homi Bhabha Road,

Pashan, Pune, 411008, INDIA

April, 2024

Supervisor: Dr. Shabana Khan

Bhavsar Parth Kalpesh

Certificate

This is to certify that this dissertation entitled "**Synthesis of Borocations and their Catalytic Application in Cyanosilylation**" towards the partial fulfillment of the MSc. degree programme at the Indian Institute of Science Education and Research, Pune, represents the study and work carried out by **Bhavsar Parth Kalpesh (Reg. No. 20226202)** at Indian Institute of Science Education and Research under the supervision of **Dr. Shabana Khan**, Associate Professor, Department of Chemistry, during the academic year 2023-2024.

Dr. Shabana Khan

Committee:

Dr. Shabana Khan

Dr. Debangsu Sil

This thesis is dedicated

to

MY PARENTS

Declaration

I hereby declare that the matter embodied in the report entitled "**Synthesis of Borocations and their Catalytic Application in Cyanosilylation**" are the results of the work carried out by me at the Department of Chemistry, Indian Institute of Science Education and Research, Pune, under the supervision of Dr. Shabana Khan and the same has not been submitted elsewhere for any other degree.

Bhavsar Parth Kalpesh

9th April, 2024

Table of Contents

List of Charts

List of Figures

List of Schemes

List of tables

List of Abbreviations

Notation	Full Name
NHC	N-Heterocyclic carbene
cAAC	Cyclic alkyl amino carbene
FLP	Frustrated Lewis Pair
OLED	Organic light-emitting diode
RT	Room temperature
Mes	$2,4,6\text{-}C_6H_2Me_3$
Ar=Dipp	$C_6H_3\text{-}2,6\text{-}^{i}Pr_2$
THF	Tetrahydrofuran
DCM	Dichloromethane
SCXRD	Single crystal X-ray diffraction
s	singlet
d	doublet
t	triplet
sept	septet
br	broad
dd	doublet of doublet
h	hours
min	minutes
g	gram
mL	millilitres
mmol	millimole
equiv.	equivalent
ppm	parts per million
mg	milligrams
°C	degree Celsius
NMR	Nuclear magnetic resonance
δ	chemical shift
IR	Infrared spectroscopy
MHz	Megahertz

1. Abstract

Boron chemistry has gained enormous traction in the last 50 years on account of the versatility of boron. Cationic boron species known as borocations have been recent favorites in organometallic chemistry due to their high electrophilic character and, thus, greater reactivity. Borocations have, therefore, been explored in organic transformations, including hydrosilylation and hydroboration. In addition, many of these species have been known to show thermochromism and luminescent properties, allowing for their use in photo-physical studies. Among the borocations, the reactivity of boronium ions has been explored to a relatively lesser extent in contrast to boreniums. Herein, we have synthesized two boronium-like cations with varying counter-ions using *N,N'*-dimesitylethanediamine as the ligand. The influence of the ligand on the steric and electronic properties of the system and, hence, the boron center has been well studied. Using literature precedence, we have justified the classification of our borocations as boronium-like cations. Furthermore, the molecular structure of the borocation **C2** has been successfully established using single crystal X-ray diffraction, and both the cations **C2** and **C3** have been characterized thoroughly using analytical tools, including NMR, IR, and HRMS. The Lewis acidic nature of both the cations has been tested via the Gutmann-Beckett method, and they have been used as efficient catalysts for the cyanosilylation of various aldehydic substrates.

2. Introduction

Transition metals have served as building blocks for several crucial organic transformations and catalysis for years.[1] However, focus on economical and sustainable chemical methodologies has resulted in the emergence of main group alternatives.[2] 21st century has marked a new dawn for main-group chemistry, with several significant breakthroughs having been achieved.[3,4] The journey that had its advent in the late 1980s ushered into a new era, especially after Philip Power's work in 2010 which broke several previous myths concerning main group elements and put them at par with their *d*-block analogs.[5]

The ability of main group elements to form multiple bonds and establish low valent derivatives with accessible coordination sites in conjunction with their low toxicity and low cost, enable their inclusion in poly-functional compounds for enhancement of reactivity and hence in carrying forth chemical transformations, σ-bond cleavages and catalysis.[4,6]

Among the main group elements, those in the *p*-block have been well explored for their chemical reactivity and subsequent formation of value-added products.[7] Incorporation of H_2 and NH_3 molecules into a stable carbene to give the respective addition/activation product as well as N_2 activation through a borylene intermediate have all been well explored by Bertrand and Braunschweig groups, respectively (**Chart 1**).[8,9] Such small molecule incorporation forms a crucial step in carrying forth a homogeneous catalytic cycle.
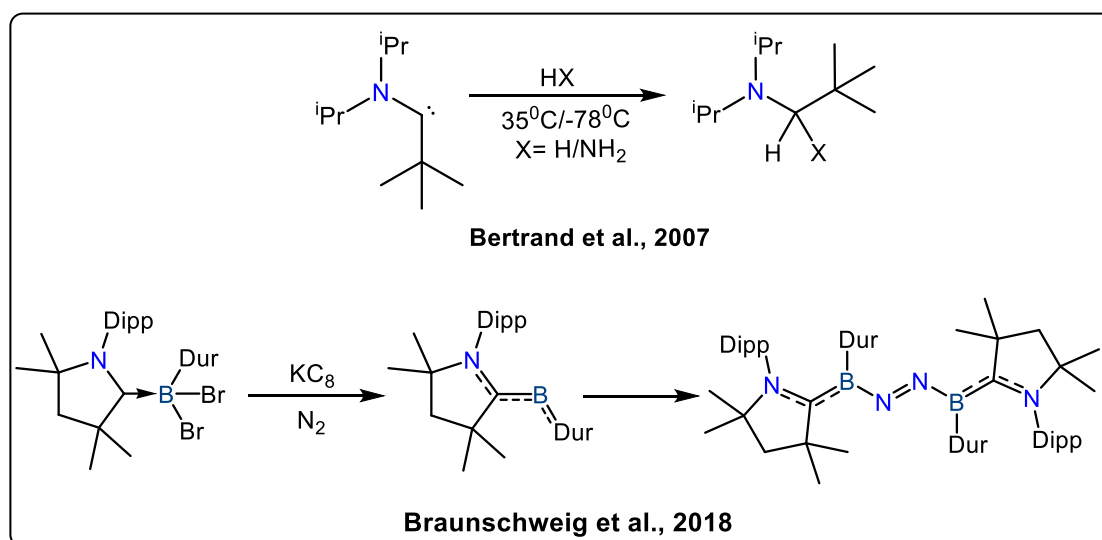
Chart 1: Small molecule activation by *p*-block elements

Subsequently, CO_2 fixation using NHC-stabilized dialumene by Weetman as well as CO_2 reduction via a cAAC stabilized boron-aluminium multiple bonded complex by Braunschweig (**Chart 2**), portray the chemical versatility of aluminium.[10,11] Additionally, aluminium-based imide complexes have also been used in CO activation by Aldridge and Goicocecha in 2020 (**Chart 2**).[12]

Braunschweig et al., 2019

Aldridge & Goicoecha, 2020
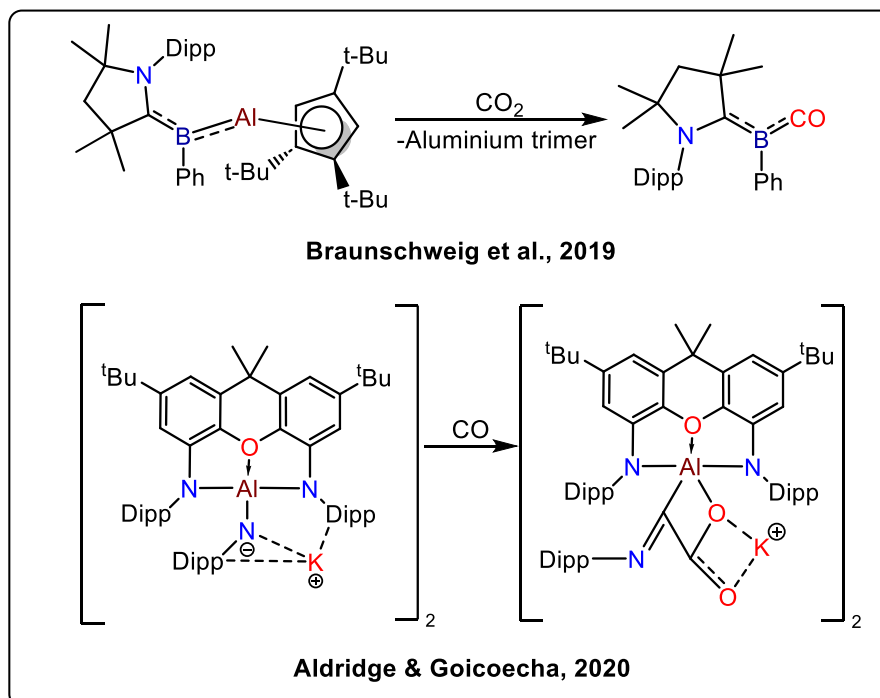
Chart 2: Reactivity of aluminium complexes

Borasilenes involving boron-silicon double bond were first established in 2006 by Sekiguchi and co-workers (**Chart 3**).[13] Thereafter, Inoue and co-workers in the year 2019, synthesized another borasilene that was Lewis base stabilized (**Chart 3**).[14] These were found to show reactivity towards chalcogens, including selenium, forming three- and four-membered rings.
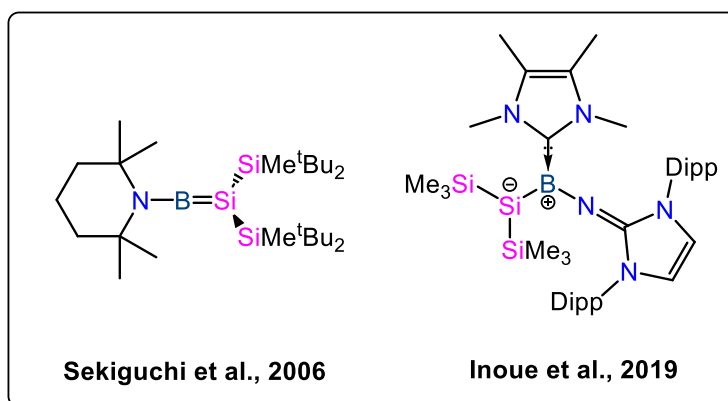
Chart 3: Schematic representation of reported borasilenes

The chemical utility of digallenes in small molecule activation (**Chart 4**) was described by Power and co-workers in 2009.[15] Additionally, in 2016, the Rivard group also demonstrated the potential ability to carry forth catalytic dehydrogenation using NHC imino-borane, avoiding the involvement of any metal in the catalytic process.[3] Meanwhile, the utilization of indene in chalcogenide dimer synthesis has been well studied by Power in 2009.[4]
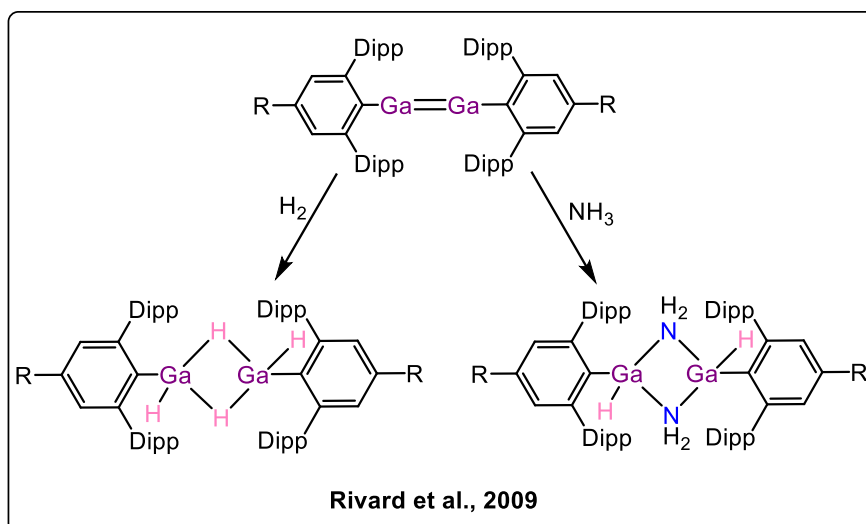
Chart 4: Digallene in small molecule activation

In 2006, Stephan and co-workers introduced the concept of Frustrated Lewis Pairs (FLPs) utilizing phosphorus and boron as a part of the molecular system.[16] Such systems prevent adduct formation via steric hindrance of phosphorus groups while aiding in the interaction of hydrogen molecules with the lone pair of phosphorus and the vacant orbital on boron. The establishment of phosphine boranes for hydrogen activation has been well described by this group (**Chart 5**).

Stephan et al., 2006
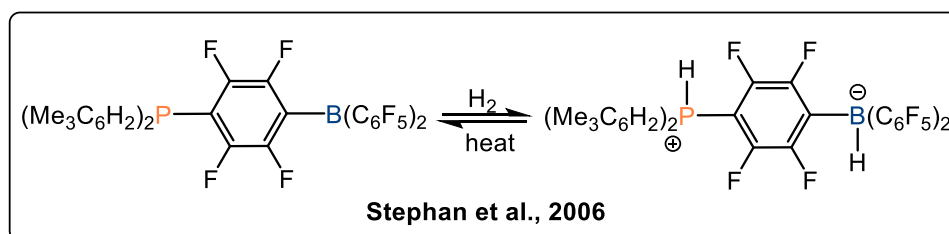
Chart 5: Hydrogen activation using Frustrated Lewis Pair

Such enhanced reactivities depicted by *p*-block elements in conjunction with the tendency to form value-added products via such reactions, motivates one to look more closely at these resplendent elements.

The element of our interest among the *p*-block elements is boron, a lightweight yet versatile periodic table element. The origin of boron in chemical transformations dates back to the year 1807 when Humphry Davy talked about wet boric acid and its electrolytic reduction.[17] Not only does boron have a higher utilization in natural chemistry, including RNA synthesis and nitrogen fixation by plants,[17] but it also has equal importance in synthetic chemistry, including in drug manufacture,[17] photo-chemical applications such as OLEDs[18] and organic transformations like catalytic dehydrocoupling, hydrogenolysis and hydroboration, etc.[17,19]

Besides its moderately high abundance and low cost, boron has a low electronegativity and an electronic configuration of *$1s^2 2s^2 2p^1$*, imparting it with an intrinsic electron-deficient nature.[20] Typical boron forms a three-coordinate neutral complex known as borane, imparting it with six valence electrons.[21] However, two vacant *2p* orbitals persist on the boron center, which can be tapped into to accept electrons and satisfy the octet. This, thus, imparts an electrophilic character to the boron center, and such a Lewis acidic boron can thereby be utilized for chemical transformations.[21]

Boron-based reagents have been known to catalyze several chemical transformations with ease. Hydroboration of carbonyls, epoxides, and unsaturated hydrocarbons using pinacolborane (HBpin), pinacolato-diboron (B$_2$pin$_{2),}$ and 1,8-diaminonaphthalatoborane (HBdan), as well as the utilization of boranes in Suzuki-Miyuara cross coupling reactions, have been well known (**Chart 6**).[22,23] Boranes and borohydrides have also served as efficient tools in selective reduction in process chemistry (**Chart 6**).[24]
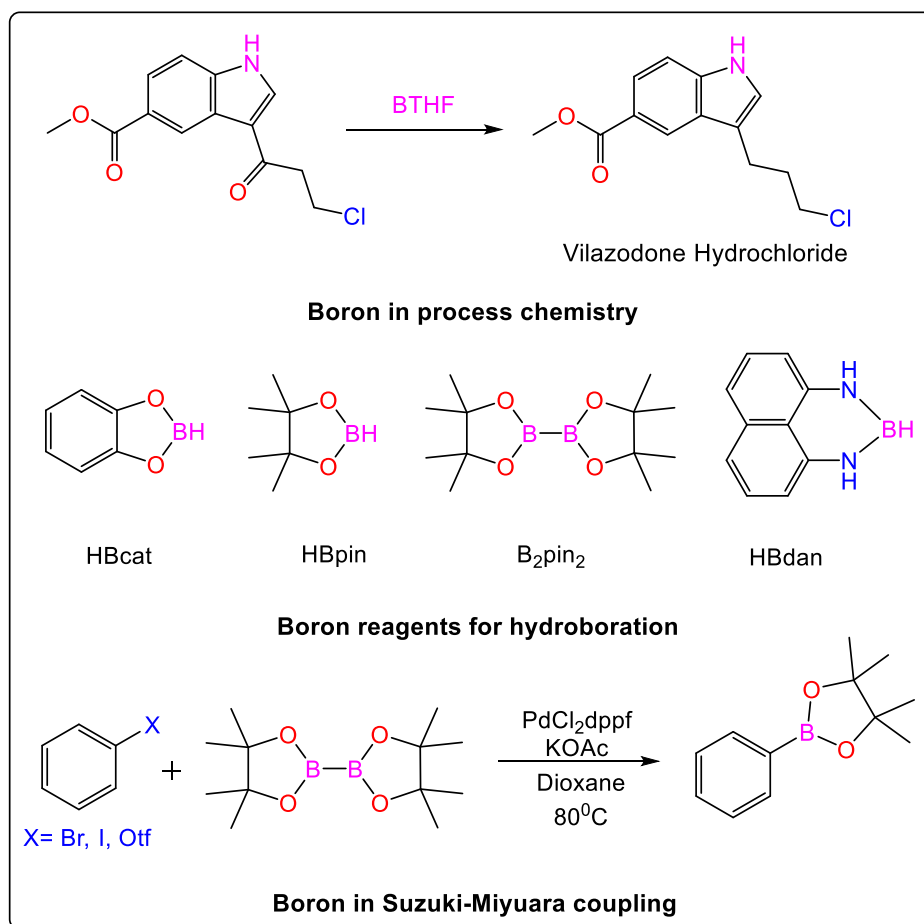
Chart 6: Chemical applications of boron reagents

Through a report in 1981, Evans and co-workers have also demonstrated stereoselective aldol condensations using boron enolates.[25] In 2017, Melen and Lawson highlighted the Lewis acidic nature and subsequent catalytic utility of tris(pentafluorophenyl) borane ($B(C_6F_5)_3$) in borylative cyclizations, carboration, (**Chart 7**), hydroboration and borylation, etc.[26]
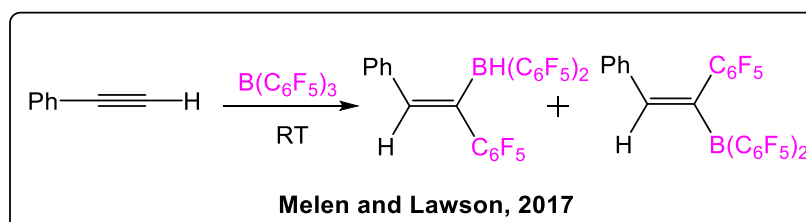
Chart 7: $B(C_6F_5)_3$ mediated carboration

In addition to neutral boron species, several reports mention the synthesis and utility of cationic and anionic boron species. Boryl anion was first reported by Auten and Kraus in 1952.[27]. Subsequently, several reports on boryl anions have come to the

forefront. In 2005, Sadighi and co-workers successfully established a borylcopper complex possessing an NHC (**Chart 8**).[28] Subsequently, Nozaki and co-workers brought to the forefront a major review in 2008, highlighting boryllithium species and their reactivities with a wide variety of electrophiles.[27] In 2008 and 2010, the Braunschweig group published two major reports on boryl anions (**Chart 8**) comprising dimetalloborylene complex and carbene-stabilized boryl anion.[29,30] Recent works have also been carried forth by Gilliard and co-workers featuring borafluorene monoanions (**Chart 8**), their luminescent properties, and reactivity in CO_2 activation.[31]
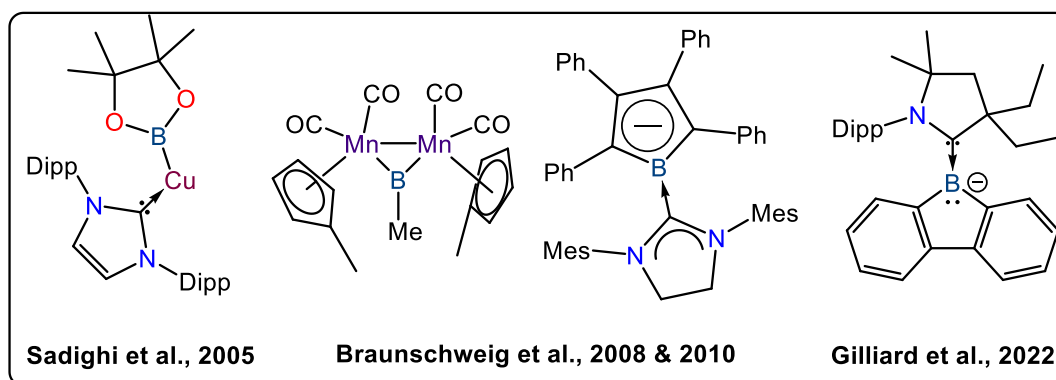
Chart 8: Schematic representation of reported boryl anions

In contrast to neutral boron centers, cationic boron species are known to exhibit enhanced electrophilic character and enhanced reactivity.[21,32] They are more Lewis acidic on account of enhanced electron deficiency, post removal of an extra electron from *2p* orbital, and due to an additional site now being available for coordination.[32] The origin of boron cations dates back to 1955 when Parry and co-workers synthesized a four-coordinate boron cation *viz.* bis(amine) boronium tetrahydroborate.[33] Soon after that, in 1970, Novikov and co-workers also reported several examples of tetra-coordinated borocations, later known as boronium ions.[34]

Borocations are generally classified into three forms of borinium, borenium, and boronium based on the subsequent electron pair coordination with the boron vacant *p*-orbitals from the surrounding moieties (**Chart 9**).[32,35,36]

As seen in the chart below, the donation of an electron pair from a surrounding moiety into the vacant *p*-orbital or π-donation from a covalently bonded substituent in the ligand backbone determines the nature of borocation formed (**Chart 9**).[32]

A boron cation stabilized by two covalent bonds and subsequent two interactions from electron pairs of the nearest neighbor classifies as a boronium ion.[32,35,36] Those borocations that are stabilized by two covalent bonds and one interaction with the electron pair of the nearest neighbor are classified as boreniums. Lastly, borinium ions are highly unstable, having only two covalent bonds coordinated to the boron center.

Literature precedence also suggests that π-donating substituents in the ligand backbone aid in controlling the electronics at the boron center.[32,36] Additionally, the choice of solvent, nature of the coordinating group, and choice of counter-ion play a crucial role in synthesizing and stabilizing these borocations.[35]

Subsequently, the reactivity of the three types of borocations proceeds in the direction opposite to their stability, with borinium ions being the most reactive and boronium ions being slightly less reactive (**Chart 9**).
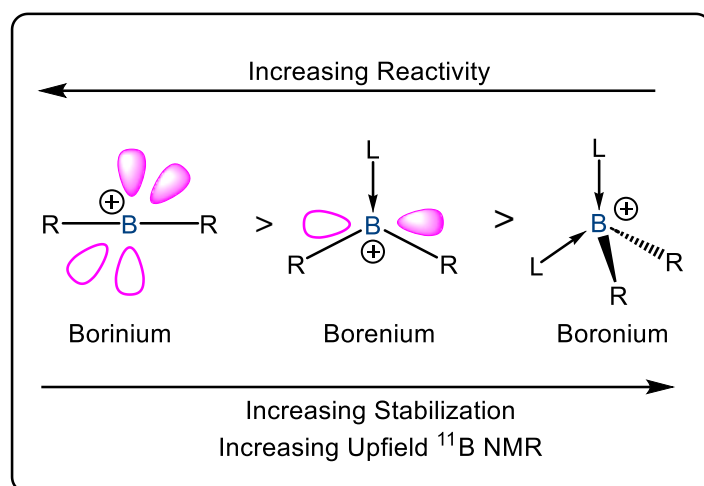
Chart 9: Comparative representation of the three types of borocations

Some of the reported borocations of the three types, synthesized by various groups, can be seen in the chart below (**Chart 10**).[33,34,37–39]
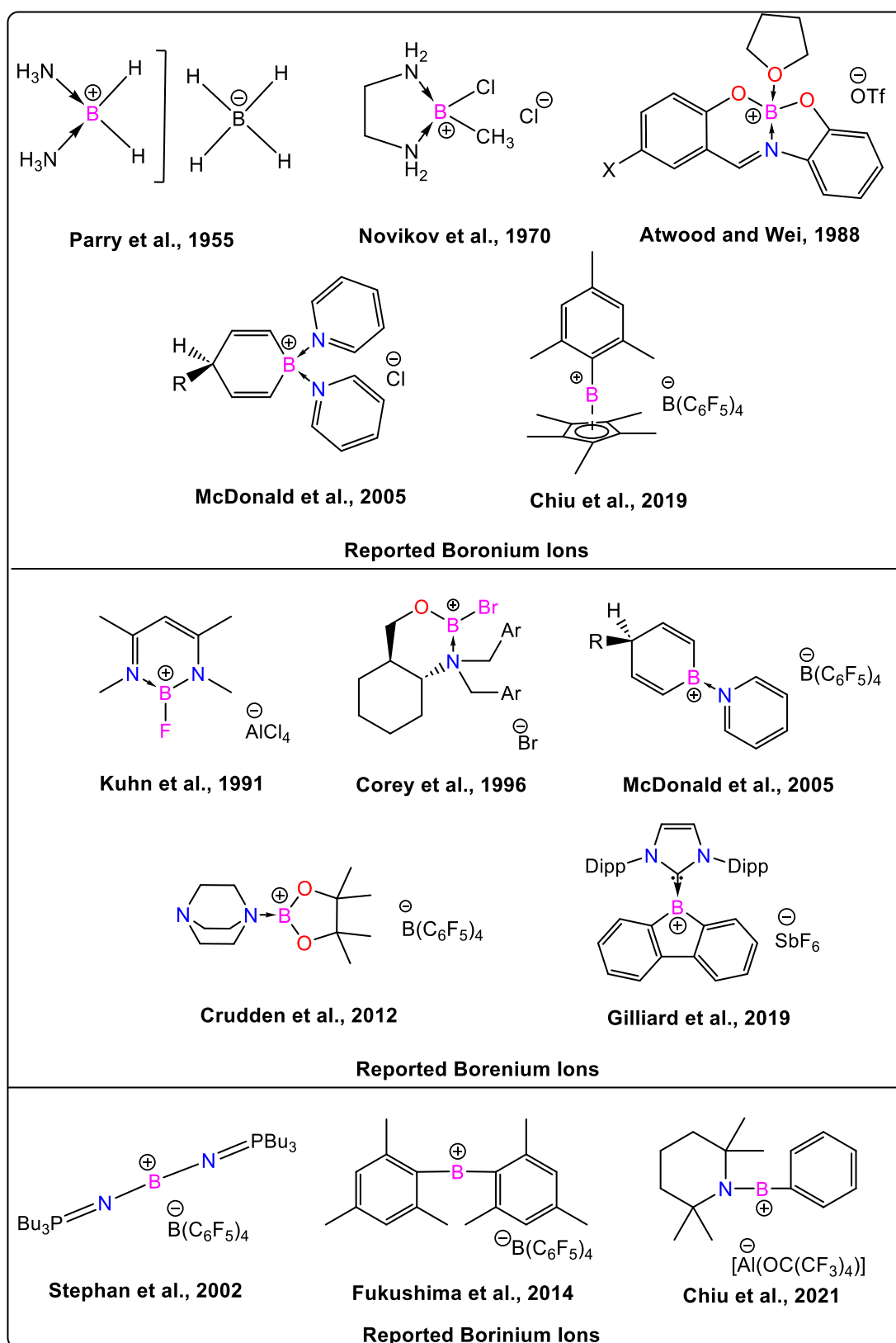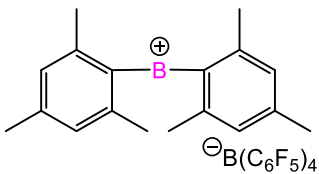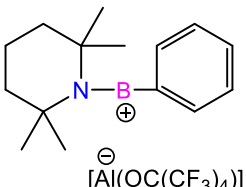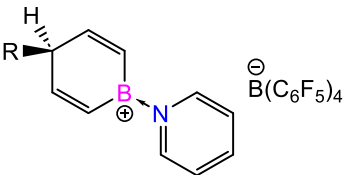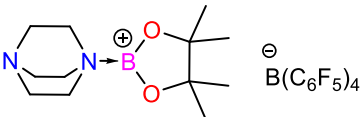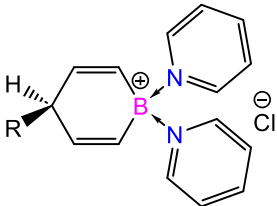
Chart 10: Diagrammatic representation of known borocations

A typical way of analyzing the choice of borocation has been by determining the ^{11}B NMR of the cationic boron center.[35,36] The greater the extent of the cationic charge

density at the boron center and the subsequent lower extent of electronic stabilization typically leads to a downfield shift in the ^{11}B NMR.[32] Thus, borinium ions are highly deshielded, giving an ^{11}B NMR above 30 ppm while corresponding borenium ions fall in the 15-25 ppm bracket. Highly stabilized boronium ions have a typical upfield shift in the ^{11}B NMR with range from 15 to -10 ppm.[32]

The table below (**Table 1**) highlights the reported ^{11}B NMR of some borocations, the ^{31}P NMR (Gutmann Beckett test) & acceptor number of some reported Lewis acidic borocations.[21,40–43]

Borocation	Type	^{11}B NMR ppm ^{31}P NMR {Acceptor No.}
Fukushima et al., 2014	Borinium	93.5 (s), -16.5 (s)
Chiu et al., 2021	Borinium	56 (s) **91.3 {86.6}**
McDonald et al., 2005	Borenium	46 (s), -19 (s)
Crudden et al., 2012	Borenium	25.4 (s), -25 (s)
McDonald et al., 2005	Boronium	0.4 (s)

$\overset{\oplus}{*Cp-B-Mes}$ $\underset{\ominus}{B(C_6F_5)_4}$ Chiu et al., 2019	Boronium	-16.74 (s), -41.69 (s) **97.6 {104.5}**
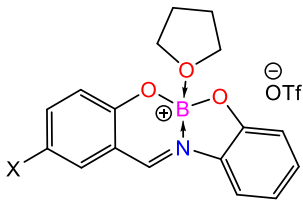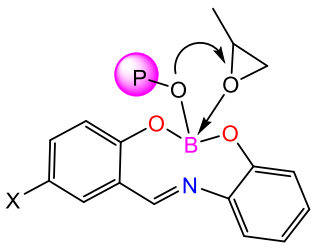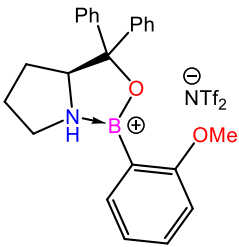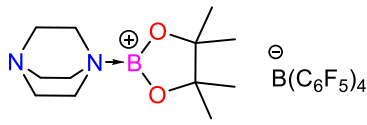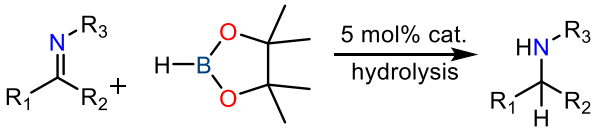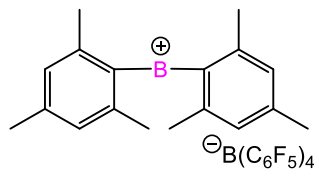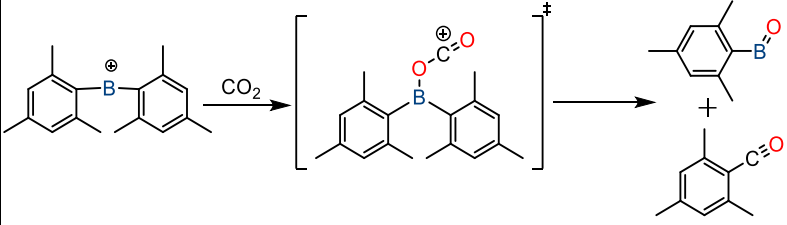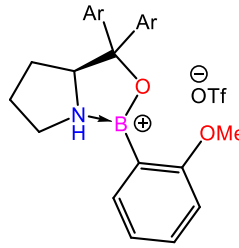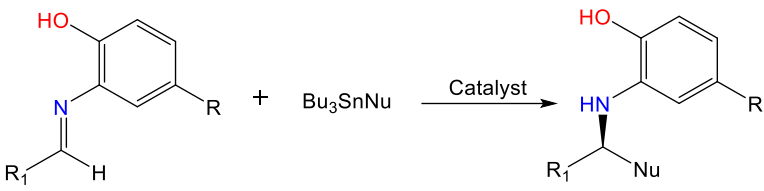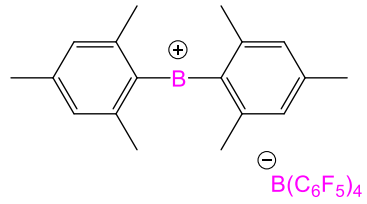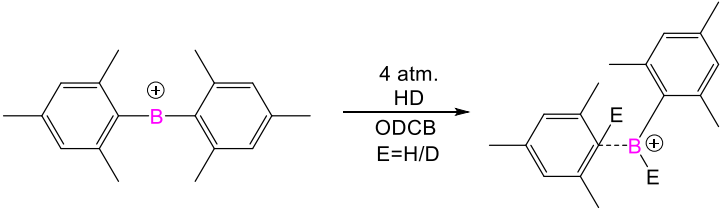
Table 1: NMR and Lewis acidity comparison table of reported borocations

Such NMR shifts thus typically provide an insight into the Lewis acidic character of these borocations, with the expected trend of boriniums being highly Lewis acidic while boroniums being relatively less Lewis acidic. However, ambiguities do arise sometimes, as in the case reported by Chiu and co-workers in 2019, wherein synthesized boronium-like cation showed exceptional electrophilicity.[43]

Nevertheless, all of these borocations have been known to show significant chemical reactivity. In 1998, Atwood and Wei synthesized a boronium cation that could potentially polymerize propylene oxide at room temperature.[44] In 2008, Corey published a report using a borenium ion for the Diels-Alder cycloaddition reaction.[32] Crudden and co-workers 2012 utilized a borenium ion as a catalyst to carry forth the hydroboration of aldimines and ketimines effectively.[42] Deoxygenation of carbon dioxide was conducted by Fukushima in 2014 using a two-coordinate boron cation.[21]

In 2019, a report by Ryu highlighted the utilization of a borenium ion as a catalyst in carrying forth the Strecker reaction utilizing a tin nucleophile.[35] Borinium ions were also tested for hydrogen and triethylsilane activation by Stephan.[45] Around the same time as Stephan's work, the team led by Chiu reported a boronium-like cation that could aid in ketone reduction.[43] The same group brought forth a novel report on a borinium ion that could be used as an efficient catalyst in the cyanosilylation and hydrosilylation of carbonyl substrates.[40]

Seen below is the table highlighting the mentioned catalytic utility of various borocations (**Table 2**)

Borocation	Reaction
Atwood and Wei, 1998	Propylene oxide polymerization
Corey et al., 2008	Diels Alder Cycloaddition
Crudden et al., 2012	Hydroboration of aldimines and ketimines
Fukushima et al., 2014	Deoxygenation of CO_2
Ryu et al., 2019	Strecker reaction
Stephen et al., 2019	H_2 activation
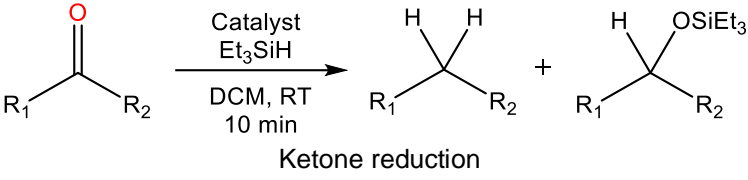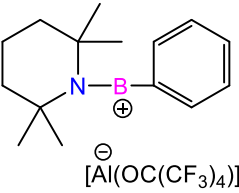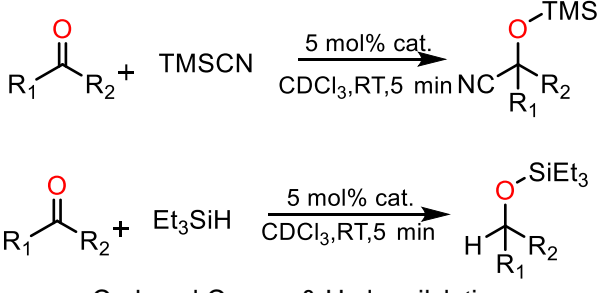
$\overset{\oplus}{*Cp-B-Mes}$ $\overset{\ominus}{B(C_6F_5)_4}$ Chiu et al., 2019	$R_1 \overset{O}{\underset{}{\diagup}} R_2$ $\xrightarrow[\substack{DCM,\ RT \\ 10\ min}]{\substack{Catalyst \\ Et_3SiH}}$ $R_1 \overset{H\ \ H}{\underset{}{\diagup}} R_2$ + $R_1 \overset{H\ \ OSiEt_3}{\underset{}{\diagup}} R_2$ Ketone reduction
(piperidine-boron cation structure) $\overset{\ominus}{[Al(OC(CF_3)_4)]}$ Chiu et al., 2021	$R_1 \overset{O}{\underset{}{\diagup}} R_2$ + TMSCN $\xrightarrow[CDCl_3, RT, 5\ min]{5\ mol\%\ cat.}$ $NC \overset{O-TMS}{\underset{R_1}{\diagup}} R_2$ $R_1 \overset{O}{\underset{}{\diagup}} R_2$ + Et_3SiH $\xrightarrow[CDCl_3, RT, 5\ min]{5\ mol\%\ cat.}$ $H \overset{O-SiEt_3}{\underset{R_1}{\diagup}} R_2$ Carbonyl Cyano- & Hydro-silylation

Table 2: Borocations in catalysis

3. Motivation

The importance of boron in chemical transformations and catalysis has enhanced significantly in the recent decade. As described above, through the extensive literature search, boron serves as a cheaper, greener, and more versatile alternative in carrying forth numerous syntheses and conversions, which would otherwise require extreme reaction conditions, leading to useful products in varying industries. Inspired by these astounding works on neutral and cationic boron complexes and the value-added benefits of boron-based products, we were keen on further exploring boron, its reactivity, and Lewis acidity. Herein, we have synthesized and characterized two cationic boron complexes. By tuning the steric and electronic properties as well as the counter-ion choice around the boron center, we have managed to vary its electrophilicity. The subsequent Lewis acidity has been measured using the Gutmann-Beckett method. Subsequently, we have attempted to demonstrate the potential application of our synthesized cations in the cyanosilylation of aldehydes.

4. Materials and Methods

4.1 General Considerations:

Unless stated otherwise, all reactions and manipulations were carried out using standard Schlenk line techniques under an argon/nitrogen atmosphere and in an argon-filled MBRAUN MB 150-G1 glovebox. All the glassware was dried at 130°C overnight, cooled to ambient temperature prior to their utilization, and purged with nitrogen/argon gas. The sensitive solid samples were handled in the argon-filled glovebox with oxygen and water levels being maintained < 0.5 ppm.

All solvents were distilled and dried under an inert atmosphere using an MBRAUN MB SPS-800 prior to use and stored in Schlenk flasks. The distillation of toluene, THF, and *n*-hexane was carried out using the standard literature protocol involving sodium metal and benzophenone, forming the ketyl radical,[46] that is responsible for turning the solution color to blue and is an indicator that the solvent under distillation is sufficiently dried. 2,6-Diisopropylaniline was distilled using potassium hydroxide pellets as the drying agent. Triethyl amine was distilled using calcium hydride as the drying agent. Methanol and absolute ethanol were used directly without any distillation.

4.2 Starting Materials:

Reagents for various syntheses were purchased from Sigma Aldrich, TCI, RANKEM, and Alfa Aesar and used directly without further purification.

4.3 Analytical Methods:

4.3.1 Nuclear Magnetic Resonance (NMR) Measurements: NMR samples for air and moisture-sensitive compounds were prepared under an inert atmosphere and maintaining the inert environment. The samples were sealed in dried NMR tubes for measurements. Deuterated solvent $CDCl_3$ was dried over calcium hydride, distilled in an inert atmosphere, and stored in sealed Schlenk flasks. Using an ARX 400 spectrometer (^1H, 400 MHz; ^{13}C, 100.61 MHz) from Bruker, ^1H-NMR and ^{13}C-NMR spectra were recorded. Additionally, using an ARX 400 spectrometer (^{11}B, 128.38 MHz; ^{19}F, 376.5 MHz; ^{31}P, 162 MHz) from Bruker, ^{11}B-NMR, ^{19}F-NMR and ^{31}P-NMR spectra were recorded.

The following abbreviations have been used to notify NMR signal multiplicity: s=singlet, d=doublet, t=triplet, q=quartet, br=broad, sept=septet

4.3.2 Mass Spectrometry: Mass spectra of specific compounds were recorded using AB Sciex, 4800 plus HRMS. Samples for sensitive compounds were prepared freshly in an inert atmosphere in an Eppendorf tube, wrapped with a parafilm cover, and taken for analysis. The mass spectra were recorded as a plot of relative intensity v/s m/z value.

4.3.3 Infrared Spectroscopy: The IR spectra were recorded using ALPHA-II ECO ATR, Bruker. Samples for the sensitive compounds were prepared identically to those for mass spectrometry analysis. Spectra were recorded as a plot of transmittance (%) v/s wavenumber (cm^{-1}).

4.3.4 Crystallographic Data: Crystallographic reflections were collected on a Bruker Smart Apex Duo diffractometer at 150 K using Mo Kα radiation (λ=0.71073 Å) for structures of complexes **C2** and **C4**. The structures were solved by direct method and refined by full-matrix least square methods against F2 (SHELXL-2014/6).

4.4 Synthesis and characterization:

4.4.1 Synthesis of Ligands

a) Synthesis of *N,N'*-dimesitylethanediimine (1)[47]

2,4,6-trimethyl aniline (Mes-aniline) (33.7 mL, 240 mmol, 2 equiv.) was suspended in absolute ethanol (50 mL) in a 250 mL round bottom flask. Aqueous glyoxal solution (40 wt.%, 5.51 mL, 120 mmol, 1 equiv.) was added to this solution, and the mixture was allowed to stir at room temperature overnight. Subsequently, a bright yellow precipitate was formed, which could be collected by vacuum filtration. Upon drying, a bright yellow solid was obtained. Yield= 27.1 g (77.4%)

Compound **1:** **^{1}H NMR (400 MHz, CDCl$_3$)** δ 8.10 (s, 2H), 6.91 (s, 4H), 2.30 (s, 6H), 2.16 (s, 12H) ppm **^{13}C NMR (100 MHz, CDCl$_3$)** δ 163.64, 147.39, 134.41, 128.82, 126.66, 20.81, 18.34 ppm **ESI-MS (m/z)**: Calculated for $C_{20}H_{24}N_2$ for [M+H]$^{+}$ 293.2012; Observed: 293.1987
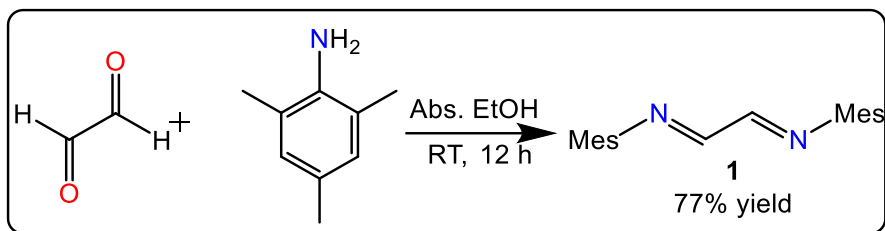
Scheme 1: Schematic representation of the synthesis of N,N'-dimesitylethanediimine (**1**)

b) Synthesis of *N,N'*-dimesitylethanediamine (L1)[47]

In a 250 mL round bottom flask, compound **1** (10 g, 34.2 mmol, 1 equiv.) was weighed and dissolved in a methanol-THF mixture (40:60). The mixture was cooled to 0°C in an ice bath, and then sodium borohydride ($NaBH_4$) (13 g, 342 mmol, 10 equiv.) was added in small batches at intervals of 10 min. The reaction mixture was then stirred for 12 h, allowing it to attain room temperature. Over time, the evolution of hydrogen ceased, and the solution became colorless. The colorless solution was subsequently dried on a rota-evaporator. A saturated ammonium chloride solution was added to the dried residue, followed by the organic phase extraction in dichloromethane. The organic layers were dried over sodium sulfate (Na_2SO_4), and the collected filtrate was concentrated in vacuum. A pale yellow oil was obtained, which, when kept at -35°C for three days, solidified to give a pale yellow solid. Yield= 9.83 g (98.3%)

Ligand **L1:** **^{1}H NMR (400 MHz, CDCl$_3$)** δ 6.85 (s, 4H), 3.18 (s, 4H), 2.31 (s, 12H), 2.26 (s, 6H) ppm **^{13}C NMR (100 MHz, CDCl$_3$)** δ 144.29, 131.06, 129.81, 129.48, 49.02, 20.64, 18.52 ppm **ESI-MS (m/z)**: Calculated for $C_{20}H_{28}N_2$ for [M+H]$^+$ 297.2325; Observed: 293.2317
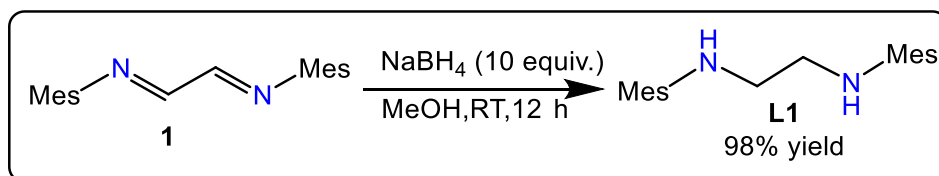
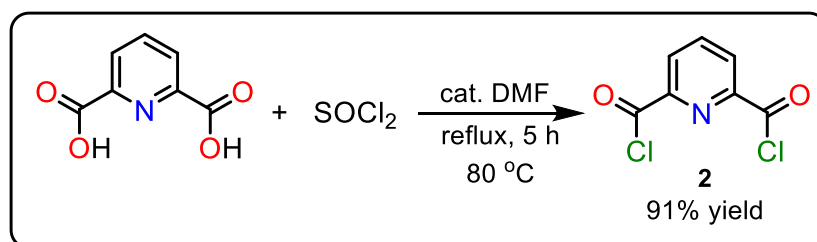**Scheme 2:** Schematic representation of the synthesis of N,N'-dimesitylethanediamine (**L1**)

c) Synthesis of 2,6-pyridine dicarboxylic acid chloride (2)[48]

2,6-pyridine dicarboxylic acid (10 g, 60 mmol, 1 equiv.) was weighed in a 250 mL Schlenk flask and dried under vacuum on the Schlenk line. A catalytic amount of dimethyl formamide (DMF) was added to it, followed by the addition of thionyl chloride (SOCl₂) (in excess). The reaction mixture was then put on reflux for 5 h at 80°C. An argon-filled balloon was attached to the top of the reflux condenser so that inert conditions were maintained. The excess thionyl chloride was removed via distillation at the end of the reflux time. A solid white color compound was obtained. Yield = 9.85 g (98%)

Compound **3:** **¹H NMR (400 MHz, CDCl₃)** δ 8.35 (d, 2H), 8.16 (t, 1H) ppm **¹³C NMR (100 MHz, CDCl₃)** δ 169.23, 150.08, 141.76, 130.23 ppm **ESI-MS (m/z)**: Calculated for $C_7H_3Cl_2N_3O_2$ for [M+H]⁺ 203.9614; Observed: 203.9598

Scheme 3: Schematic representation of the synthesis of 2,6-pyridine dicarboxylic acid chloride (**2**)

d) Synthesis of *N,N'*-Bis (2,6-diisopropylphenyl)-2,6-pyridinedicarboxamide (L2)[49]

To a 250 mL Schlenk flask containing Compound **2** (5 g, 24.5 mmol, 1 equiv.) and 60 mL distilled THF, distilled 2,6-diisopropyl aniline (Dipp-aniline) (9.22 mL, 49 mmol, 2 equiv.) and dried triethyl amine (NEt₃) (6.95 mL, 50 mmol, 2.05 eqiv.) were added at 0°C. The reaction mixture was then warmed to room temperature and stirred at room temperature for 12 h. The precipitated NEt₃.HCl salt was removed thereafter via filtration, and the filtrate that was obtained was dried under vacuum. Subsequent washing with a small amount of pentane resulted in a creamy white solid. Yield= 11.68 g (98%)

Ligand **L2:** **¹H NMR (400 MHz, CDCl₃)** δ 9.05 (s, 2H), 8.55 (d, 2H), 8.18 (t, 1H), 7.35 (t, 2H), 7.25 (d, 4H), 3.14 (sept, 4H), 1.23 (d, 24H) ppm **¹³C NMR (100 MHz, CDCl₃)** δ 162.95, 150.17, 146.88, 140.07, 132.31, 128.97, 126.25, 124.87, 29.75, 24.88 ppm

ESI-MS (m/z): Calculated for $C_{31}H_{39}N_3O_2$ for [M+H]$^+$ 486.3115; Observed: 486.3122

ν$_{max}$ (ATR-IR)/cm^{-1} (key stretches only): 3386 (N-H), 1748 (C=O).
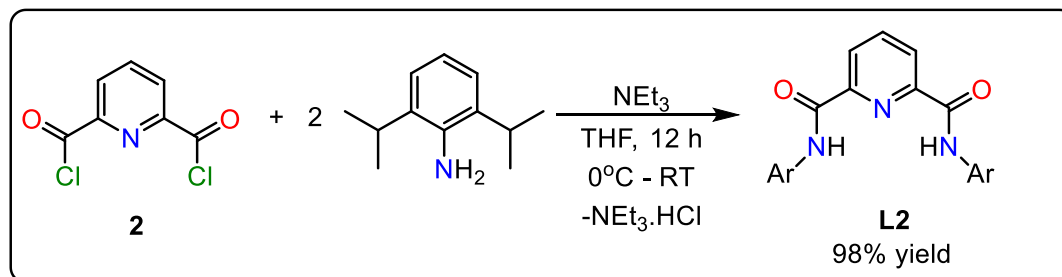
Scheme 4: Schematic representation of the synthesis of N,N'-Bis (2,6-diisopropylphenyl)-2,6-pyridinedicarboxamide (**L2**)

4.4.2 Synthesis of complexes:

a) Synthesis of 2-bromo-1,3-dimesityl-1,3,2-diazaborolidine (C1)[27]

L1 (3 g, 10.12 mmol, 1 equiv.) was weighed in an oven-dried 250 mL Schlenk flask and dissolved in 50 mL DCM. The reaction mixture was cooled to -40°C, and then boron tribromide (BBr$_3$) (1.05 mL, 11.13 mmol, 1.1 equiv.) was added dropwise to it. After the addition, the solution was brought to room temperature and stirred for one hour. The solution was again cooled to -20°C, and N,N-diisopropylethyl amine (iPr$_2$NEt) (4.41mL, 25.3 mmol, 2.5 equiv.) was added dropwise. Thereon, the solution was stirred for 1.5 hours at ambient temperatures. At the end of the reaction time, the solvents were evaporated in vacuum, and toluene was added to the residue. The precipitated salt was removed via filtration. Drying of the collected solvent, followed by subsequent washing with hexane, gave the desired product, an off-white solid, that was scratched and stored in the glovebox. Yield: 3.4 g (87%)

Complex **C1**: **^{1}H NMR (400 MHz, CDCl$_3$)** δ 6.94 (s, 4H), 3.69 (s, 4H), 2.32 (s, 12H), 2.29 (s, 6H) ppm **^{13}C NMR (100 MHz, CDCl$_3$)** δ 138.43, 136.96, 136.20, 129.45, 50.03, 21.43, 18.45 ppm **^{11}B {^{1}H} NMR (128.38 MHz, CDCl$_3$)** δ 26.01 (br) ppm **ESI-MS (m/z):** Calculated for $C_{20}H_{26}BBrN_2$ for [M+H]$^+$ 385.1445; Observed: 385.1429 **ν$_{max}$ (ATR-IR)/cm^{-1}** (key stretches only): 1487.94 (B-N).
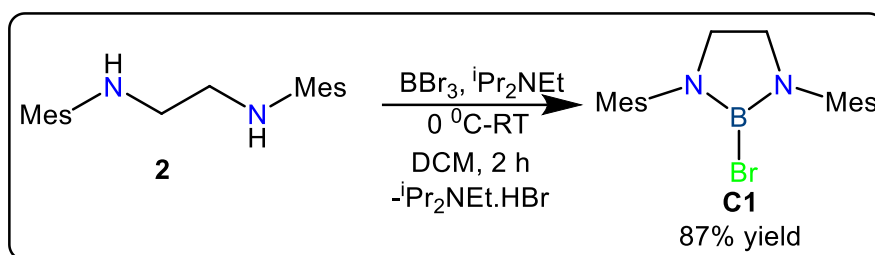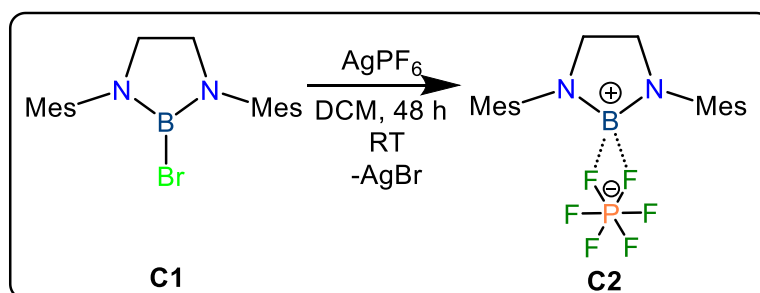
Scheme 5: Schematic representation of the synthesis of 2-bromo-1,3-dimesityl-1,3,2-diazaborolidine (**C1**)

b) Synthesis of 1,3-dimesityl-1,3,2-diazaborolidin-2-ylium hexafluorophosphate (C2)

An oven-dried 100 mL Schlenk flask was taken into the glove box where **C1** (500 mg, 1.3 mmol, 1 equiv.) and silver hexafluorophosphate (AgPF$_6$) (329 mg, 1.3 mmol, 1 equiv.) were weighed. The flask was covered with an aluminium foil and brought to the Schlenk line. Under an inert atmosphere and in the dark, DCM was added to the flask containing the weighed reactants. The flask was sealed thoroughly, and the reaction mixture was stirred for a period of 48h. The accommodated brown precipitate of silver bromide (AgBr) was removed via filtration. The obtained clear solution was reduced till about 4 mL of DCM was left in the flask. To this 2-3 mL of pentane was added, and the flask was then packed and stored at -30°C for 3 days. Colourless needle-shaped crystals were obtained, which were suitable for SCXRD.

Complex **C2: ^{1}H NMR (400 MHz, CDCl$_3$)** δ 6.92 (s, 4H), 3.42 (s, 4H), 2.42 (s, 12H), 2.24 (s, 6H) ppm ^{13}**C NMR (100 MHz, CDCl$_3$)** δ 138.12, 136.57, 135.90, 129.14, 49.72, 21.12., 18.14 ppm ^{11}**B {^{1}H} NMR (128.38 MHz, CDCl$_3$)** δ -1.00 (s) ppm ^{19}**F {^{1}H} NMR (376.5 MHz, CDCl$_3$)** δ -57.98 (s), -60.25 (s) ppm ^{31}**P {^{1}H} NMR (162 MHz, CDCl$_3$)** δ 11.71 (s), 5.57 (s) ppm **ESI-MS (*m/z*):** Calculated for C$_{20}$H$_{26}$BN$_2$$^+$ [M+2H]$^+$ 307.2330; Observed: 307.2170 **v$_{max}$ (ATR-IR)/cm^{-1}:** 1486.82 (B-N)
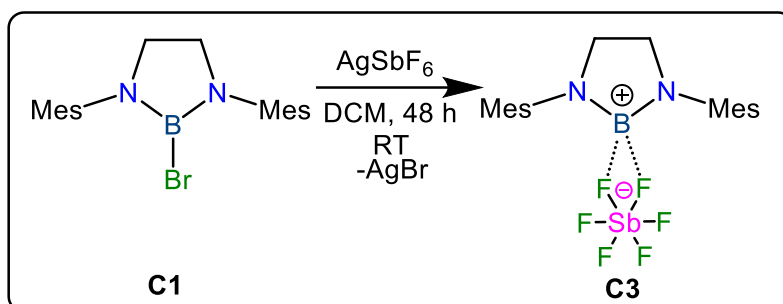
Scheme 6: Schematic representation of the synthesis of 1,3-dimesityl-1,3,2-diazaborolidin-2-ylium hexafluorophosphate (**C2**)

Synthesis of 1,3-dimesityl-1,3,2-diazaborolidin-2-ylium hexafluoroantimonate (C3)

An oven-dried 100 mL Schlenk flask was taken into the glove box where **C1** (500 mg, 1.3 mmol, 1 equiv.) and silver hexafluoroantimonate (AgSbF$_6$) (447 mg, 1.3 mmol, 1 equiv.) were weighed. The flask was covered with an aluminium foil and brought to the Schlenk line. Under an inert atmosphere and in the dark, DCM was added to the flask containing the weighed reactants. The flask was sealed thoroughly, and the reaction mixture was stirred for a period of 48h. The accommodated brown precipitate of silver bromide (AgBr) was removed via filtration. The clear solution was dried completely, and NMR, IR and HRMS analysis was carried out.

Complex **C3**: **¹H NMR (400 MHz, CDCl₃)** δ 6.83 (s, 4H), 3.41 (s, 4H), 2.35 (s, 12H), 2.24 (s, 6H) ppm **¹³C NMR (100 MHz, CDCl₃)** δ 137.79, 136.34, 135.57, 128.82, 49.40, 20.79, 17.81 ppm **¹¹B {¹H} NMR (128.38 MHz, CDCl₃)** δ -0.65 (s) ppm **¹⁹F {¹H} NMR (376.5 MHz, CDCl₃)** δ -131.35 (s), -131.07 (s) ppm **ESI-MS (*m/z*):** Calculated for $C_{20}H_{26}BN_2^+$ [M+2H]$^+$ 307.2330; Observed: 307.2240 **v$_{max}$ (ATR-IR)/cm⁻¹:** 1487.52 (B-N)

Scheme 7: Schematic representation of the synthesis of 1,3-dimesityl-1,3,2-diazaborolidin-2-ylium hexafluoroantimonate (**C3**)

d) Synthesis of *N*,2-bis(2,6-diisopropylphenyl)-3-oxo-2,3-dihydro-1H-8λ⁴-[1,3,2] diazaborolo[1,5-a]pyridine-7-carboxamide (C4)

In a clean oven-dried 250 mL Schlenk flask, **L1** (1 g, 2.06 mmol, 1 equiv.) was weighed, and freshly distilled toluene was added to it. Dimethyl sulfide borane (BH₃.SMe₂) (0.22 mL, 2.3 mmol, 1.1 equiv.) was added dropwise to the solution. The

reaction mixture was then attached to a reflux condenser and subjected to reflux at 115°C for 3 days. At the end of the designated time period, the reaction mixture was cooled to ambient temperatures, and the solvent was dried in vacuum to give a yellow solid. Recrystallization was done in THF to yield colorless crystals which were obtained by storing the solution at -30°C overnight. Yield= 907 mg (89%)

Complex **C4:** **^{1}H NMR (400 MHz, CDCl$_3$)** δ 9.03 (s, 1H), 8.78 (d, 1H), 8.57 (d, 1H), 8.50 (t, 1H), 7.34 (dd, 2H), 7.24 (d, 4H), 3.13 (sept, 2H), 2.98 (sept, 2H), 1.23 (d, 12H), 1.22 (d, 12H) ppm **^{13}C NMR (100 MHz, CDCl$_3$)** δ 160.56, 159.52, 150.18, 149.00, 146.50, 146.22, 142.95, 132.76, 129.84, 129.66, 129.17, 126.00, 125.41, 125.13, 123.85, 29.21, 28.71, 24.57, 23.74 ppm **^{11}B NMR (128.38 MHz, CDCl$_3$)** δ 0.5 (t, BH$_2$) ppm **^{11}B {^{1}H} NMR (128.38 MHz, CDCl$_3$)** 0.04 (s) ppm **ESI-MS (*m/z*):** Calculated for C$_{31}$H$_{40}$BN$_3$O$_2$ [M+H] $^+$ 498.3280; Observed: 498.3292 **v$_{max}$ (ATR-IR)/cm^{-1}** (key stretches only): 3491.19 (N-H uncoordinated), 2785.32 (B-H), 1684.44 (C=O)
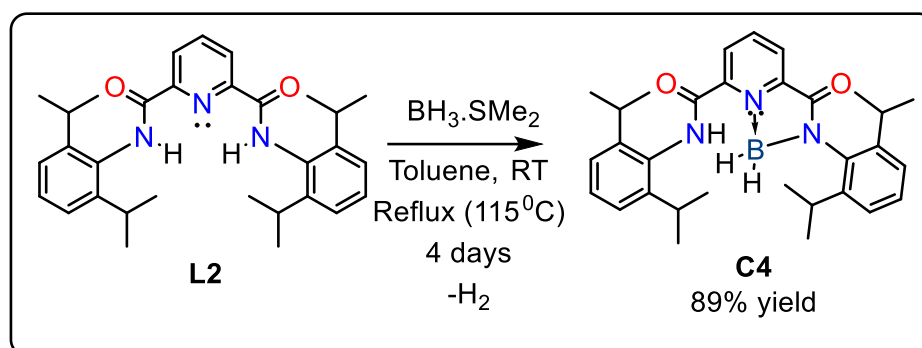
Scheme 8: Schematic representation of synthesis of **C4**

5. Results and Discussion

The advent of our synthesis towards borocations began with the synthesis of our ligand system. The choice of our ligand backbone was N^1,N^2-Bis(2,4,6-trimethylphenyl)-1,2-ethylenediamine, which was first used by Gudat and co-workers in the year 2000 while synthesizing the phosphorus analogs of Arduengo carbene (**Chart 11**).[50] The system was selected due to its ability to stabilize several low-valent main group element complexes, including those of tin, arsenic, and antimony, most of which were later synthesized by Gudat (**Chart 11**).[51,52] In sync with the same, our group brought upon a slight modification to this ligand system and utilized the same for the establishment of a stibenium cation, which was tested as a cyanosilylation catalyst (**Chart 11**).[53]
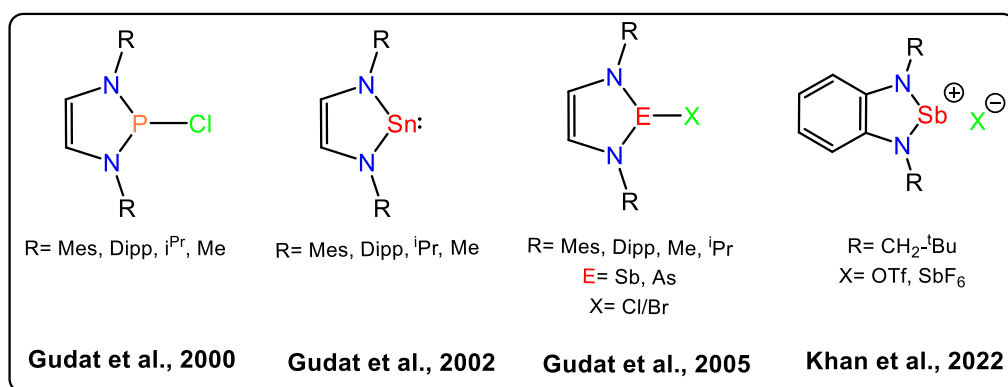

R= Mes, Dipp, iPr, Me

R= Mes, Dipp, iPr, Me

R= Mes, Dipp, Me, iPr
E= Sb, As
X= Cl/Br

R= CH_2-tBu
X= OTf, SbF_6

Gudat et al., 2000   **Gudat et al., 2002**   **Gudat et al., 2005**   **Khan et al., 2022**

Chart 11: Schematic representation of reported complexes using ethylenediamine backbone

However, utilizing a phenyl ring or a double bond in the ligand backbone means that electron delocalization would occur, affecting the electrophilicity at the metal center. Our aim was thus to establish a complex system utilizing the saturated form of the system, which would help enhance the Lewis acidic character at the element center.

Combining this with the literature known versatility of boron, we proceeded to establish a cationic boron complex, characterize it, and understand its potential reaction utility.

As stated earlier, for synthesizing any borocation, the choice of stabilizing ligand, the solvent choice, and the nature of the counter-ion play a crucial role.[35] Reports suggest that utilization of only bulky counter-ions like $B(C_6F_5)_4^-$, BArF, and $Al(OC(CF_3)_3)_4$ etc., can aid in the stabilization of the established borocation.[35,40] Our boronium-like cations thus stand out as they are stabilized by relatively less bulky counter-ions, *viz.*

hexafluorophosphate and hexafluoroantimonate. In addition, boronium-like cations synthesized using a saturated ethanediamine backbone have been known to a lesser extent.

Hence, we started our venture by the synthesis of N,N'-dimesitylethanediimine and its subsequent reduction to N,N'-dimesitylethanediamine (**L1**) using the protocol available in the literature.[47] The choice of this ligand satisfies the primary goal of stabilizing the complex through bulky substituents, yet at the same time not significantly reducing the electrophilicity at the boron center.

Once established, our immediate aim was to synthesize a haloborane complex, which could then be subjected to a salt metathesis reaction in order to form the borocation. We attempted three different methodologies for the synthesis of the same. However, as seen through the scheme below (**Scheme 9**), the methods of lithiation and that of using triethylamine as the base either resulted in poor yields or subsequent adduct/by-product formation, which were difficult to isolate.
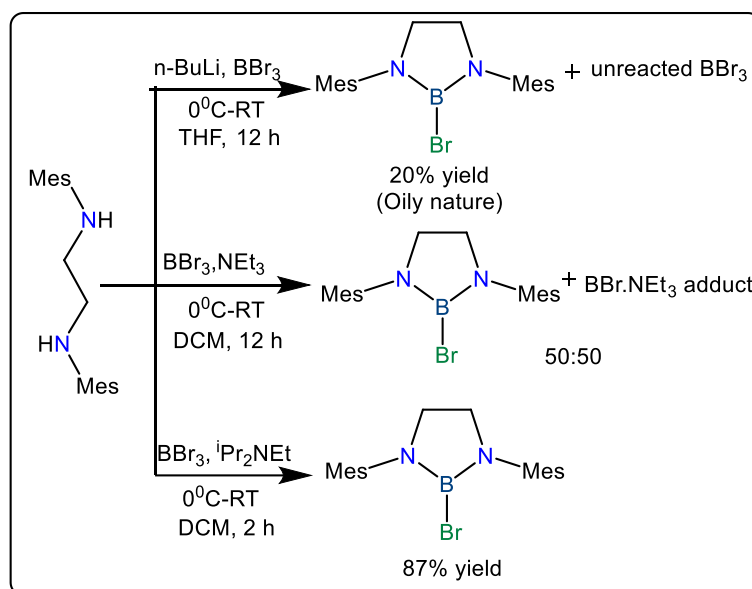
Scheme 9: Schematic representation of three attempted protocols for **C1** synthesis

Hence, by using the protocol established by Nozaki and co-workers[27] as our guiding path, we treated the ligand **L1** with BBr_3 and $^iPr_2NEt$ in DCM to establish 2-bromo-1,3-dimesityl-1,3,2-diazaborolidine (**C1**) as our precursor to the borocation. The pure product was obtained with a good yield of 87%, and its characterization was carried forth using NMR, IR, and Mass Spectrometry. The obtained data matches with what is known in the literature.[27]

For the synthesis of borocation **C2**, we weighed **C1** and $AgPF_6$ in an oven-dried Schlenk flask in the glove box where inert conditions prevailed. Covered with an aluminium foil, the flask was brought to the Schlenk line, DCM was added in inert conditions and the solution was stirred for 48 hours. After work-up, a dull red-colored solution was obtained, to which pentane was added. The flask was then stored at -30°C for 4 days, and colorless needle-shaped crystals formed. Primary characterization of the crystal was carried out using SCXRD, which resulted in obtaining the structure below (**Figure 1)**.
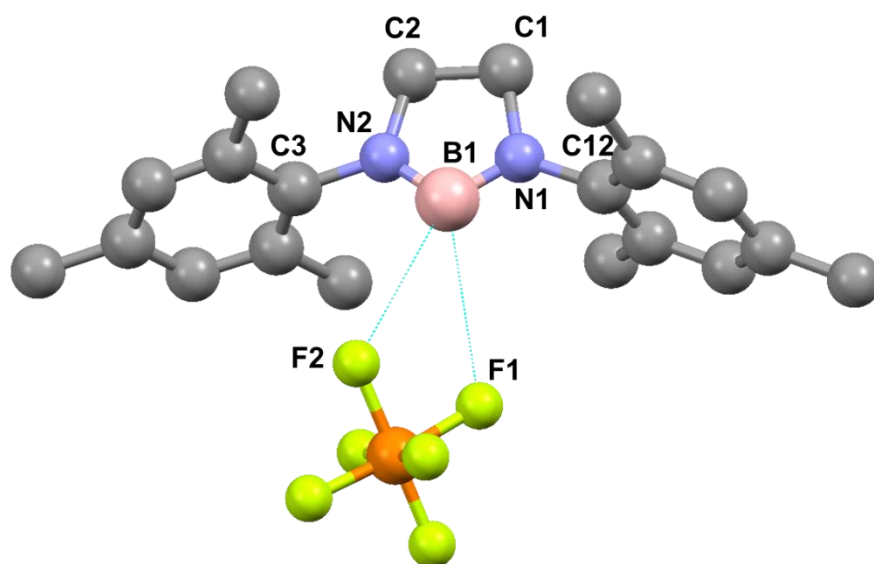

Figure 1: Molecular structure of borocation **C2.** The anisotropic displacement parameters are depicted at the 50% probability level. Hydrogen atoms and solvent are omitted for clarity. Selected bond distances (Å) and bond angles (°): N1-B1 1.298 (4), N2-B1 1.287 (3), N1-C3 1.475 (6), N2-C12 1.432 (3), N1-C1 1.524 (8), N2-C2 1.497 (5), C1-C2 1.520 (2), B1-F1 3.245 (3), B1-F2 3.307 (4) and N2-B1-N1 110.30 (7), C3-N2-B1 125.61 (4), C12-N1-B1 126.79 (8), C2-N2-B1 114.27 (3), C1-N1-B1 11.17 (4).

Subsequently, we carried forth the ^{1}H, ^{13}C, [11]B, ^{31}P, and ^{19}F spectroscopic analysis of the obtained borocation.

A comparative analysis of the obtained crystal structure suggests that the obtained borocation classifies as a boronium-like cation. NMR analysis also validates our hypothesis that the formed borocation is a boronium-like cation owing to the peak at -1.00 ppm.[35,36,41,43] In 2019, Chiu and co-workers reported a boronium-like cation with $B\{C_6F_5)_4^-$ as a counter ion.[43] The cation was found to have an ^{11}B NMR value at -16.74

ppm for the cationic boron center. Based on the ^{11}B NMR value, we can say that our boron center, much like Chiu's, is being pumped in with electrons, resulting in the shift heading upfield.

Subsequently, our ^{31}P and ^{19}F NMR also support our understanding. Both the NMRs show a significant downfield shift compared to the starting $AgPF_6$. As such it can be said that fluorine is pumping electrons from phosphorus and subsequently pushing these electrons towards boron, to stabilize it. Electron concentration at both is thus experiencing a decline, resulting in them undergoing a downfield shift in the respective NMR analysis. Our ^{19}F NMR value matches those of other reported shifts, including those reported by Lichtenberg and co-workers, using the same counter-ion.[54]

Additionally, our boronium-like cation also displays a relatively high stability, much like Chiu's,[43] when stored under inert conditions and moderate stability lasting upto 24 hours when stored at ambient temperature.

The XRD analysis portrays the N1-B1-N2 bond angle to be measured to be around 110.3° slightly distorting from the tetrahedral nature but in close proximity to reported bond angles like C-B-C angle of 112.9° in the boronium reported by McDonald and co-workers[41] and C-B-N angle of 111.4° by Jutzi, Howes and co-workers.[55] The geometry also matches to the known geometry of tetrahedral to distorted tetrahedral at the boron center in previously reported boronium studies.[41,55]

Figure 2: Unit cell representation of the borocation **C2**

A key highlight of the obtained unit cell (**Figure 2)** is that one unit's boron interacts with the adjacent unit's counter-ion. We hypothesize that the planarity of the amine backbone, including the bulky mesityl groups, prevents the closer approach of the counter-ion, hexafluorophosphate. The B-F bond length, however, falls within the sum of the Van der Waals radii[56], allowing for the interaction of the lone pair on fluorine atoms of the counter with cationic boron-center, validating the boronium-like cation formation hypothesis.

The validation of the B-N single bond is obtained by known B-N bond lengths[37,43] and subsequent B-N IR stretching frequency. The B-N stretching frequency in the **C1** and **C2** complexes are nearly the same, falling in the B-N single bond in-plane stretching vibration zone, resonating that no double bond character exists between the cationic boron and immediate nitrogen atoms. This also rules out the formation of any borinium ion which are known to have a double/ partial-double bond character between the boron center and the adjacent atom.

With the successful establishment of one borocation, we decided to move further and vary the counter-ion.

Counter-ions form the crucial secondary coordination sphere for any complex. In 2023, Ferran and co-workers, through their report, pointed out that by meer variation of the counter-ion, one can vary the selectivity for a given chemical transformation. They highlighted the same for hydroboration of alkynes.[57] Hence we felt that counter-ion variation may affect the Lewis acidity and the borocation's reactivity.

To attain the desired goal, we followed the same protocol for obtaining borocation **C2.** However, silver hexafluorophosphate was replaced with silver hexafluoroantimonate to give **C3**. Our NMR analysis suggested that **C3** might also be a boronium-like cation with ^{11}B NMR at -0.46ppm, slightly downfield with respect to **C2.** Thus, all the points for the analysis of C2 are also valid for **C3**. Our efforts to isolate the molecular structure for **C3** continue positively.

Having established these two borocations, we were interested in testing for their Lewis acidity. Although the coordination of the lone pair on the fluorine with the vacant p-orbital on boron does seem to affect the electron concentration at boron, reports

suggest that boroniums are still sufficiently Lewis acidic in nature, although lesser than boriniums and boreniums.[35,55] The borocation reported by Chiu had a boronium-like electronic structure but significantly high Lewis acidity, which was measured using the Gutmann-Beckett method. [43] Using this as our stepping stone, we decided to test for the Lewis acidity of our established cations using the same protocol.

The Guttmann-Beckett Method aids in determining the relative Lewis acidity of the compound by measuring the changes in the compound's physicochemical properties on binding with a Lewis base, which acts as a probe.[58] The test utilizes the shift in ^{31}P, which is obtained on the binding of triethylphosphine oxide (Et_3PO) with a Lewis acid, to determine the compound's relative Lewis acidic character. Triethylphosphine oxide is the ideal choice for the probe on account of its high solubility in the deuterated solvents. The higher the ^{31}P NMR value relative to Et_3PO, the more Lewis acidic the compound is. Subsequently, the acceptor number is also determined for comparative purposes.

We began the probe by first preparing and recording the ^{31}P NMR of neat Et_3PO in $CDCl_3$, which gave us a peak of 52.40ppm, matching the known literature value.[40,43] For a comparative purpose, we then dissolved $B(C_6F_5)_3$ in the same NMR tube and probed its phosphorus NMR. Analysis of the same gave us a sharp peak at 75.88 ppm. Thereafter, we proceeded with an analysis of the Lewis acidity of our established boronium like cation **C2**. The ^{31}P NMR analysis suggests a major peak at 78.55ppm, indicating that the established cation is quite Lewis acidic. Subsequently, **C3** was also subjected to the Gutmann-Beckett test. **C3** gave a ^{31}P NMR at 78.70 ppm, suggesting that it is slightly more Lewis acidic than **C2**. However, in comparison to the borocation established by Chiu and co-workers in 2019, our borocations are slightly less Lewis acidic in nature.[43]

The high acceptor number determined by the Gutmann-Beckett test suggests that while our borocations have a boronium-like electronic nature, they are quite Lewis acidic, with the ^{31}P shifts nearing that of borenium ions.

The calculated acceptor number of $B(C_6F_5)_3$ and our cation is shown in the table below.

Lewis acid	^{31}P NMR δ (ppm)	^{31}P NMR Δδ (ppm)[a]	Acceptor Number (AN)[b]

B(C$_6$F$_5$)$_3$	75.88	23.48	51.89
[C$_{20}$H$_{26}$BN$_2^+$][PF$_6^-$] (**C2**)	78.55	26.15	57.79
[C$_{20}$H$_{26}$BN$_2^+$][SbF$_6^-$] (**C3**)	78.70	26.3	58.12
[Cp*-B$^+$-Mes][B(C$_6$F$_5$)$_4$]	97.6	47.3	104.5

aEt$_3$PO: ^{31}P δ = 52.40 ppm in CDCl$_3$; **b**AN=2.21 x Δδ

Table 3: Gutmann Beckett acidity determination result

With these Lewis acidic boronium ions in hand, we decided to test for the catalytic application of our established cations. Cyanosilylation of carbonyl substrates has been a well-known reaction for the formation of carbon-carbon bonds. Subsequently, the cyanosilylated products have great biological utility as α-amino acids and β-amino alcohols, which are used further for drug synthesis and in pharmaceuticals.[59] While several reports on cyanosilylation using neutral boranes as catalysts have been reported, those involving cationic boron species are relatively smaller. Utilizing this background in conjunction with the greater synthetic utility of cyanosilylated products, we decided to carry forth cyanosilylation of aldehydes using our cations.

All our reactions were carried out in an NMR tube with CDCl$_3$ as the solvent and dibromomethane (CH$_2$Br$_2$) as the internal standard. We started our investigation by conducting a comparative analysis between our complex **C1** and established borocations **C2** and **C3**. The cyanosilylation of benzaldehyde with trimethylsilyl cyanide (TMSCN) (1.1 equiv.) in the presence of each catalyst was carried forth. The catalyst loading was fixed at 5 mol%, and the reaction was carried out for 30 minutes.

As seen from the table below, **C1** and **C2** yielded 78% and 92% respectively. However, **C3** portrayed an excellent yield of >99%. This matches with the acceptor number calculation in Lewis acidity determination. **C3,** having a greater acceptor number and being more Lewis acidic, carries forth the transformation more readily.

Sr.No.	Catalyst	Mol (%)	Time (mins)	Yield (%)
1.	**C1**	5	30	78
2.	**C2**	5	30	92
3.	**C3**	5	30	>99

Table 4: Comparison of **C1-C3** as catalysts for cyanosilylation

With **C3** being established as our catalyst of choice, we proceeded further with the optimization of our reaction condition.

We began the same process by varying the catalyst loading from 5 mol% to 1 mol%, as seen in the table below. We were delighted to find that quantitative (>99%) conversion of benzaldehyde to the cyanosilylated equivalent was observed, even with 1 mol% of catalyst loading.

Subsequently, we attempted to optimize the duration of our reaction. We began optimizing the same by carrying out reactions with time spans ranging from 5 minutes to 30 minutes. As seen from the optimized conditions, benzaldehyde showed an excellent conversion (>99%) to the desired product when the reaction was carried forth for a duration of 15 minutes.
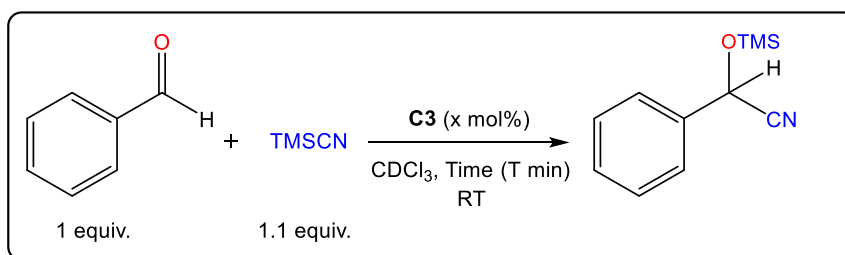
Sr. No.	Catalyst	Mol (%)	Reaction Time	TMSCN (equiv.)	Yield (%)[a]
1.	**C3**	5	30 mins	1.5	>99
		5	30 mins	1.1	98
		3	30 mins	1.1	97
		2	30 mins	1.1	98
		1	30 mins	1.1	>99
2.	**C3**	1	5 mins	1.1	63
		1	10 mins	1.1	84
		1	15 mins	1.1	>99
		1	20 mins	1.1	99
		1	25 mins	1.1	>99
3.	No catalyst	-	30 mins	1.1	Trace amount

Table 5: Optimization of reaction conditions for cyanosilylation reaction of aldehydes with trimethyl silyl cyanide using catalyst C3; **a**= NMR yields using dibromomethane as internal standard

Using our catalyst, we went a step further using these optimized conditions to probe the substrate scope of various aldehydes for cyanosilylation.
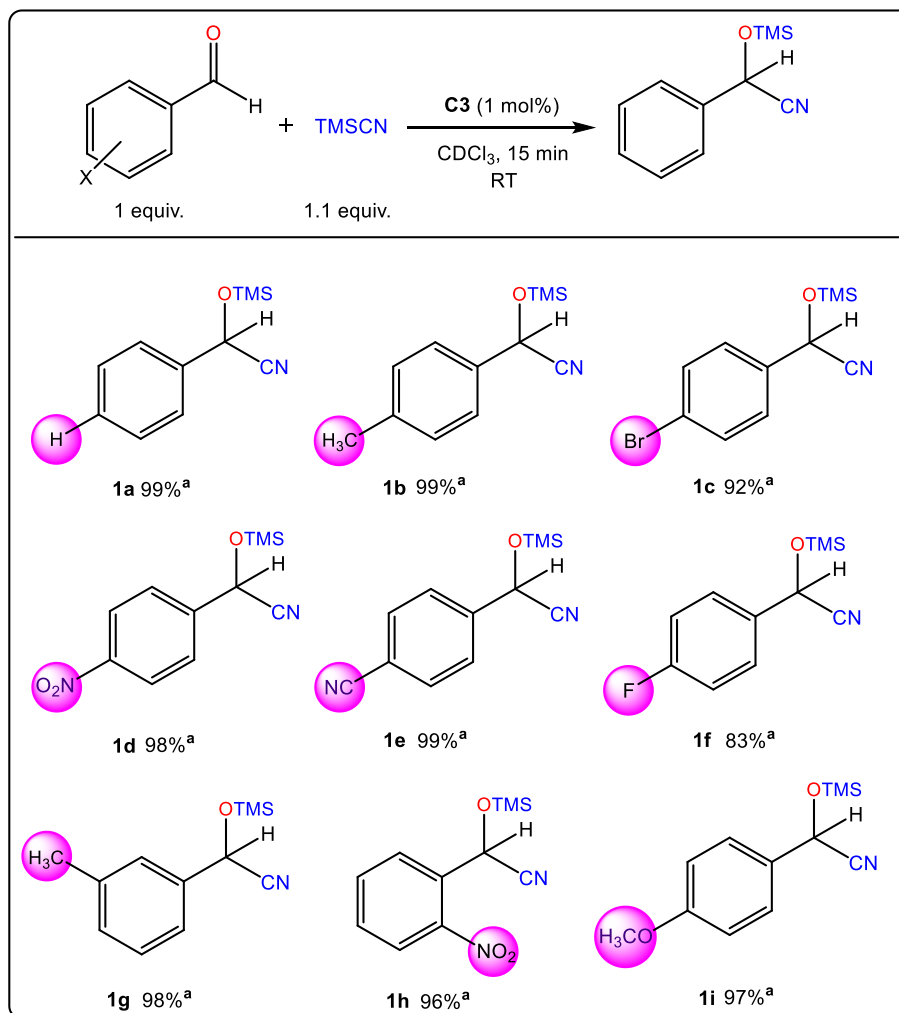
Table 6: Substrate scope for **C3** catalyzed cyanosilylation of various aldehydic substrates; **a**= NMR yields using dibromomethane as internal standard

As the table above shows, a wide variety of aldehydic substrates transformed into their cyanosilylated form in good to excellent yields. Substituted benzaldehydes containing electron-donating groups (-CH$_3$, OMe) and electron-withdrawing groups (-F, -NO$_2$, -CN, -Br) showed tolerance to cyanosilylation catalyzed by **C3.**

6. Conclusion

In summary, two new boronium-like cations *viz.* **C2** and **C3**, with PF_6^- and SbF_6^- as the stabilizing counter-ions, have been synthesized and characterized. Subsequently, the molecular structure of **C2** has been successfully isolated. Both the borocations have been found to exhibit relatively high stability. Despite having a boronium-like electronic nature, both the borocations have been found to showcase a high Lewis acidic character, nearing those of borenium ions. Subsequently, one of these boronium-like cations, *viz*, **C3,** has been established as an efficient catalyst in the cyanosilylation of numerous aldehydic substrates. At present, we are exploring the catalytic activity of both the borocations in hydrofunctionalization reactions. We are also attempting to change the chemical environment about the boron center by carrying forth modifications to the ligand backbone and choice of counter-ion. We believe that such transformations will be able to aid in securing enhanced reactivity as well as selectivity in organic transformations.

7. Miscellaneous

With the successful isolation and characterization of the borocations and testing for their catalytic utility in cyanosilylation, we decided to attempt to synthesize another borocation with a varying ligand backbone. While exploring several ligand options, we came by the NNN pincer system which has been widely used for establishing several transition metal complexes (**Chart 12**). The benefit of using *N,N'*-Bis (2,6-diisopropylphenyl)-2,6-pyridinedicarboxamide as the ligand choice rests in the presence of the *π*-accepting carbonyl groups, which tend to pull electrons and enhance the electrophilicity at the element center. In addition, the electron delocalization across the system helps stabilize the complex.
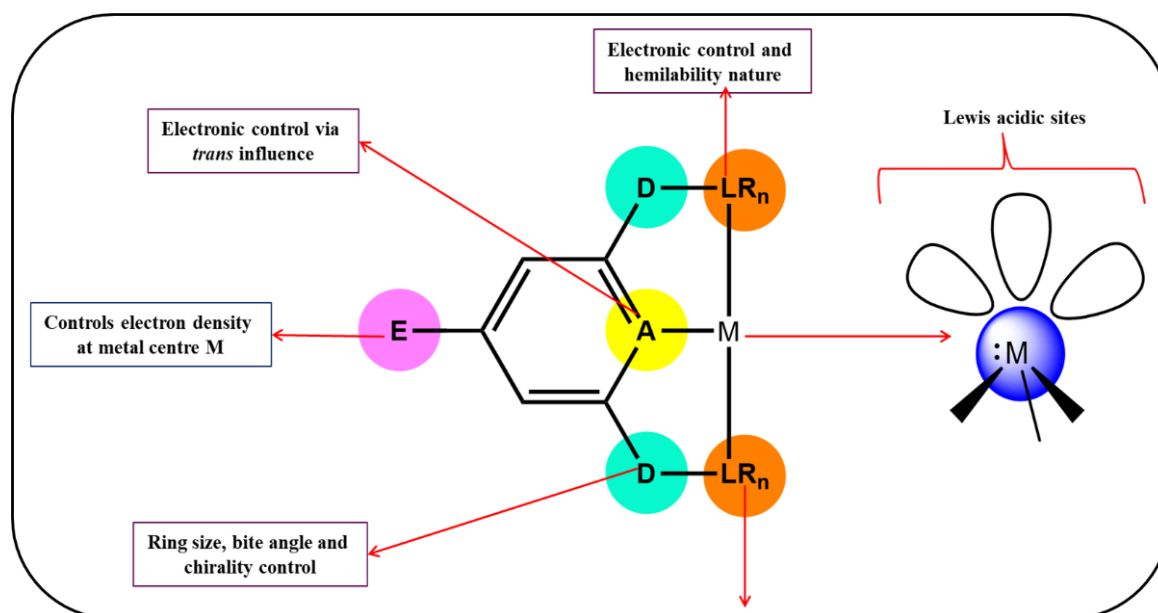
Chart 12: Schematic representation of a pincer-based complex depicting electronic and steric control

We thus moved forward to establish a boron complex with this system. The synthesis of ligand was carried forth using the protocol established by Wasilke and co-workers.[49] For the synthesis of the boron complex, we decided to use $BH_3.SMe_2$ as our reagent to form a boron complex with all three nitrogen atoms coordinated to the boron center. However, as seen through the synthetic protocol above (check Scheme 8, Materials and Methods), we could isolate a boron complex with only two nitrogen coordination (one covalent and the other coordinate) (**C4**).

The complex was characterized using NMR, IR and HRMS. The crystal for the same was obtained by recrystallization of the yellow solid in THF. The molecular structure and some bond parameters have been shown below.
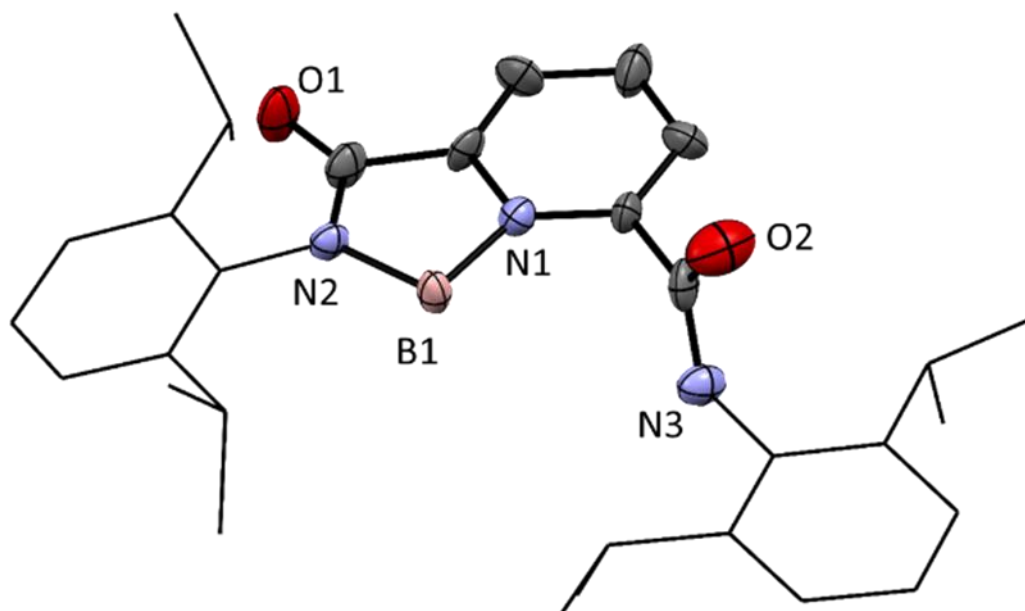
Figure 3: Molecular structure of boron complex **C4.** The anisotropic displacement parameters are depicted at the 50% probability level. Hydrogen atoms and solvent are omitted for clarity. Selected bond distances (Å) and bond angles (°): N1-B1 1.674 (3), N2-B1 1.529 (5), C-O1 1.197 (2), C-O2 1.352 (3) and N2-B1-N1 96.06 (2), N2-C-O1 134.66 (4), N3-C-O2 129.21 (4).

8. References

1   Q. L. Zhou, *Angew. Chem. Int. Ed.*, 2016, **55**, 5352–5353.

2   S. Inoue, R. L. Melen and S. Harder, *Eur. J. Inorg. Chem.*, e20200414

3   C. Weetman, *Chem. - A Eur. J.*, 2021, **27**, 1941–1954.

4   C. Weetman and S. Inoue, *ChemCatChem*, 2018, **10**, 4213–4228.

5   P. P. Power, *Nature*, 2010, **463**, 171–177.

6   E. Rivard, *Dalt. Trans.*, 2014, **43**, 8577–8586.

7   S. Yadav, S. Saha and S. S. Sen, *ChemCatChem*, 2016, **8**, 486–501.

8   G. D. Frey, V. Lavallo, B. Donnadieu, W. W. Schoeller and G. Bertrand, *Science (80-.).*, 2007, 439–441.

9   E. Welz, I. Krummenacher, B. Engels and H. Braunschweig, *Science.*, 2018, **359**, 896–900.

10   C. Weetman, P. Bag, T. Szilvási, C. Jandl and S. Inoue, *Angew. Chem. Int. Ed.*, 2019, **58**, 10961–10965.

11   A. Hofmann, M. A. Légaré, L. Wüst and H. Braunschweig, *Angew. Chem. Int. Ed.*, 2019, **58**, 9776–9781.

12   A. Heilmann, J. Hicks, P. Vasko, J. M. Goicoechea and S. Aldridge, *Angew. Chem. Int. Ed.*, 2020, **59**, 4897–4901.

13   N. Nakata and A. Sekiguchi, *J. Am. Chem. Soc.*, 2006, **128**, 422–423.

14   D. Franz, T. Szilvási, A. Pöthig and S. Inoue, *Chem. - A Eur. J.*, 2019, **25**, 11036–11041.

15   Z. Zhu, X. Wang, Y. Peng, H. Lei, J. C. Fettinger, E. Rivard and P. P. Power, *Angew. Chem. Int. Ed.*, 2009, **48**, 2031–2034.

16   D. W. Welch, G. C., San Juan, R. R., Masuda, J. D., Stephan, *Science*, 2006, **314**, 1124–1126.

17   M. Fan, X. Liang, Q. Li, L. Cui, X. He and X. Zou, *Chinese Chem. Lett.*, 2023, **34**, 107275.

18   T. Agou, J. Kobayashi and T. Kawashima, *Inorg. Chem.*, 2006, **45**, 9137–9144.

19   Q. Yin, S. Kemper, H. F. T. Klare and M. Oestreich, *Chem. - A Eur. J.*, 2016, **22**, 13840–13844.

20   V. Nori, F. Pesciaioli, A. Sinibaldi, G. Giorgianni and A. Carlone, *Catalysts*, 2022, **12**, 1–27.

21   Y. Shoji, N. Tanaka, K. Mikami, M. Uchiyama and T. Fukushima, *Nat. Chem.*, 2014, **6**, 498–503.

22   A. D. Bage, K. Nicholson, T. Langer and S. P. Thomas, *ACS Catal.*, 2020, **10**, 13479–13486.

23   N. Miyaura and A. Suzuki, *J. Chem. Soc. Chem. Commun.*, 1979, 866–867.

24   E. R. Burkhardt and K. Matos, *Chem. Rev.*, 2006, **106**, 2617–2650.

25   T. L. Evans, D. A., Bartroli, J., Shih, *J. Am. Chem. sosciety*, 1981, **103**, 2127–2129.

26   J. R. Lawson and R. L. Melen, *Inorg. Chem.*, 2017, **56**, 8627–8643.

27   Y. Segawa, Y. Suzuki, M. Yamashita and K. Nozaki, *J. Am. Chem. Soc.*, 2008, **130**, 16069–16079.

28   D. S. Laitar, P. Müller and J. P. Sadighi, *J. Am. Chem. Soc.*, 2005, **127**, 17196–17197.

29   H. Braunschweig, M. Burzler, R. D. Dewhurst and K. Radacki, *Angew. Chem. Int. Ed.*, 2008, **47**, 5650–5653.

30   H. Braunschweig, C. W. Chiu, K. Radacki and T. Kupfer, *Angew. Chem. Int. Ed.*, 2010, **49**, 2041–2044.

31   K. E. Wentz, A. Molino, L. A. Freeman, D. A. Dickie, D. J. D. Wilson and R. J. Gilliard, *Inorg. Chem.*, 2022, **61**, 17049–17058.

32   W. E. Piers, S. C. Bourke and K. D. Conroy, *Angew. Chem. Int. Ed.*, 2005, **44**, 5016–5036.

33   P. Kolle and H. Noth, *Chem. Rev.*, 1985, **85**, 399–418.

34   C. Transition, *Russ. Chem. Rev.*, 1970, **39**, 905–922.

35   K. Stefkova, L. Gierlichs, D. Willcox and R. L. Melen, *Borocations in Catalysis*, 2020,1-37.

36   P. Eisenberger and C. M. Crudden, *Dalt. Trans.*, 2017, **46**, 4874–4887.

37   N. Kuhn, A. Kuhn, J. Lewandowski and M. Speis, *Chem. Ber.*, 1991, **124**, 2197–2201.

38   W. Yang, K. E. Krantz, L. A. Freeman, D. A. Dickie, A. Molino, A. Kaur, D. J. D. Wilson and R. J. Gilliard, *Chem. - A Eur. J.*, 2019, **25**, 12512–12516.

39   S. Courtenay, J. Y. Mutus, R. W. Schurko and D. W. Stephan, *Angew. Chem. Int. Ed.*, 2002, **41**, 498–501.

40   P. H. Chen, C. P. Hsu, H. C. Tseng, Y. H. Liu and C. W. Chiu, *Chem. Commun.*, 2021, **57**, 13732–13735.

41   I. Ghesner, W. E. Piers, M. Parvez and R. McDonald, *Chem. Commun.*, 2005, 2480–2482.

42   P. Eisenberger, A. M. Bailey and C. M. Crudden, *J. Am. Chem. Soc.*, 2012, **134**, 17384–17387.

43   H. C. Tseng, C. T. Shen, K. Matsumoto, D. N. Shih, Y. H. Liu, S. M. Peng, S. Yamaguchi, Y. F. Lin and C. W. Chiu, *Organometallics*, 2019, 4516–4521.

44   P. Wei and D. A. Atwood, *Inorg. Chem.*, 1998, **37**, 4934–4938.

45   K. L. Bamford, Z. W. Qu and D. W. Stephan, *J. Am. Chem. Soc.*, 2019, **141**, 6180–6184.

46   R. Inoue, M. Yamaguchi, Y. Murakami, K. Okano and A. Mori, *ACS Omega*, 2018, **3**, 12703–12706.

47   S. Medvedko, M. Ströbele and J. P. Wagner, *Chem. - A Eur. J.*, 2023, **29**, 1–15.

48   N. Kleigrewe, W. Steffen, T. Blömker, G. Kehr, R. Fröhlich, B. Wibbeling, G. Erker, J. C. Wasilke, G. Wu and G. C. Bazan, *J. Am. Chem. Soc.*, 2005, **127**, 13955–13968.

49 J. C. Wasilke, G. Wu, X. Bu, G. Kehr and G. Erker, *Organometallics*, 2005, **24**, 4289–4297.

50 D. Gudat, A. Haghverdi, H. Hupfer and M. Nieger, *Chem. - A Eur. J.*, 2000, **6**, 3414–3425.

51 T. Gans-eichler and D. Gudat, *Angew Chem Int. Ed*, 2002, **41**, 1888–1891.

52 T. Gans-Eichler, D. Gudat and M. Nieger, *Heteroat. Chem.*, 2005, **16**, 327–338.

53 N. Sen, P. Gothe, P. Sarkar, S. Das, S. Tothadi, S. K. Pati and S. Khan, *Chem. Commun.*, 2022, **58**, 10380–10383.

54 T. Dunaj, J. Schwarzmann, J. Ramler, A. Stoy, S. Reith, J. Nitzsche, L. Völlinger, C. von Hänisch and C. Lichtenberg, *Chem. - A Eur. J.*, 29, e2022014012

55 P. Jutzi, B. Krato, M. Hursthouse and A. J. Howes, *Chem. Ber.*, 1987, **120**, 1091–1098.

56 M. Mantina, A. C. Chamberlin, R. Valero, C. J. Cramer and D. G. Truhlar, *J. Phys. Chem. A*, 2009, **113**, 5806–5812.

57 A. Martínez-Bascuñana, J. L. Núñez-Rico, L. Carreras and A. Vidal-Ferran, *ACS Catal.*, 2023, **13**, 10447–10456.

58 P. Erdmann and L. Greb, *Angew. Chem. Int. Ed.*, 61, e202114550.

59 S. Pahar, G. Kundu and S. S. Sen, *ACS Omega*, 2020, **5**, 25477–25484.

9. Appendix
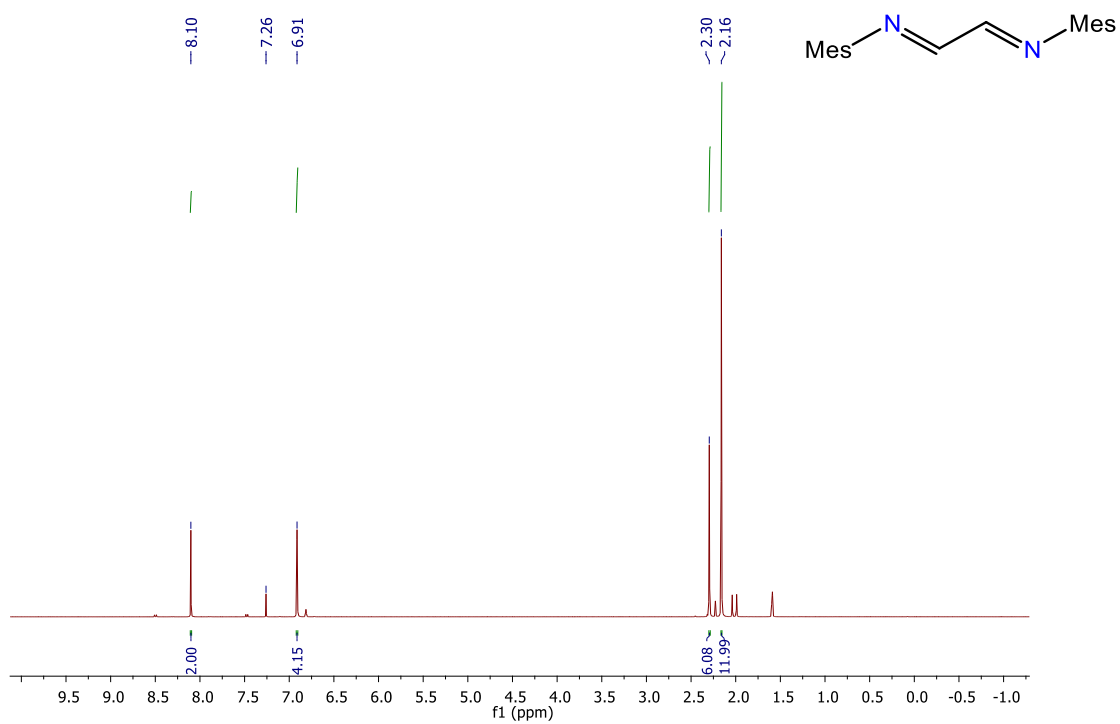
^{1}H NMR spectra of **1**

^{1}H NMR spectra of **L1**

8.36
8.34
8.18
8.16
8.14
7.26

^{1}H NMR spectra of **2**

9.05
8.56
8.54
8.20
8.18
8.16
7.37
7.35
7.33
7.26
7.25
7.23
3.18
3.16
3.14
3.13
3.11
1.23
1.22

1.94
2.00
1.00
2.07
4.02
4.09
24.09
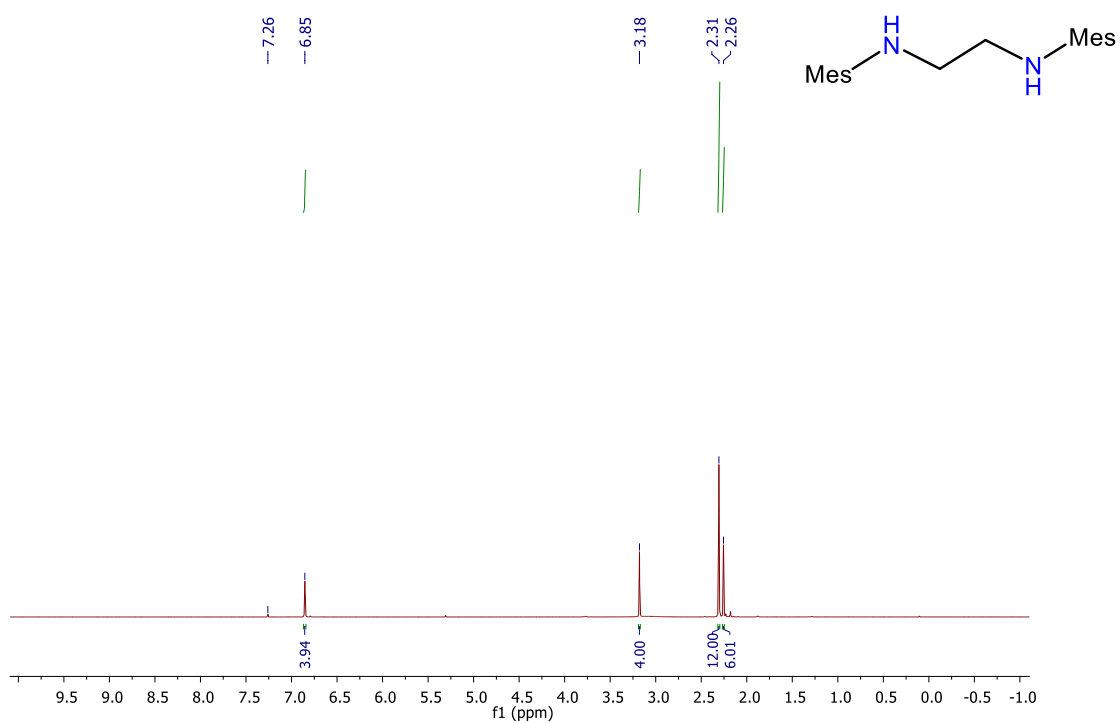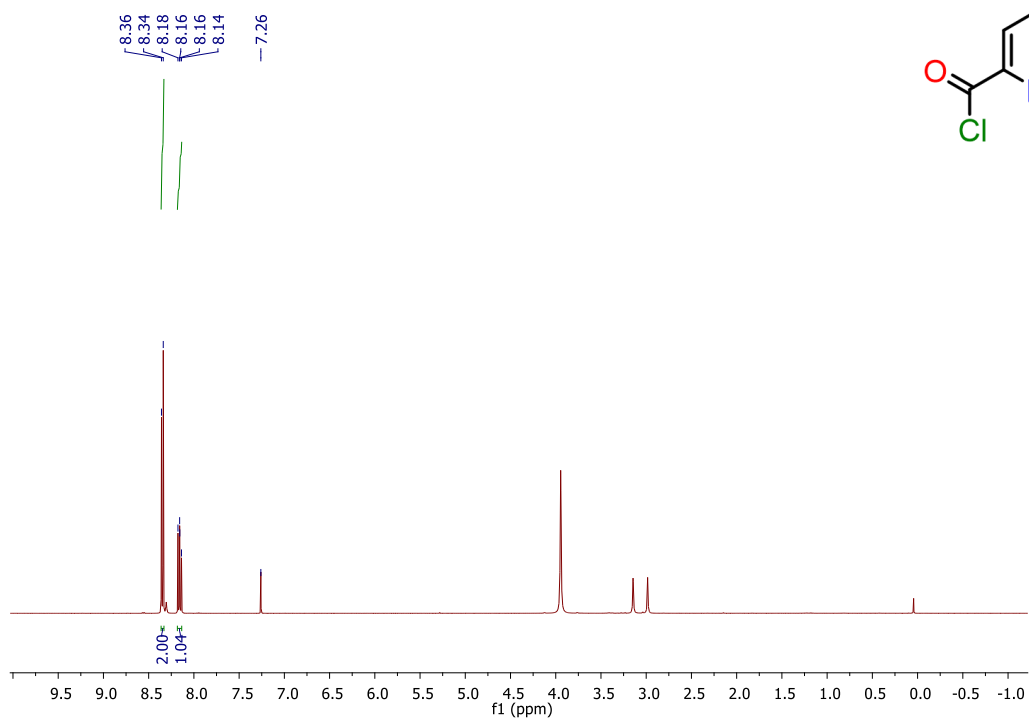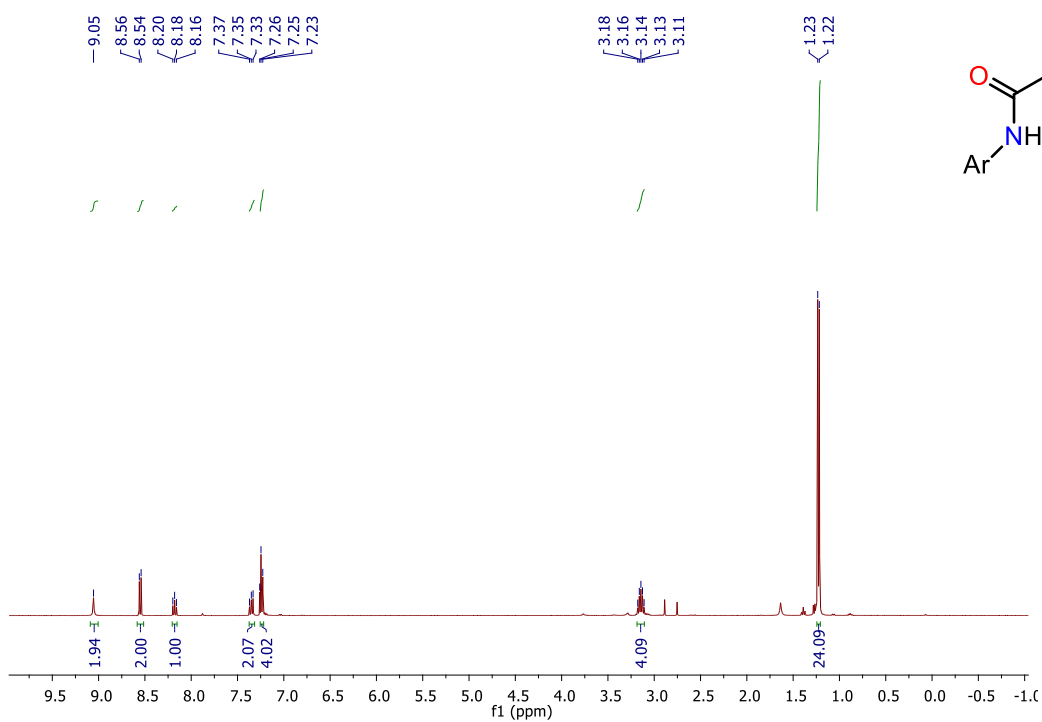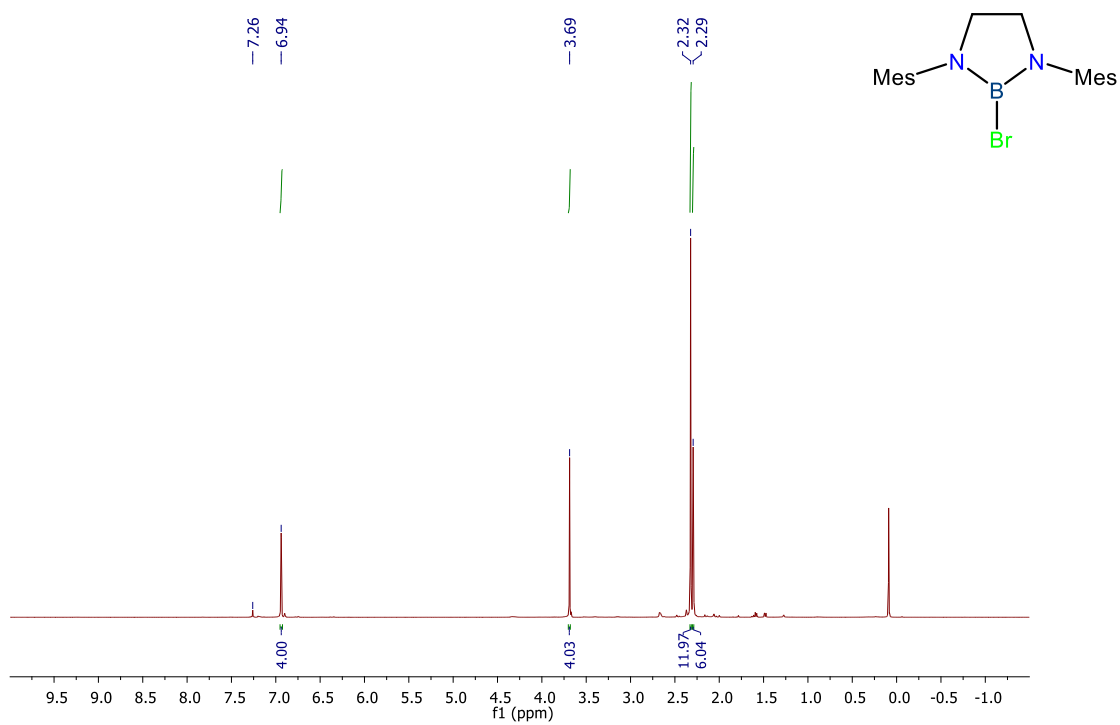
^{1}H NMR spectra of **L2**

^{1}H NMR spectra of **C1**
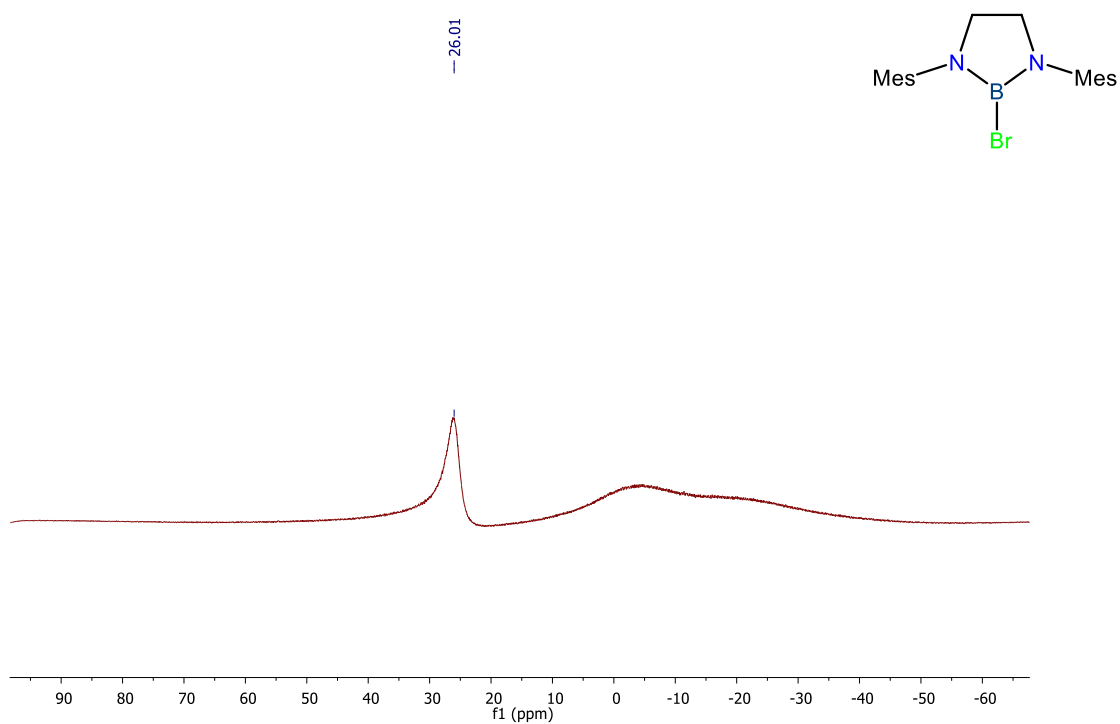
^{11}B NMR spectra of **C1**
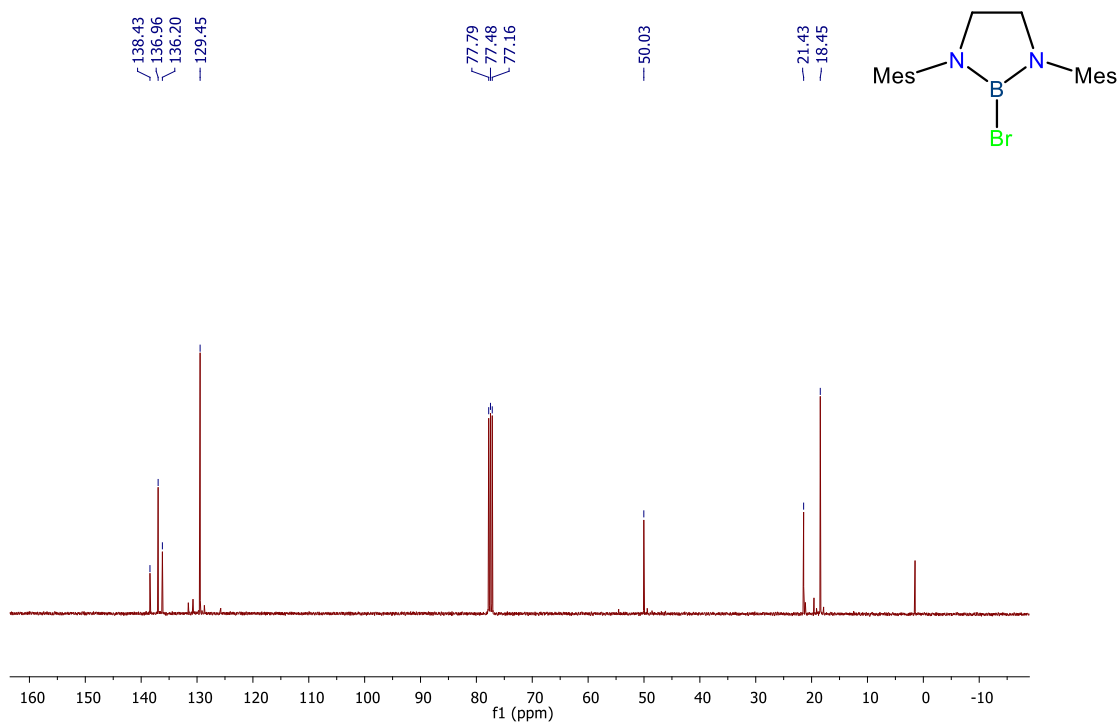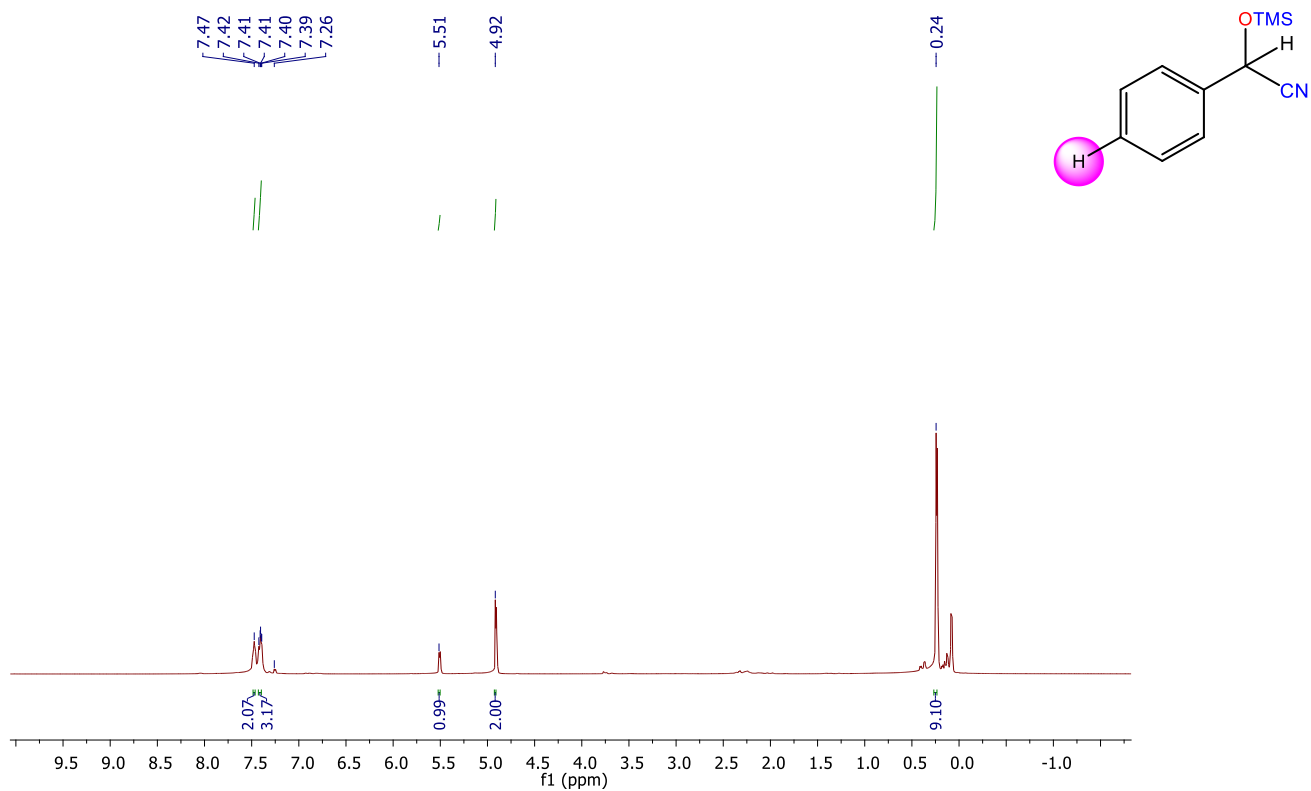
^{13}C NMR spectra of **C1**
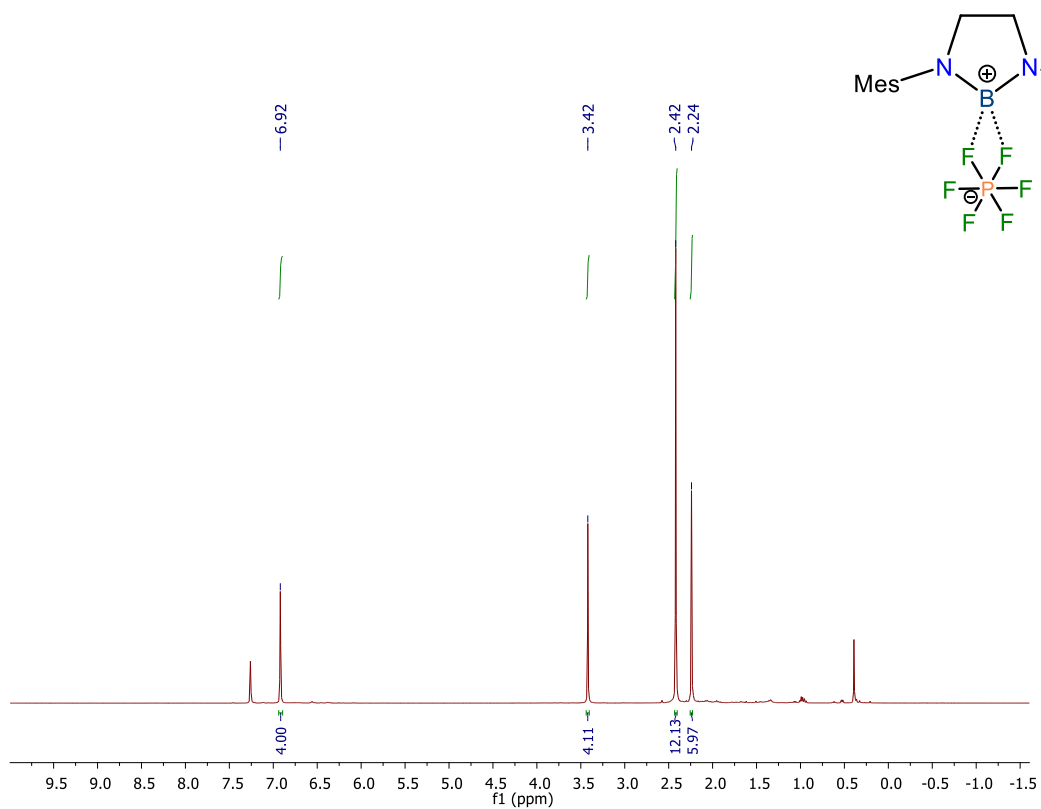
^{1}H NMR spectra of **C2**

−−1.00
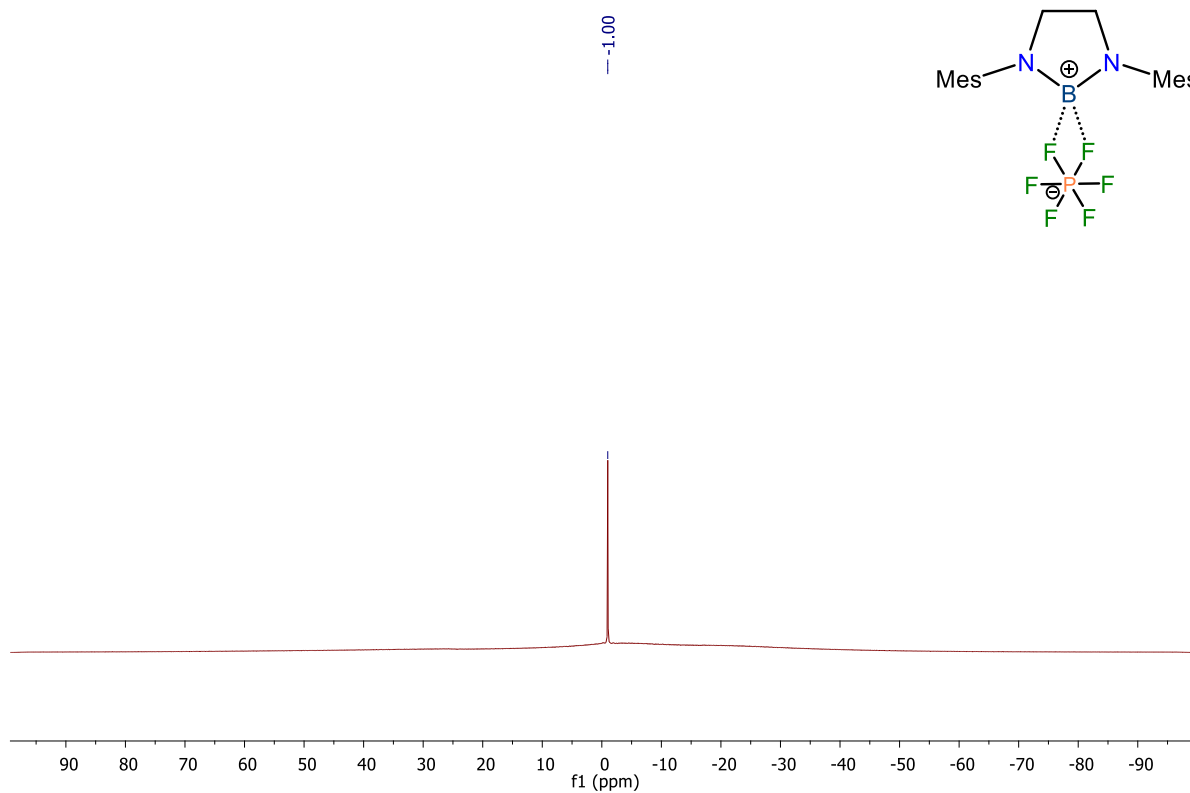
¹¹B NMR spectra of **C2**

⟨ −57.98
   −60.25
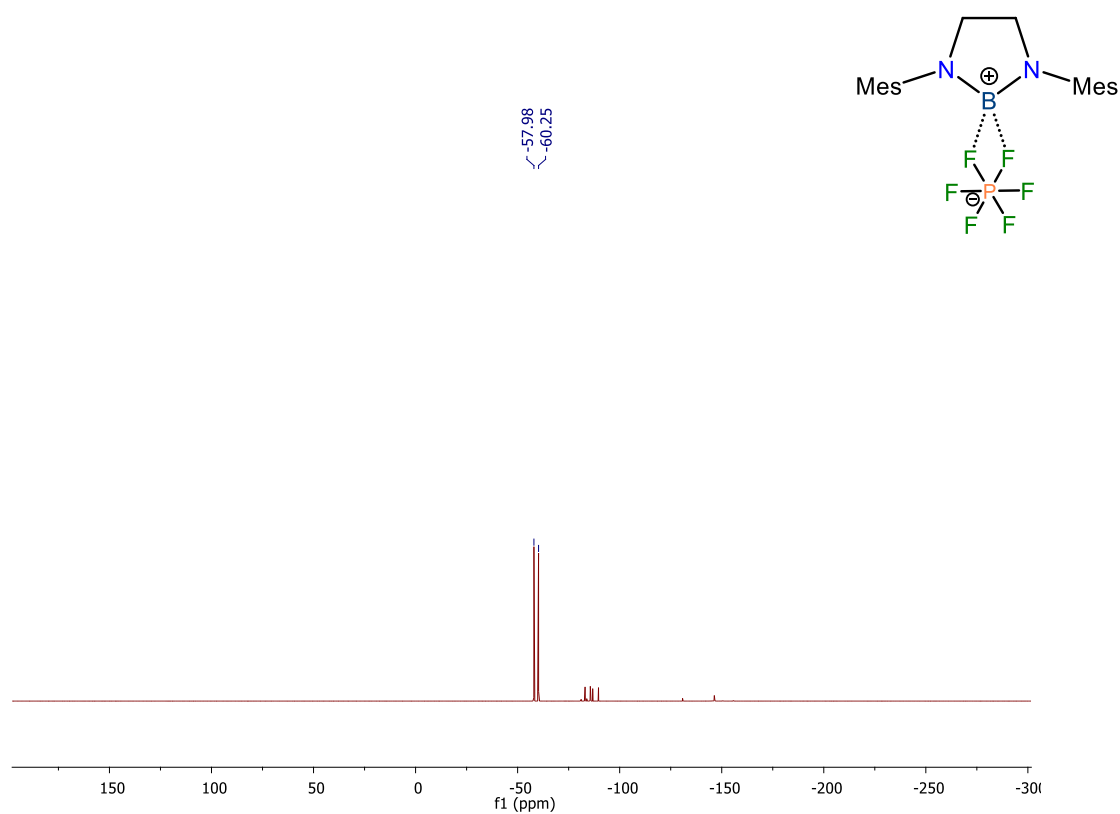
¹⁹F NMR spectra of **C2**
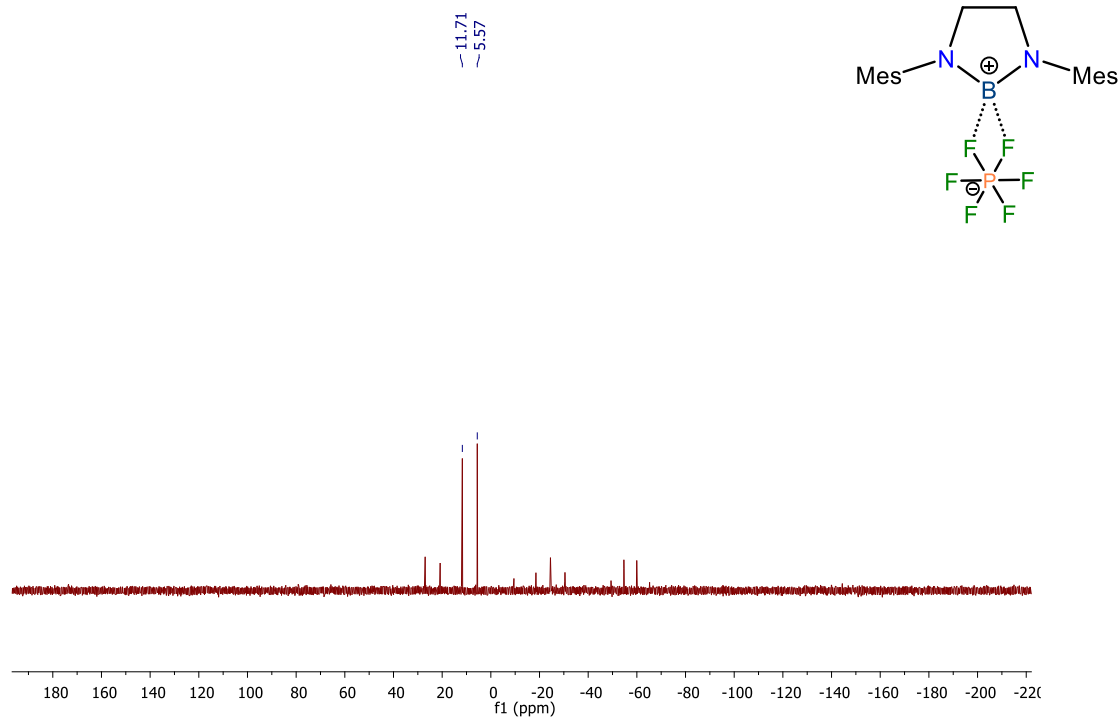
^{31}P NMR spectra of **C2**
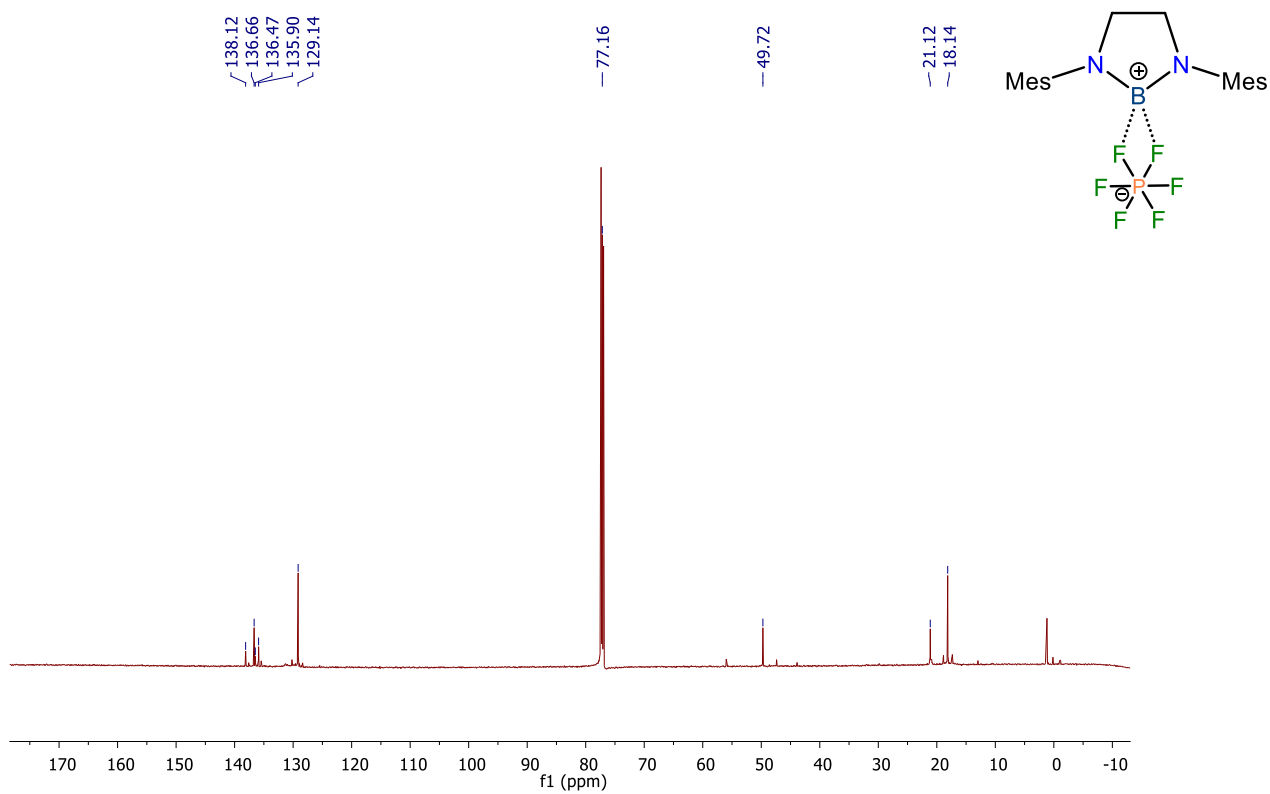
^{13}C NMR spectra of **C2**
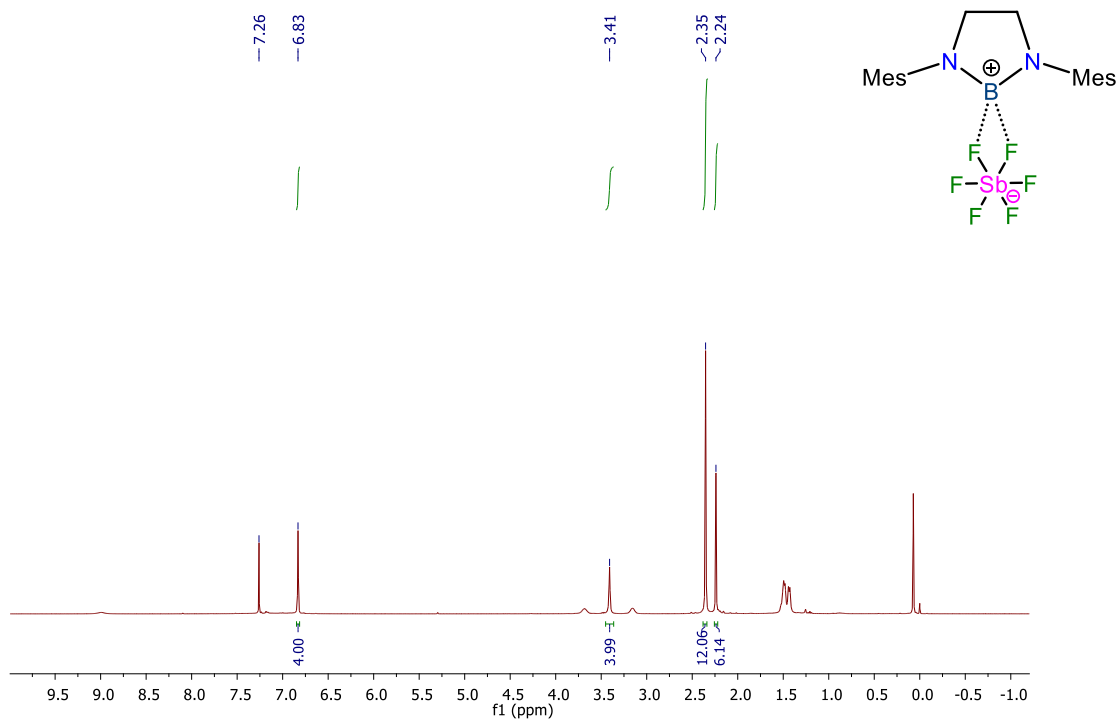
^{1}H NMR spectra of **C3**

^{11}B NMR spectra of **C3**

-131.07
-131.35

^{19}F NMR spectra of **C3**

137.79
136.34
135.57
128.82

77.16
76.84
76.53

49.40

20.79
17.81
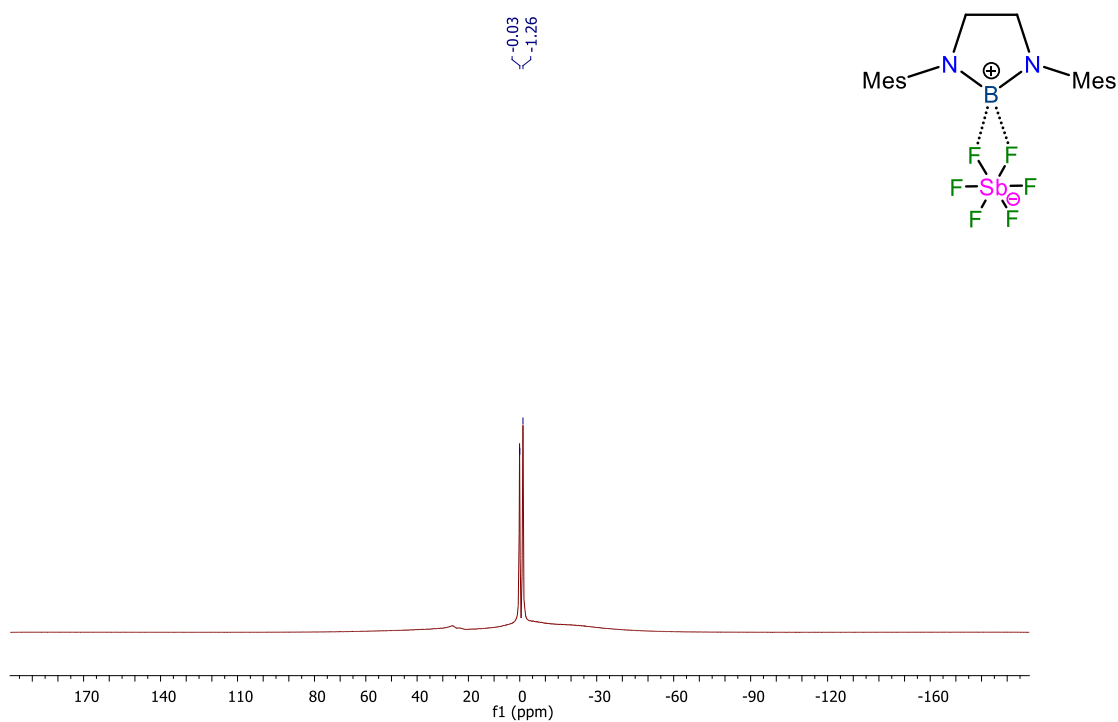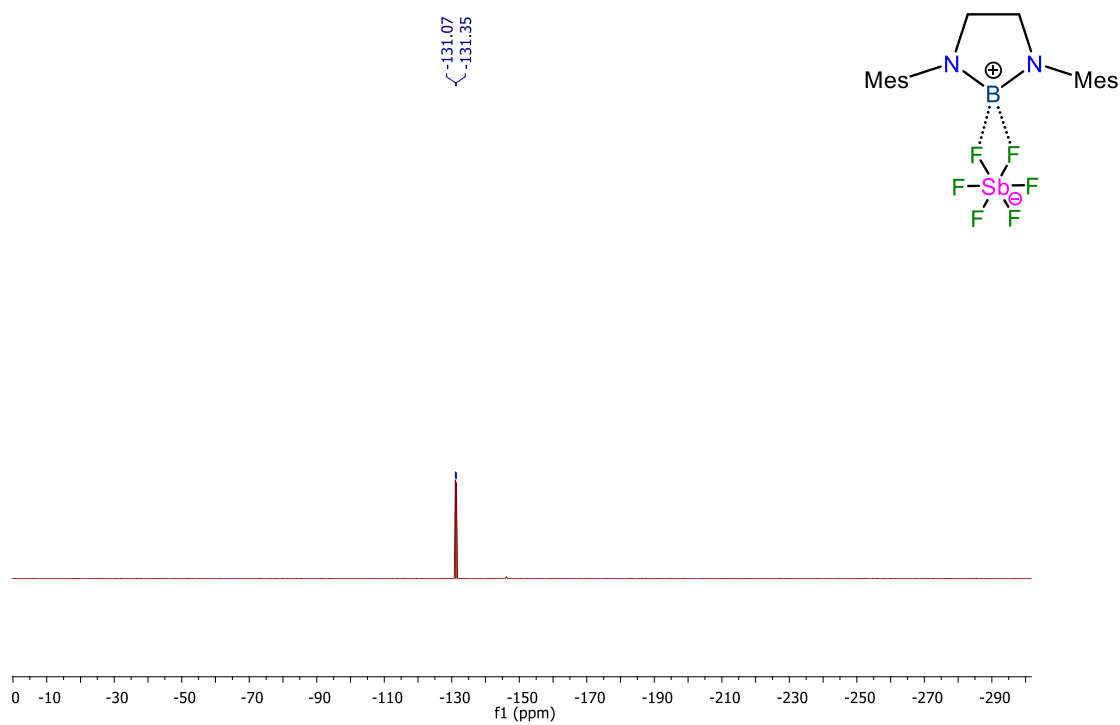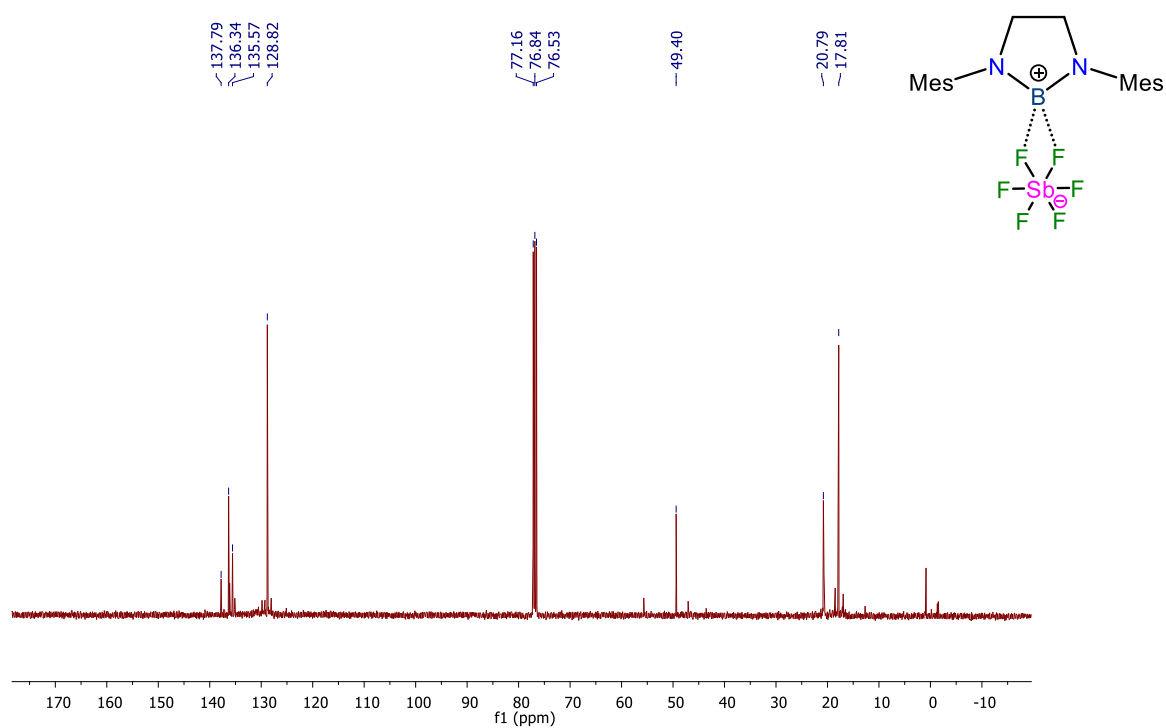
^{13}C NMR spectra of **C3**
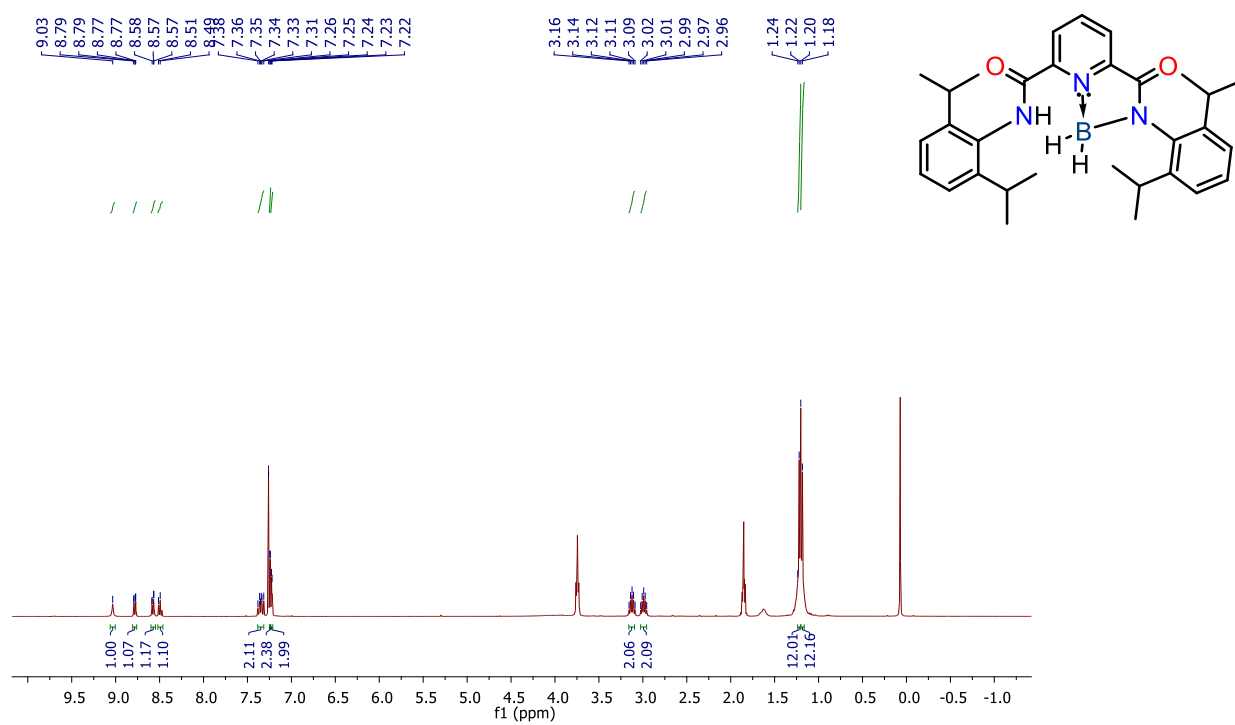
^{1}H NMR spectra of **C4**
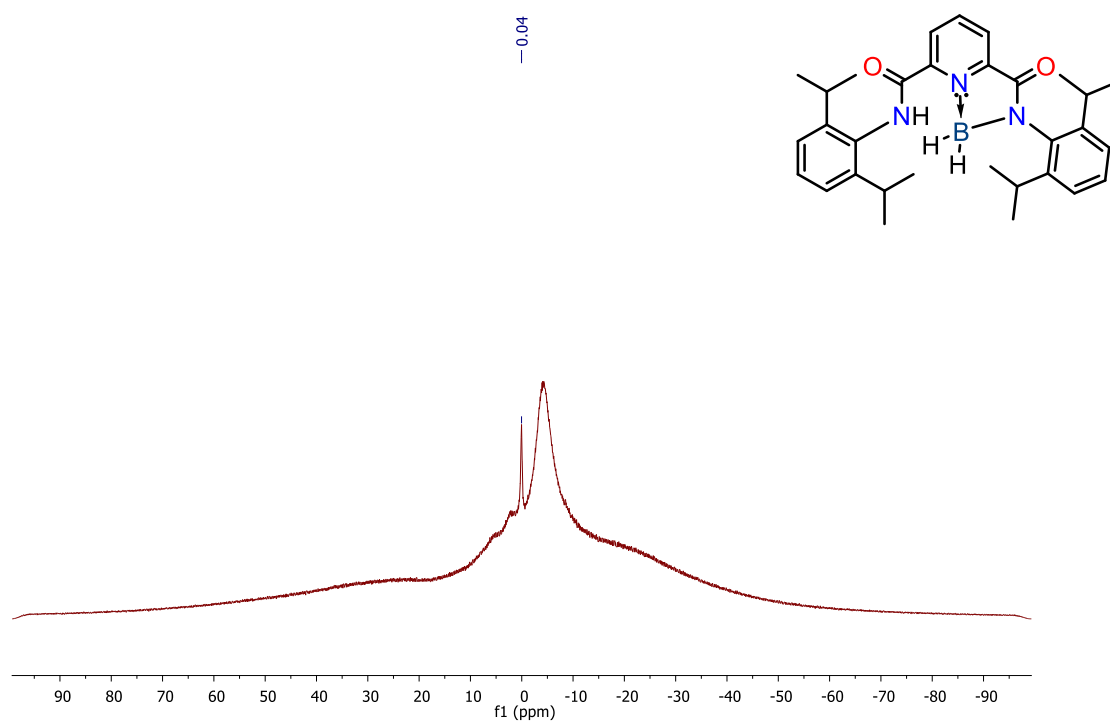
^{11}B{^{1}H} NMR spectra of **C4**

0.01
−0.89
−1.73

^{11}B NMR spectra of **C4**

160.56
159.52
150.18
146.50
146.22
146.03
142.95
137.97
132.76
132.53
129.84
129.66
129.20
129.15
128.34
128.12
126.00
125.41
125.13
123.90
123.81
77.48
77.16
76.84
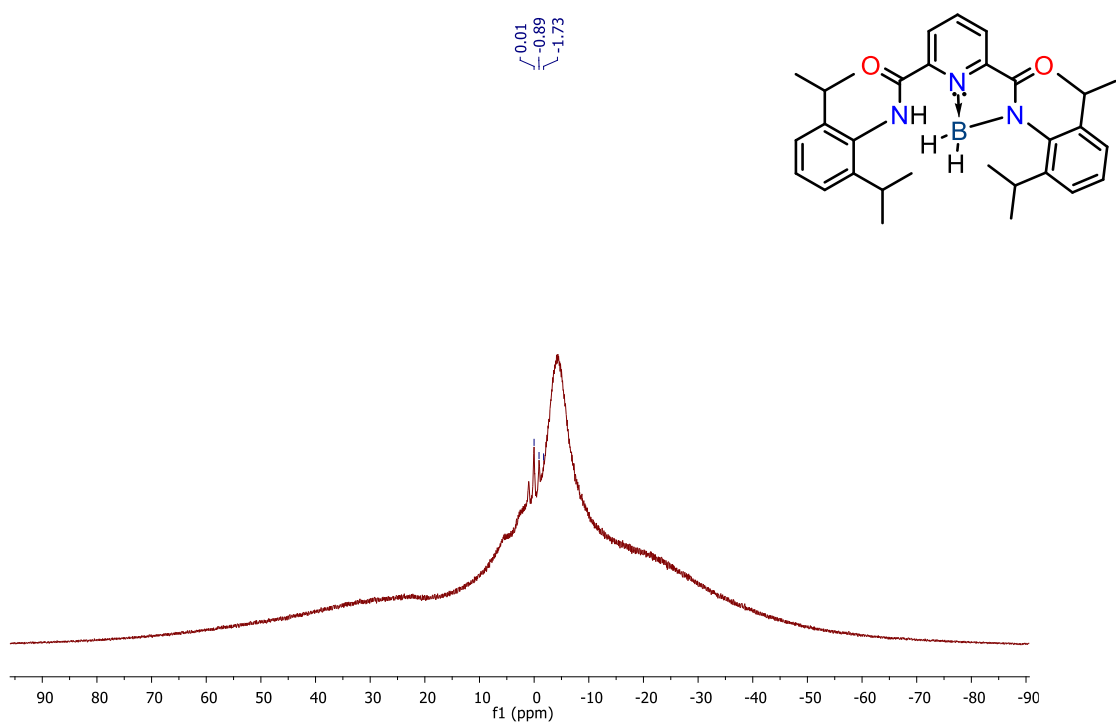
29.21
29.10
28.71
24.57
24.23
23.74
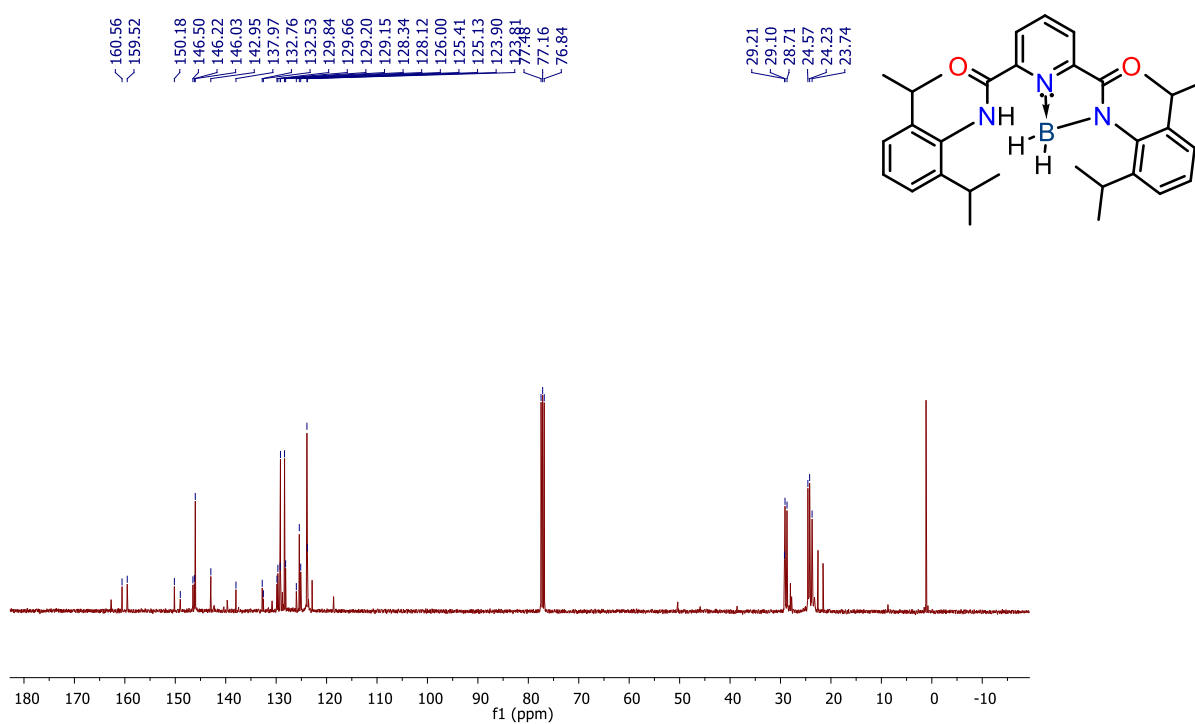
^{13}C NMR spectra of **C4**

52.47
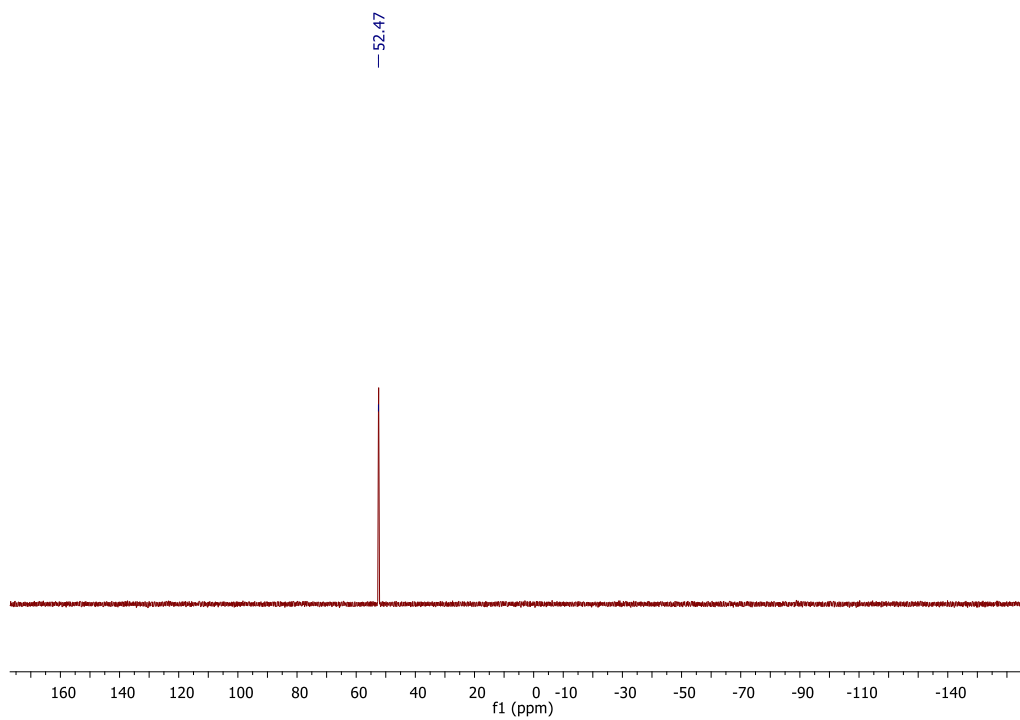
^{31}P NMR spectra of neat **Et₃PO**

75.88
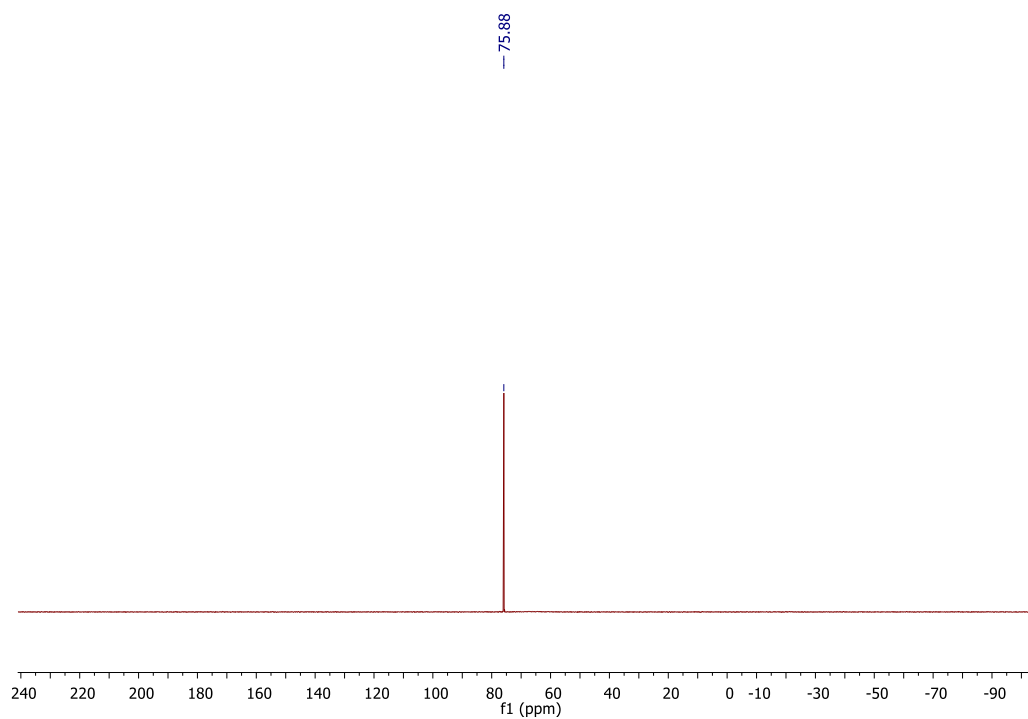
^{31}P NMR spectra of **Et₃PO-B(C₆F₅)₃ adduct**

−78.55

Unreacted Et$_3$PO

f1 (ppm)
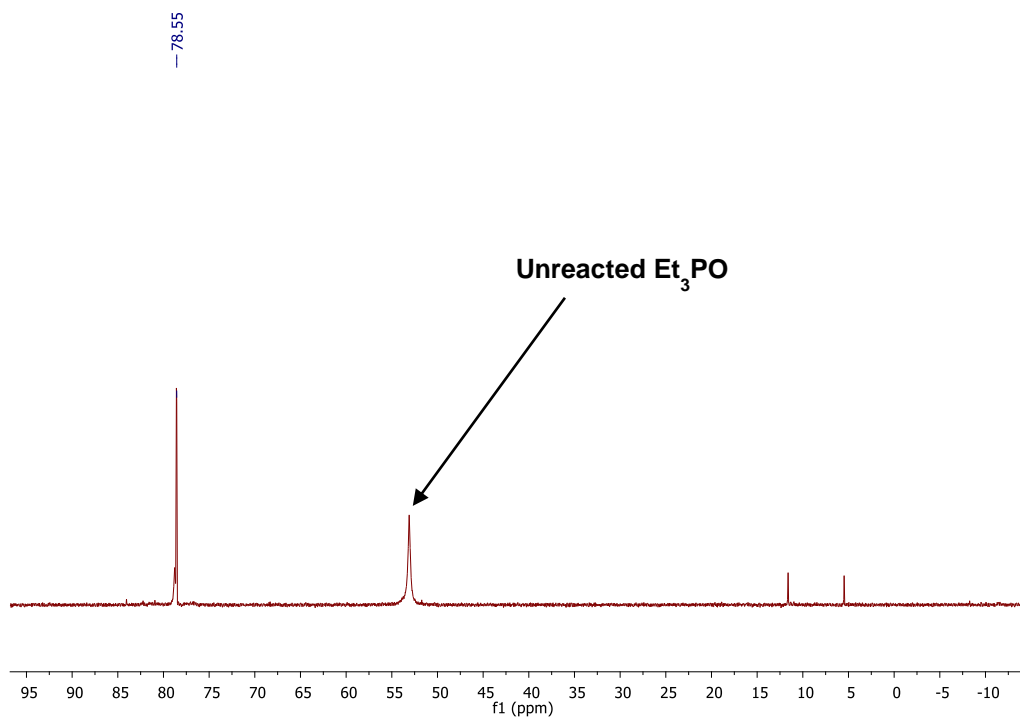
^{31}P NMR spectra of **Et$_3$PO-C2 adduct**

−78.68

f1 (ppm)
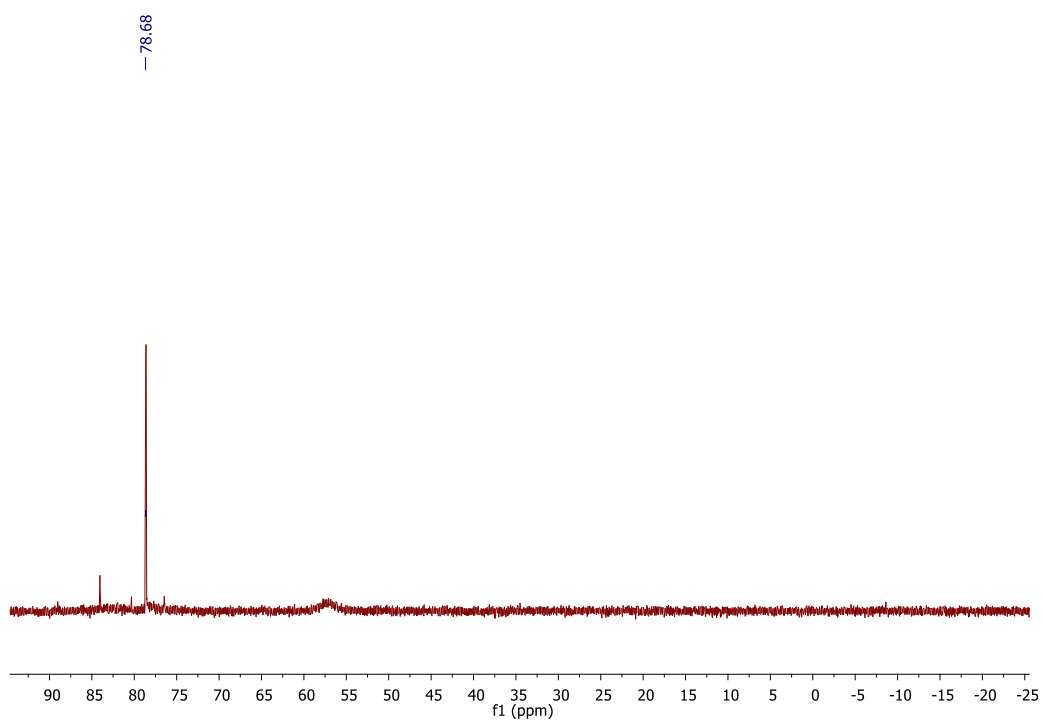
^{31}P NMR spectra of **Et$_3$PO-C3 adduct**

^{1}H NMR spectra of **1a** (Internal standard-CH$_2$Br$_2$ at δ=4.92 ppm)
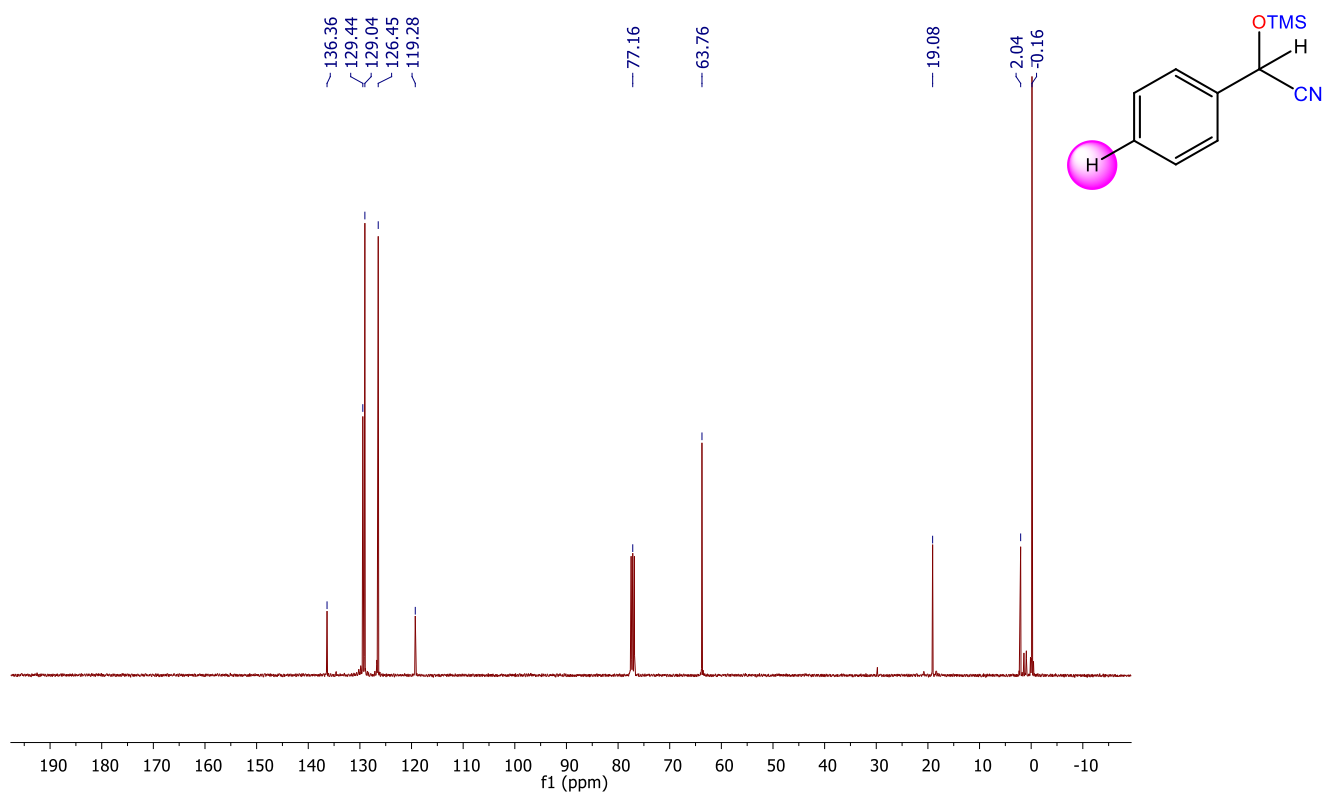
^{13}C NMR spectra of **1a** (Internal standard-CH$_2$Br$_2$ at δ=19.08 ppm)
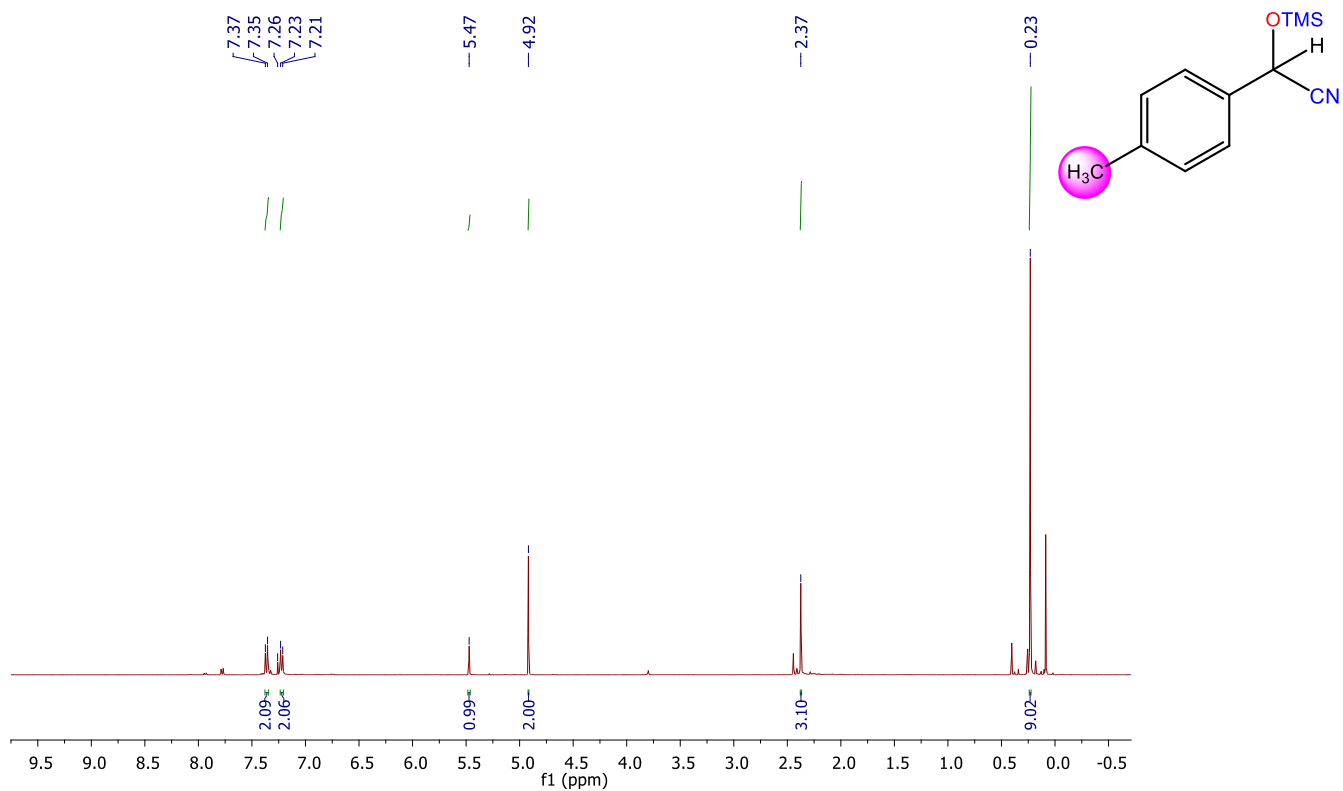
^{1}H NMR spectra of **1b** (Internal standard-CH$_2$Br$_2$ at δ=4.92 ppm)
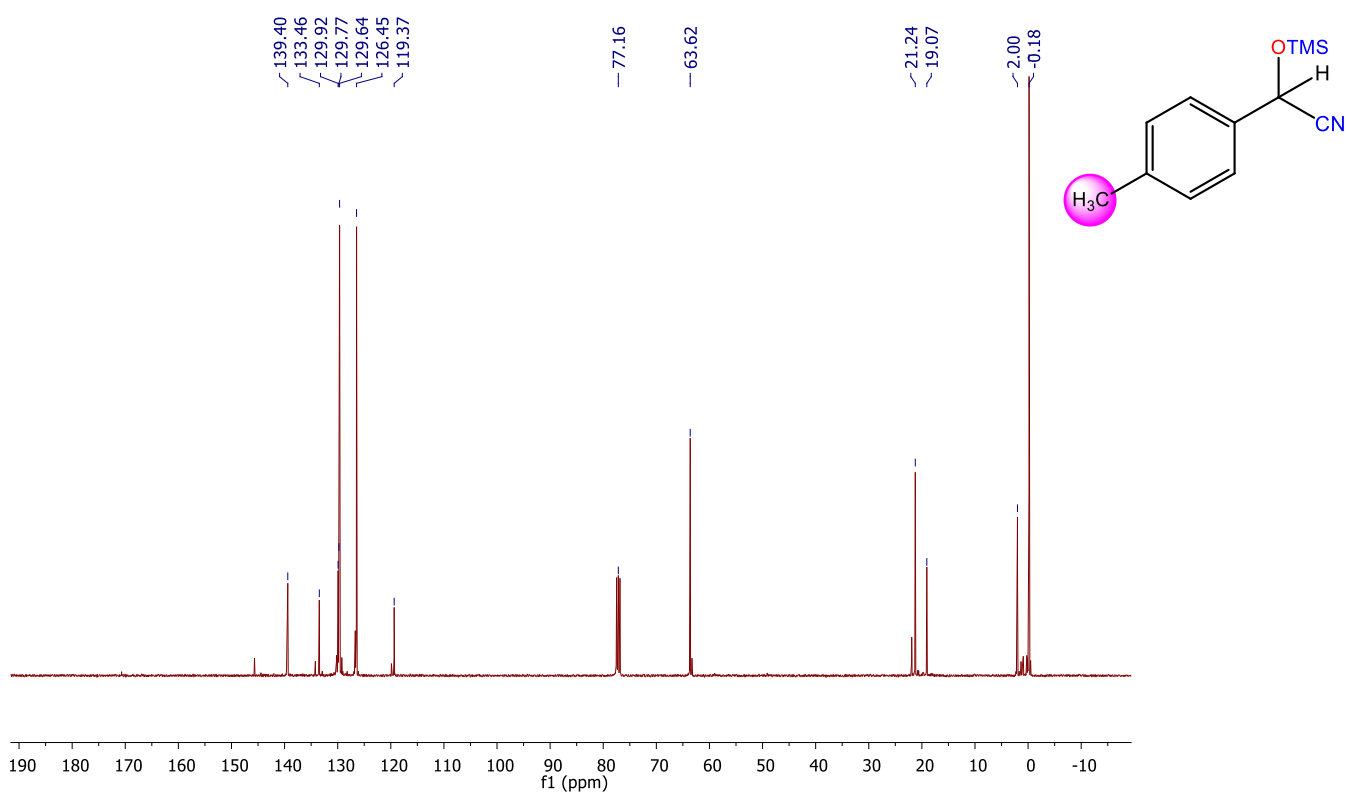
^{13}C NMR spectra of **1b** (Internal standard-CH$_2$Br$_2$ at δ=19.08 ppm)
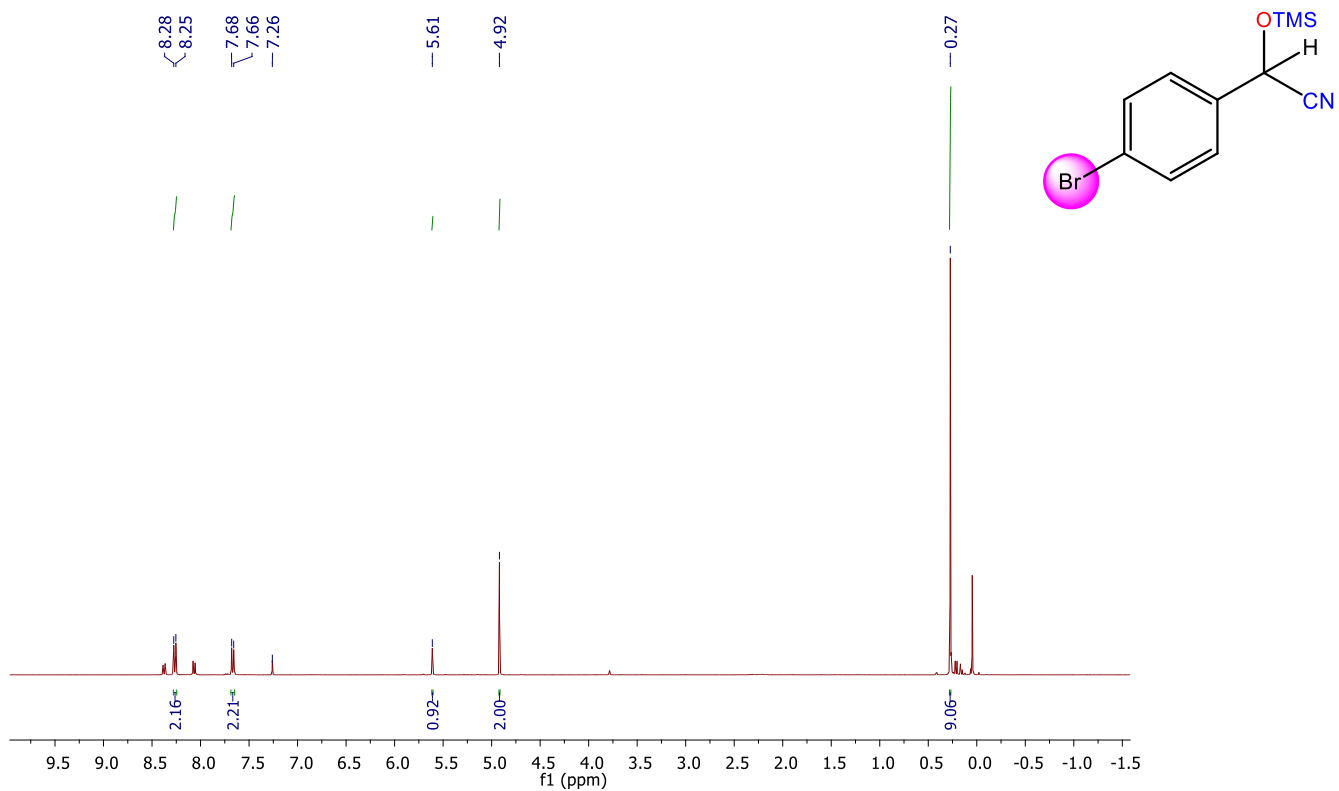
^{1}H NMR spectra of **1c** (Internal standard-CH$_2$Br$_2$ at δ=4.92 ppm)
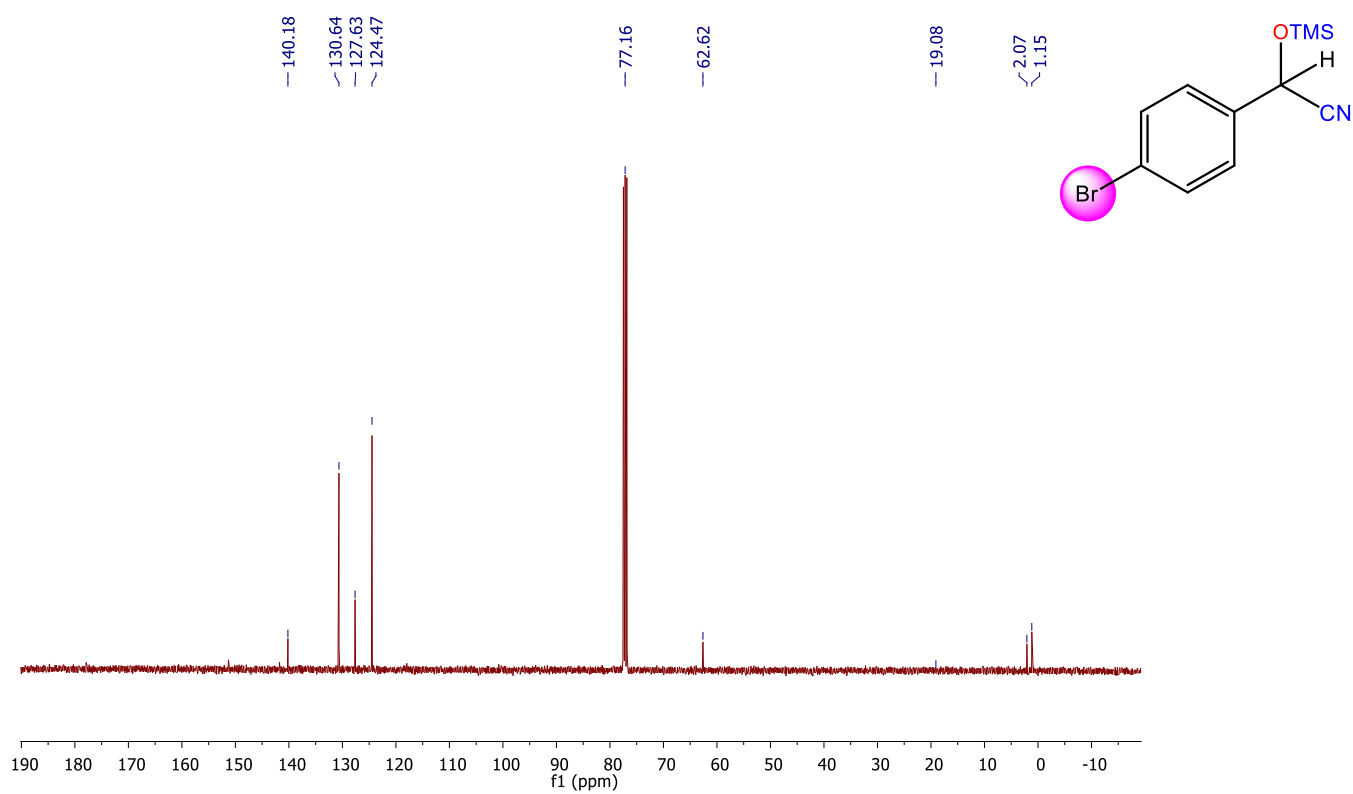
^{13}C NMR spectra of **1c** (Internal standard-CH$_2$Br$_2$ at δ=19.08 ppm)
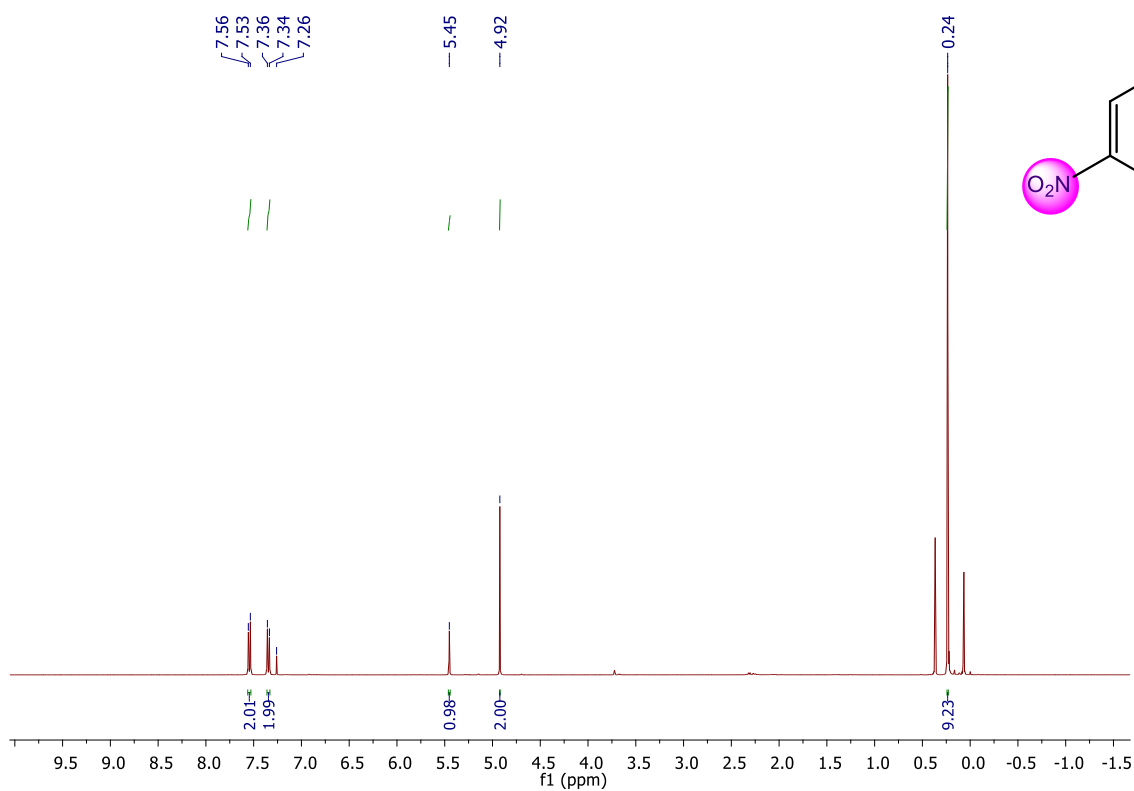
^{1}H NMR spectra of **1d** (Internal standard-CH$_2$Br$_2$ at δ=4.92 ppm)
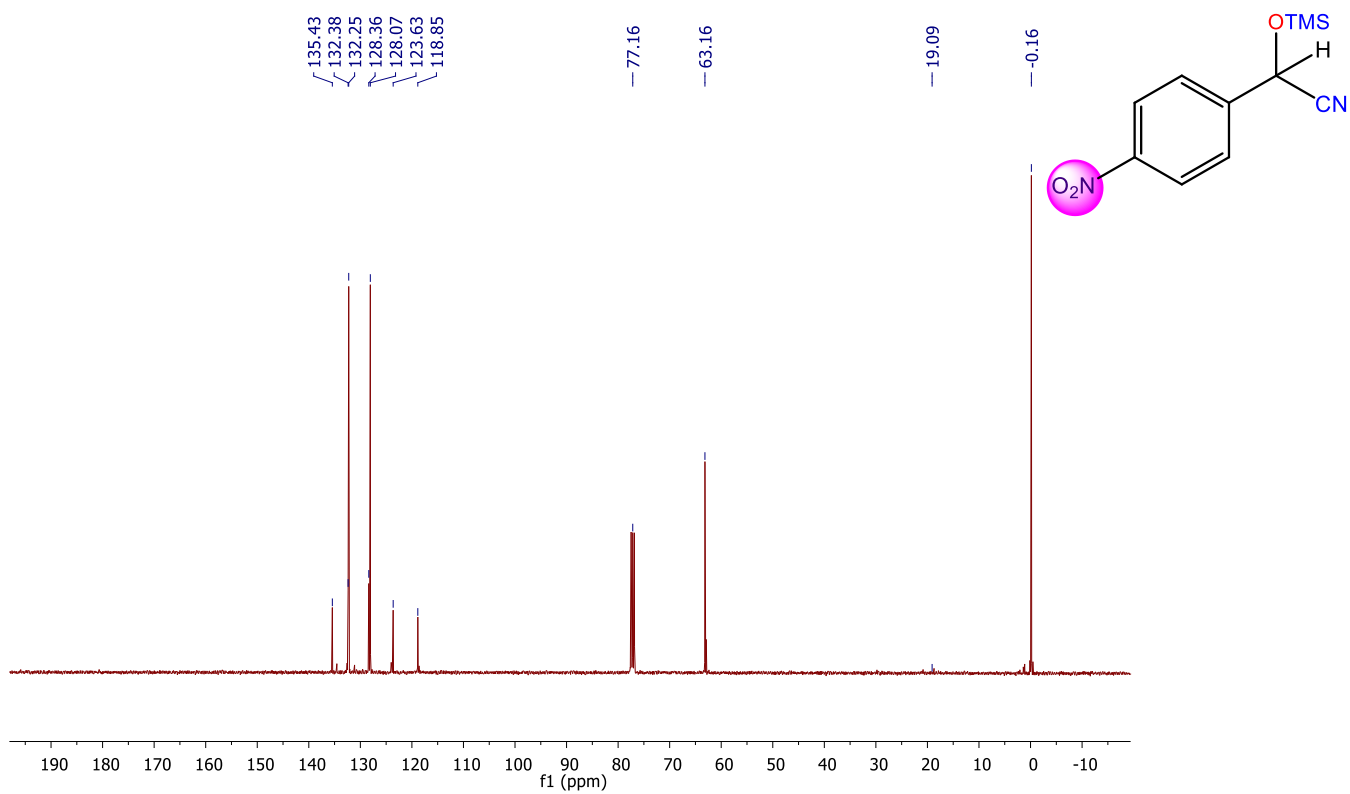
^{13}C NMR spectra of **1d** (Internal standard-CH$_2$Br$_2$ at δ=19.08 ppm)
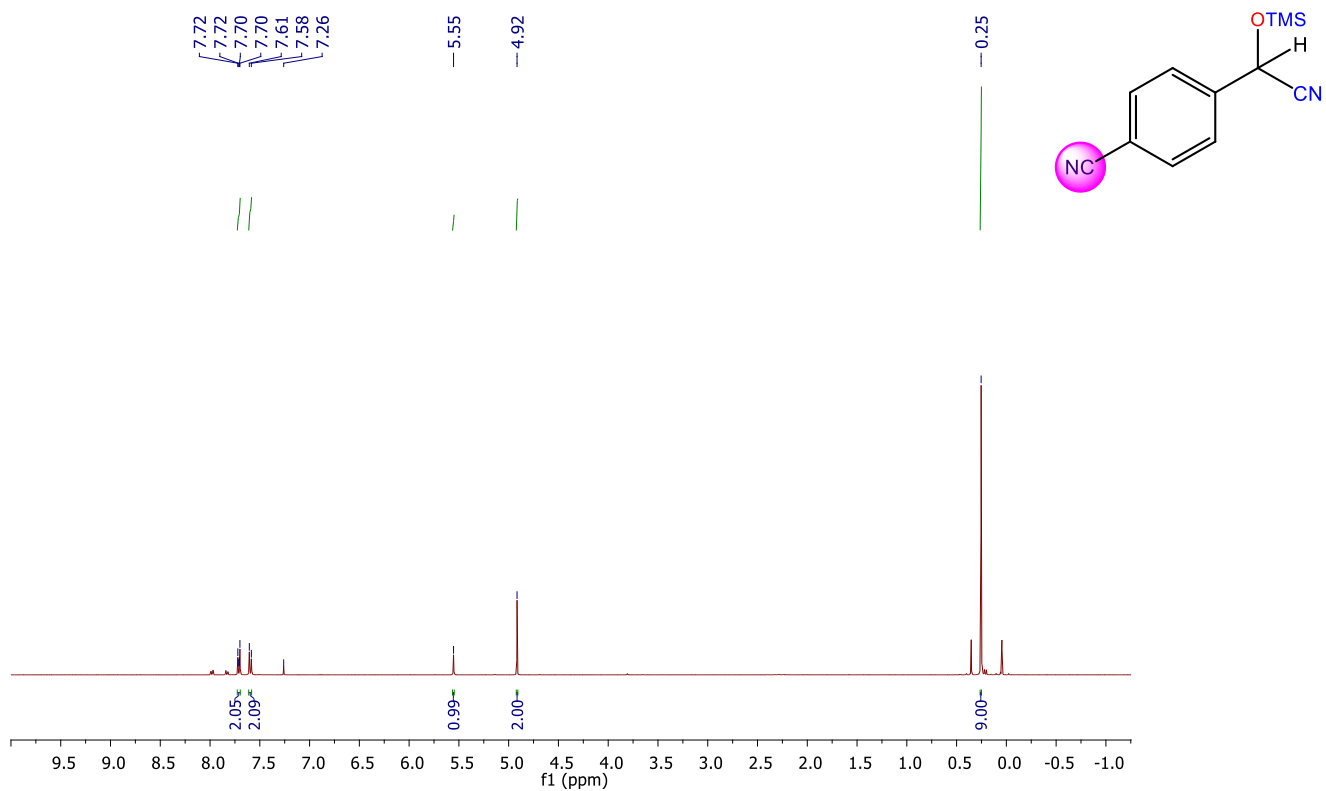
^{1}H NMR spectra of **1e** (Internal standard-CH$_2$Br$_2$ at δ=4.92 ppm)
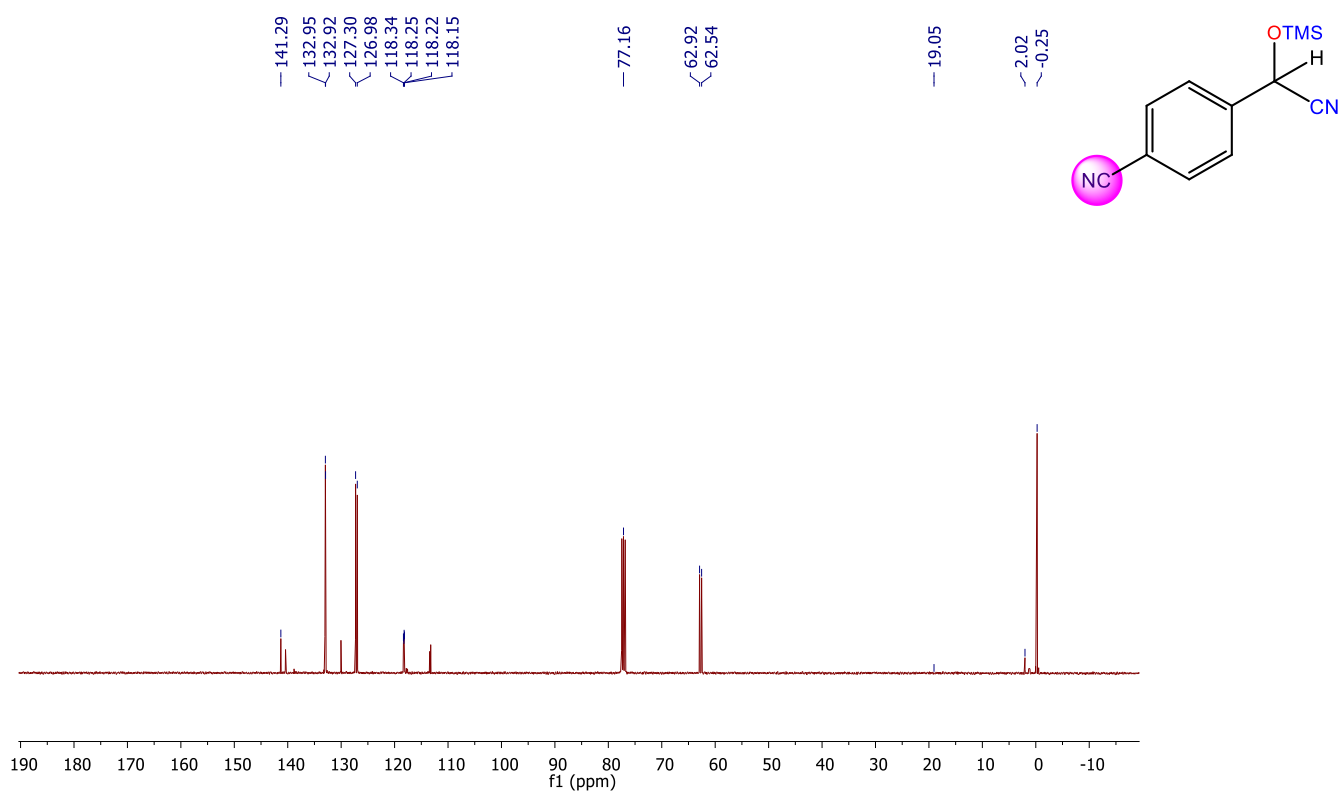
^{13}C NMR spectra of **1e** (Internal standard-CH$_2$Br$_2$ at δ=19.08 ppm)
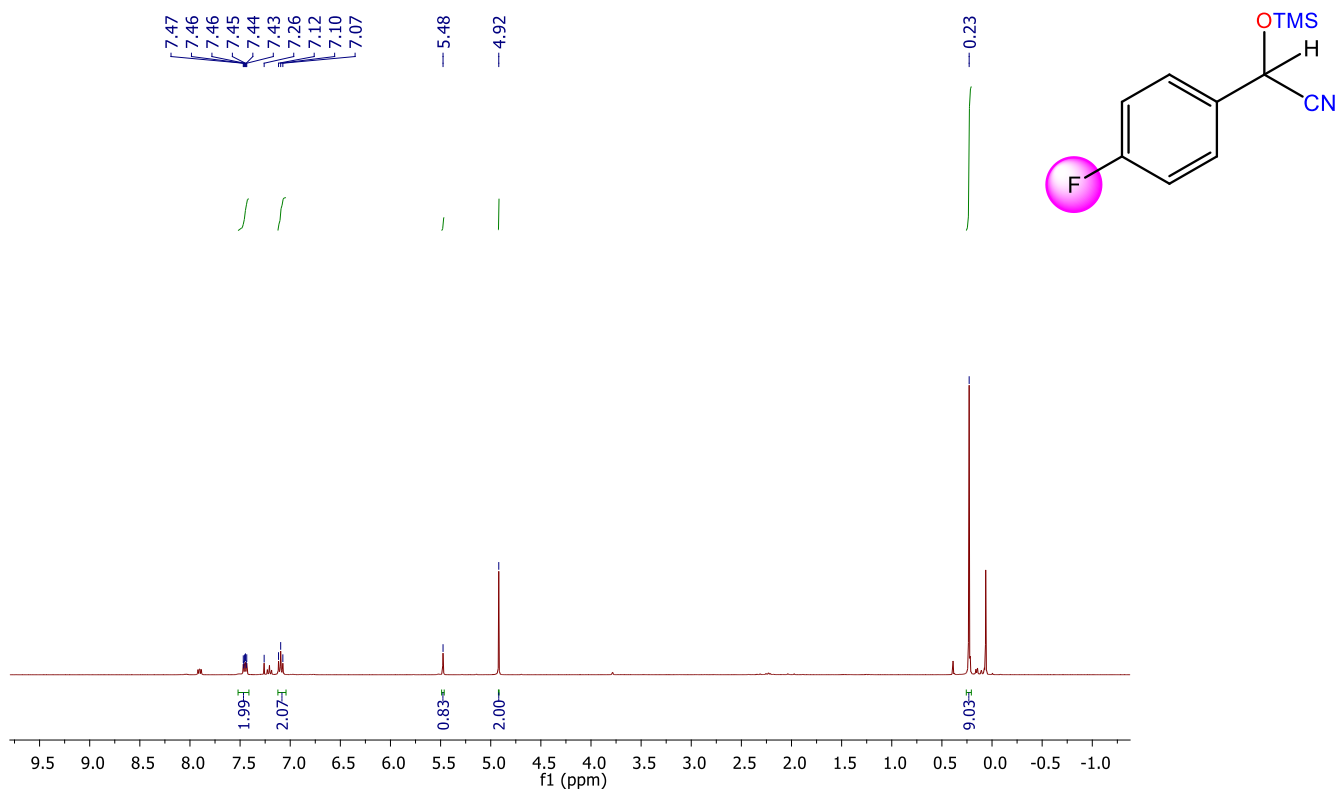
^{1}H NMR spectra of **1f** (Internal standard-CH$_2$Br$_2$ at δ=4.92 ppm)
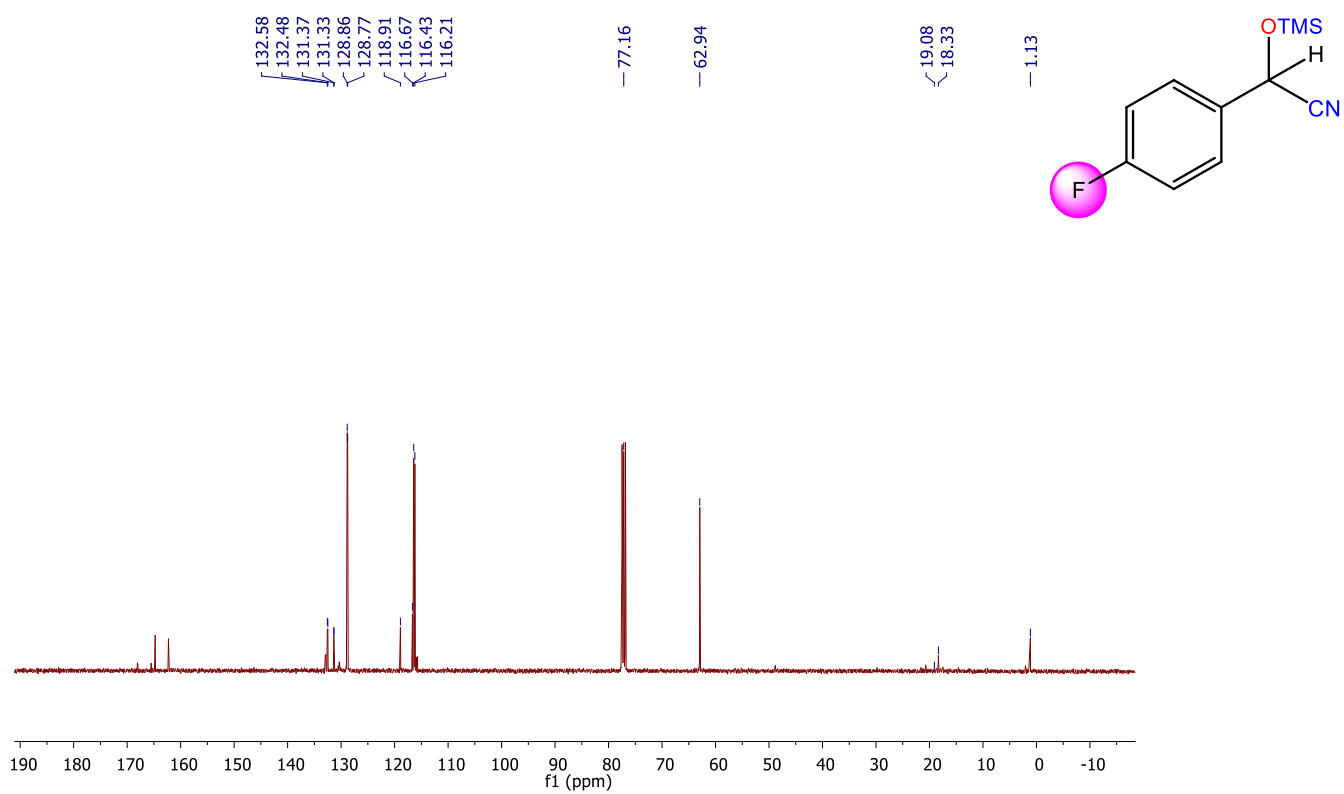
^{13}C NMR spectra of **1f** (Internal standard-CH$_2$Br$_2$ at δ=19.08 ppm)
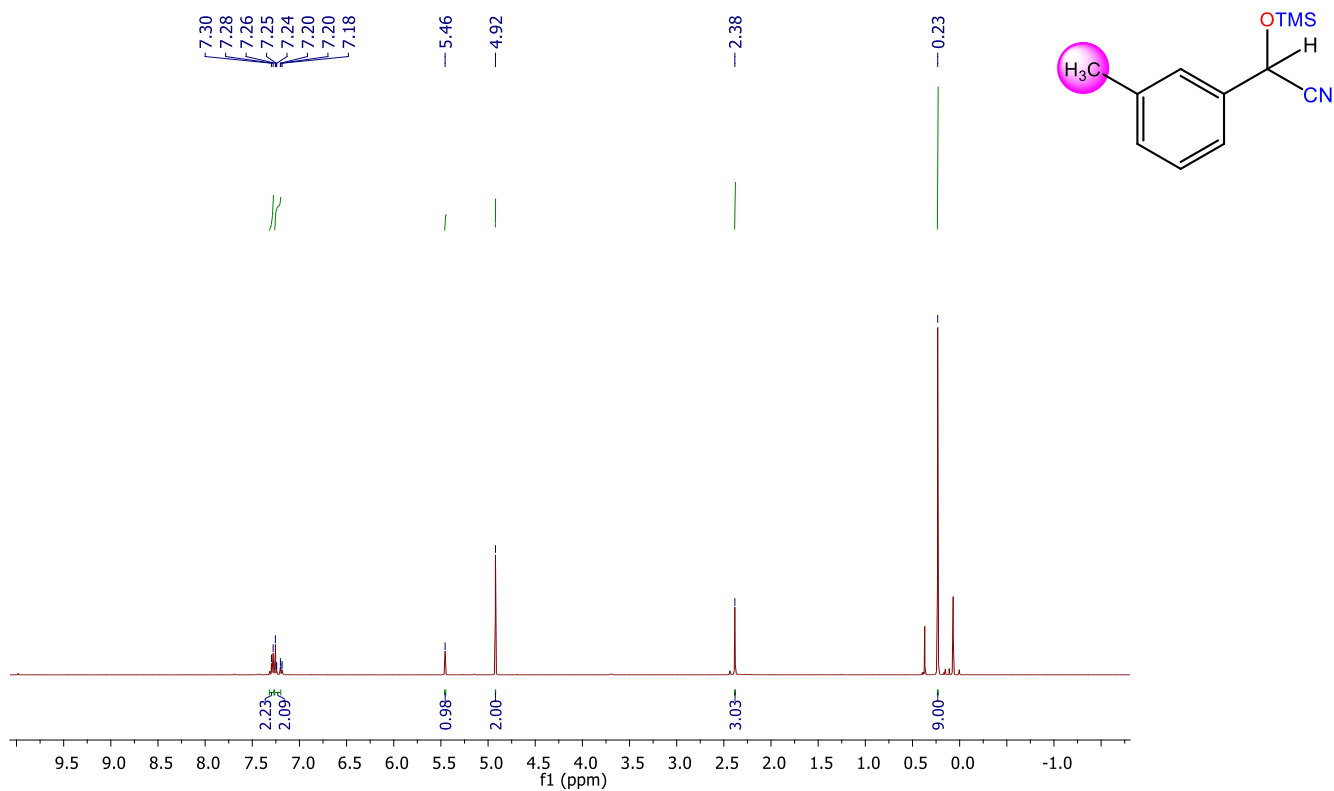
^{1}H NMR spectra of **1g** (Internal standard-CH$_2$Br$_2$ at δ=4.92 ppm)
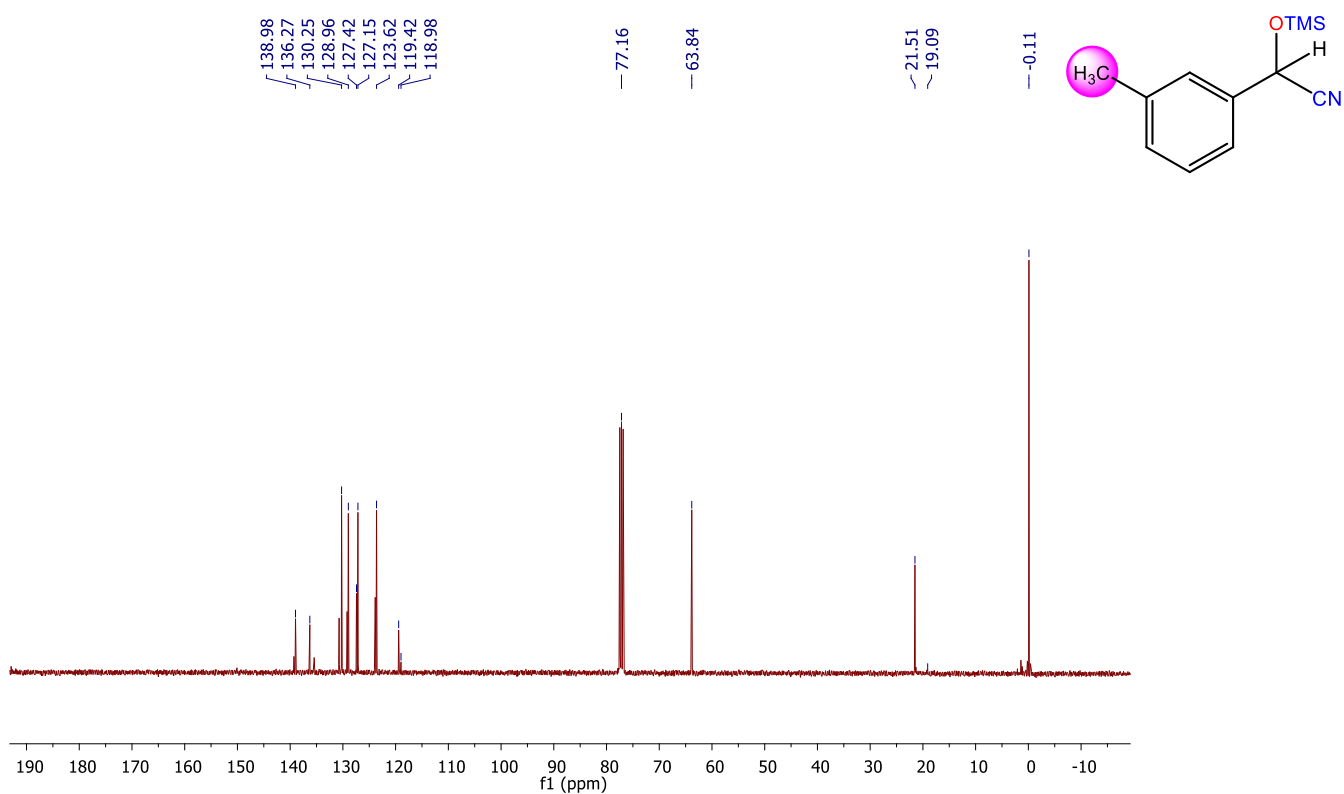
^{13}C NMR spectra of **1g** (Internal standard-CH$_2$Br$_2$ at δ=19.08 ppm)
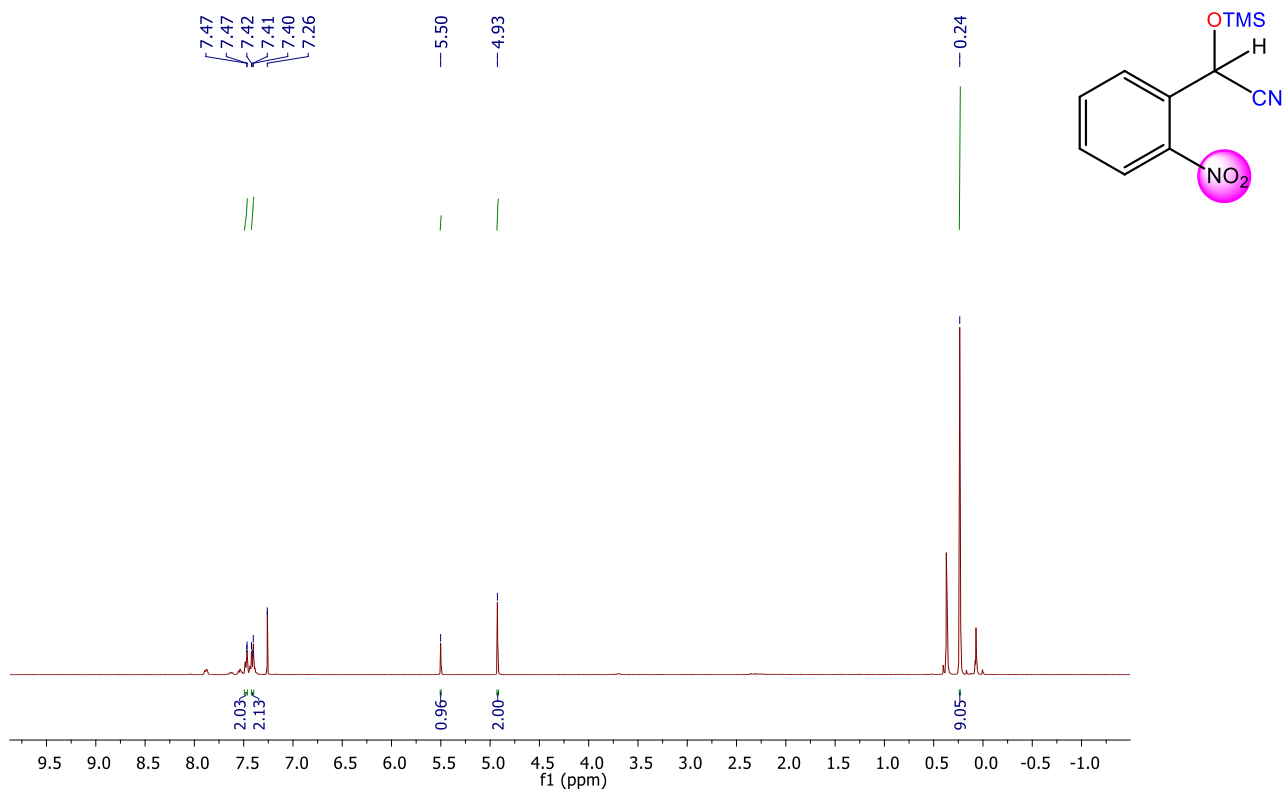
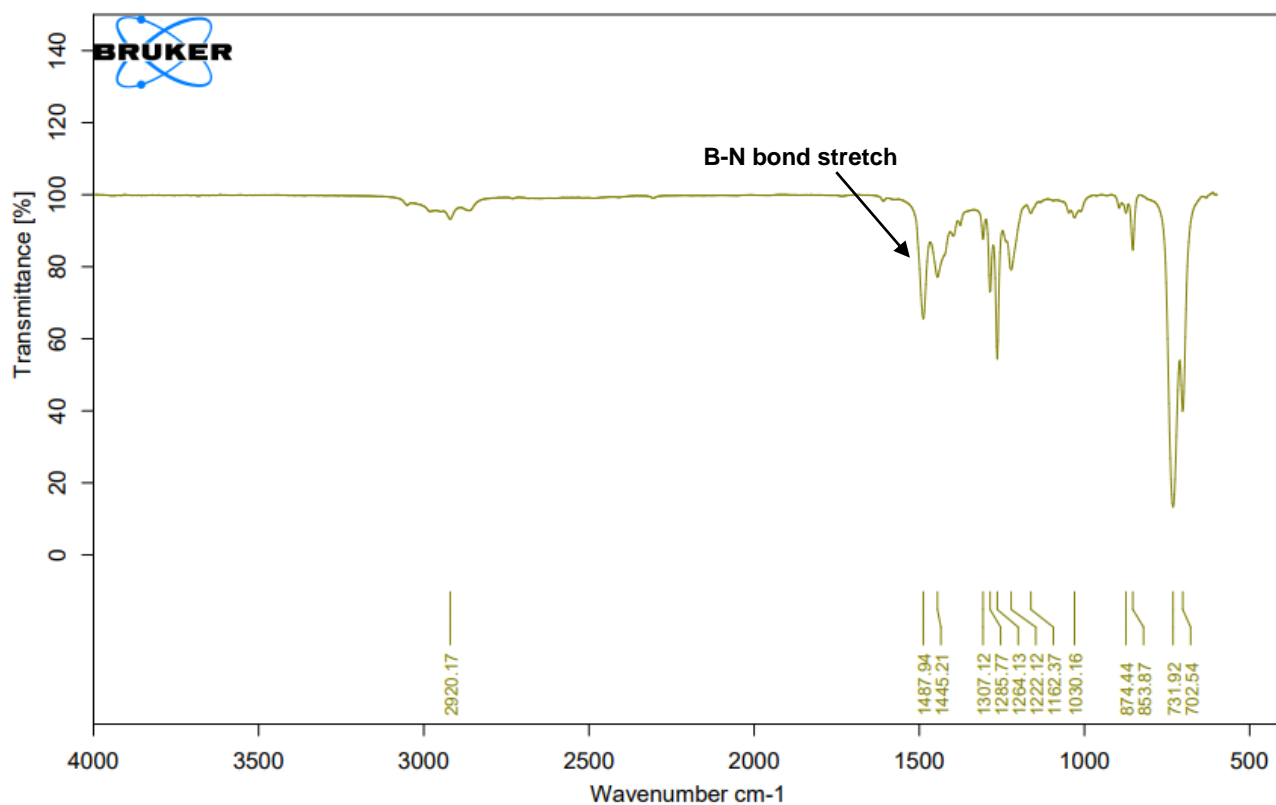^{1}H NMR spectra of **1h** (Internal standard-CH$_2$Br$_2$ at δ=4.92 ppm)
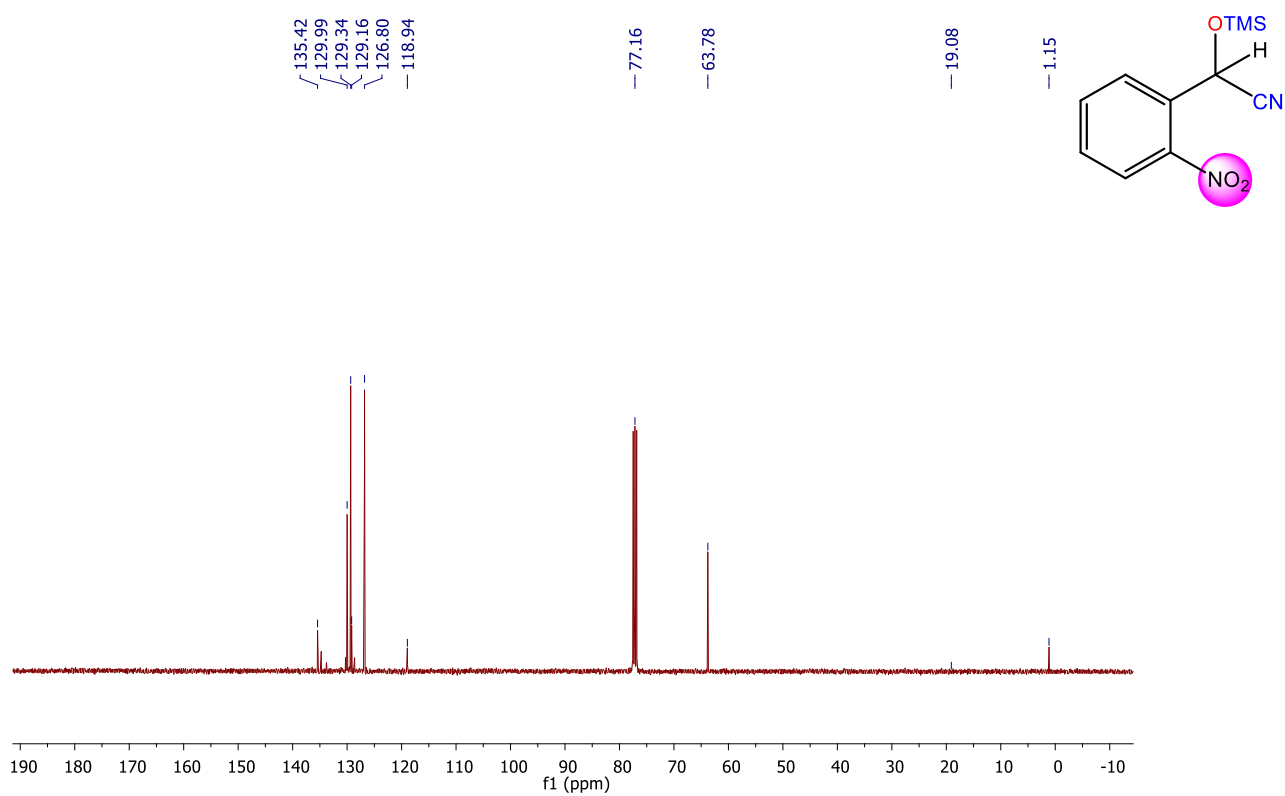
^{13}C NMR spectra of **1h** (Internal standard-CH$_2$Br$_2$ at δ=19.08 ppm)
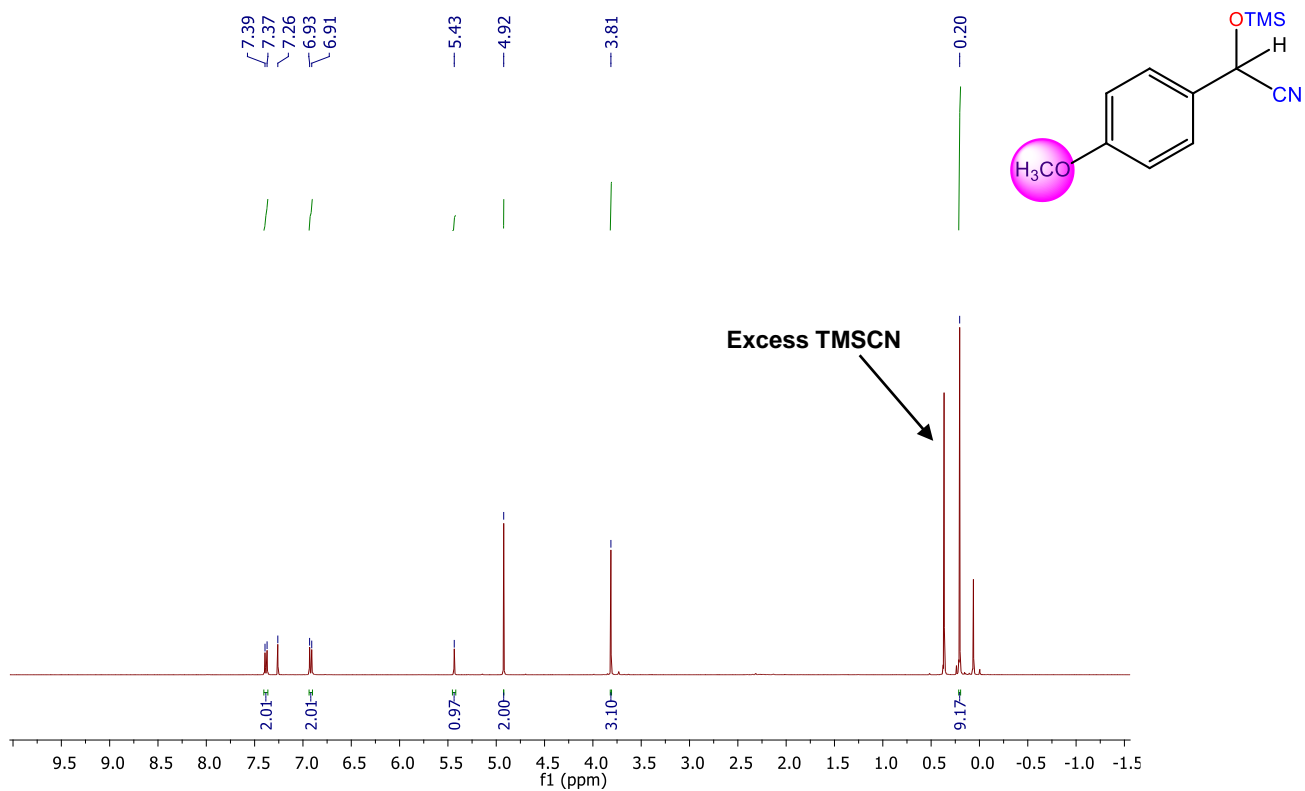
^{1}H NMR spectra of **1i** (Internal standard-CH$_2$Br$_2$ at δ=4.92 ppm)
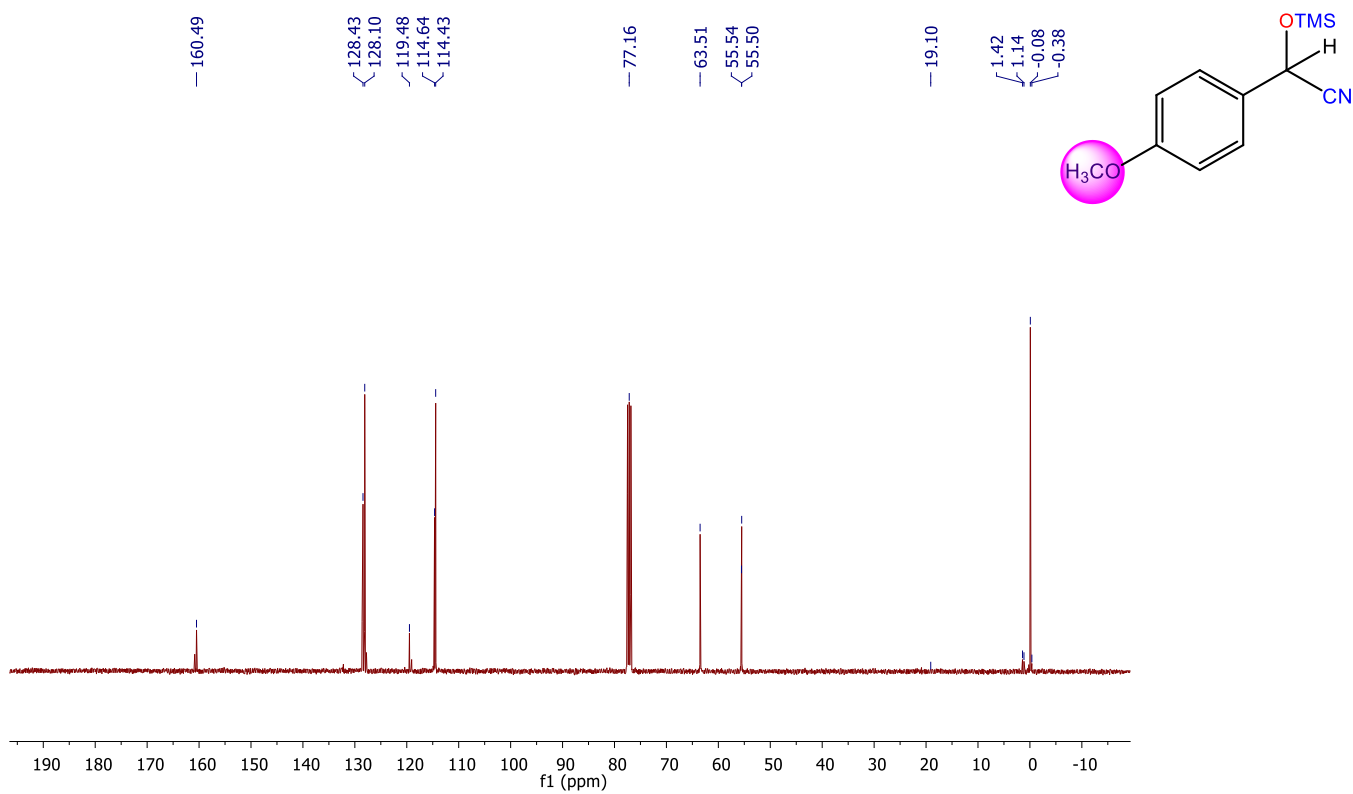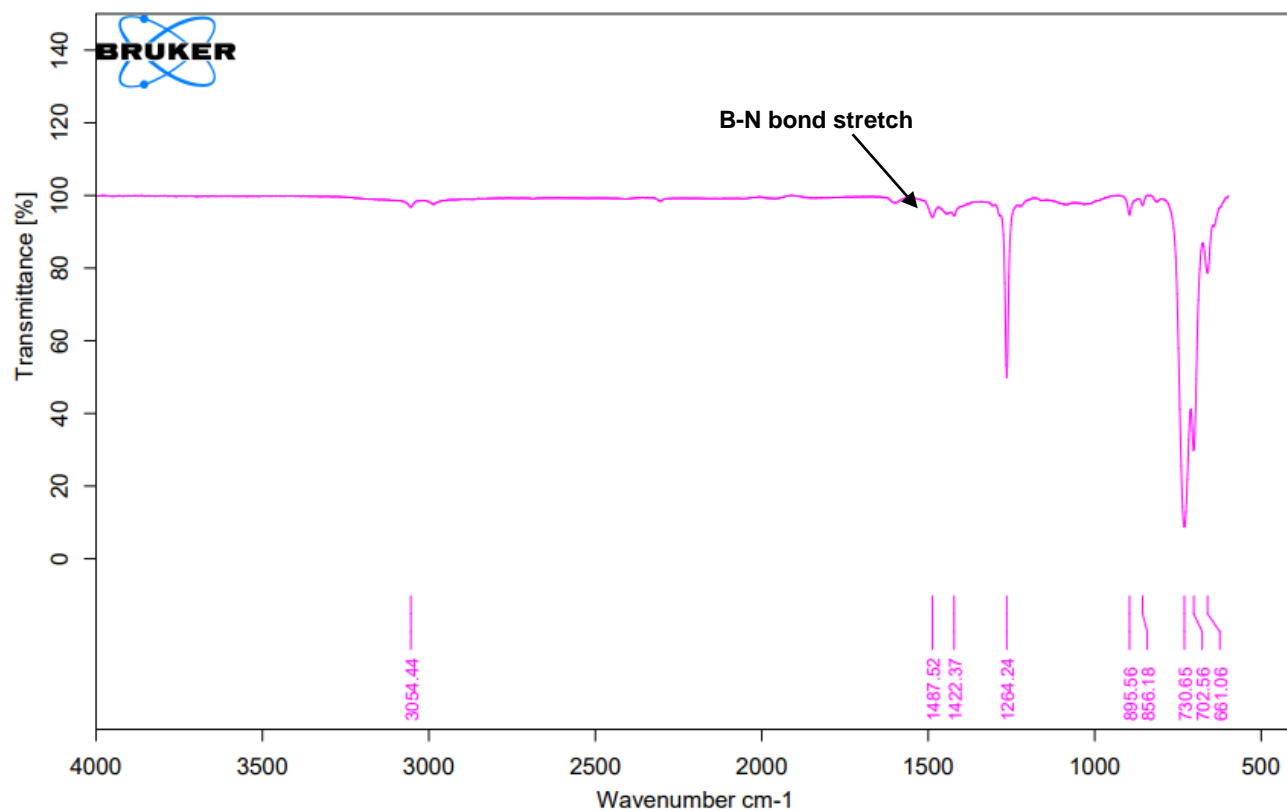

^{13}C NMR spectra of **1i** (Internal standard-CH$_2$Br$_2$ at δ=19.08 ppm)

IR spectrum of **C1**
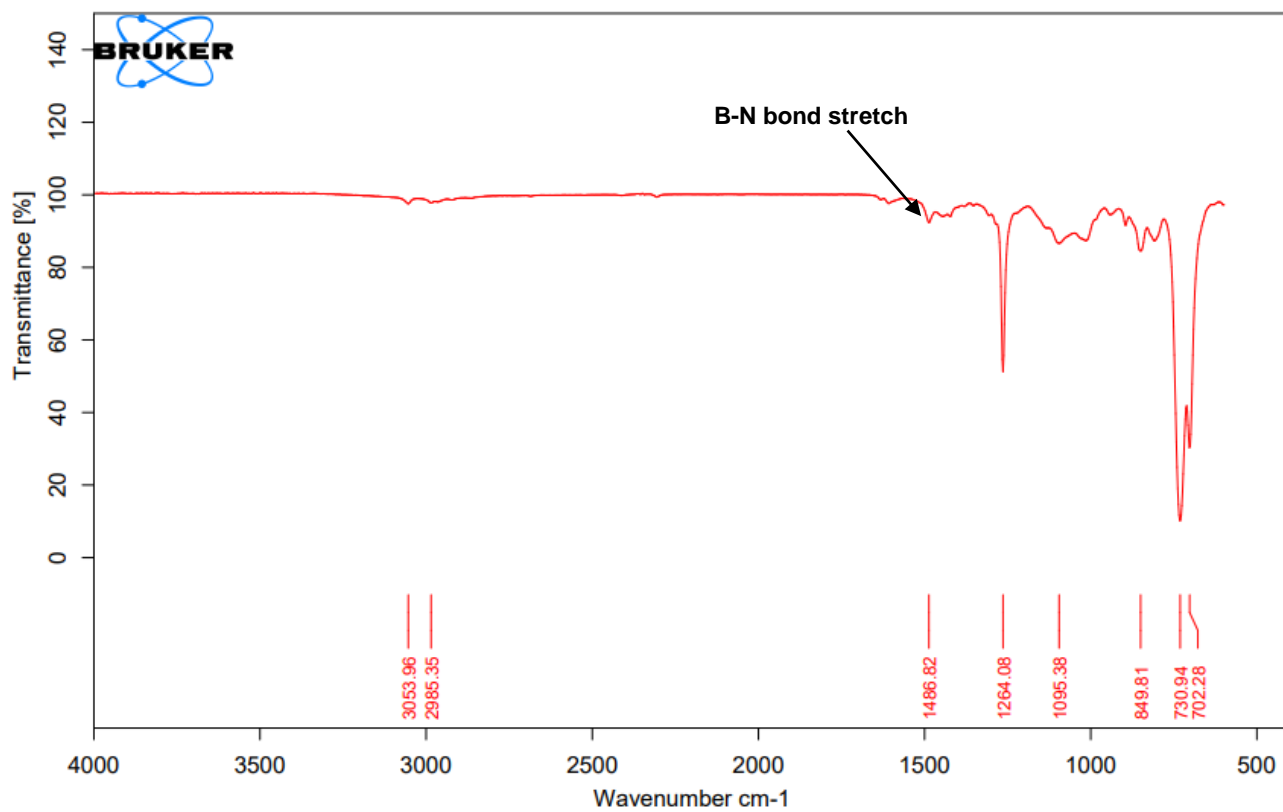
IR spectrum of **C2**

IR spectrum of **C3**